“G. d’Annunzio” University of Chieti-Pescara

School of Advanced Studies “G. d’Annunzio”

DOCTORATE OF RESEARCH IN:

BIOMOLECULAR AND PHARMACEUTICAL SCIENCES

CYCLE XXXVIII

“Endothelial dysfunction and impaired angiogenesis in chronic hyperglycaemia: from molecular mechanisms to emerging therapeutic strategies”

Department of Medical, Oral and Biotechnological Sciences

Scientific Disciplinary Sector BIOS-10/A

PhD Student

Dr. Ilaria Cappellacci

Coordinator and Tutor

Prof. Assunta Pandolfi

Co-Tutor

Prof. Caterina Pipino

Academic Years 2022/2025

TABLE OF CONTENTS

1 ABSTRACT 1

2 INTRODUCTION 3

2.1 DIABETES MELLITUS 3

2.1.1 TYPE 1 DIABETES 4

2.1.2 TYPE 2 DIABETES 6

2.1.3 OTHER DIABETES MELLITUS TYPES 10

2.1.4 GESTATIONAL DIABETES 11

2.2 DIABETES COMPLICATIONS 16

2.3 DIABETIC FOOT ULCER 18

2.3.1 WOUND HEALING MECHANISMS 19

2.3.2 WOUND ANGIOGENESIS 23

2.4 ENDOTHELIAL DYSFUNCTION 27

2.5 HUMAN UMBILICAL VEIN ENDOTHELIAL CELLS OF GESTATIONAL DIABETIC MOTHERS 29

2.6 NATURAL BIOACTIVE COMPOUNDS 31

2.6.1 POLYPHENOLS 32

2.7 AMNIOTIC MEMBRANE 33

3 AIMS 38

4 VASCULAR INFLAMMATION: ROLE OF OLIVE LEAF PHENOLIC EXTRACTS (*AIM 1)* 40

4.1 MATERIALS AND METHODS 40

4.1.1 Olive leaf samples 40

4.1.2 Extraction of phenolic compounds and their analysis by HPLC-ESI-TOF-MS 40

4.1.3 Clinical characteristics of umbilical cords donors and newborns 40

4.1.4 HUVEC isolation and culture 42

4.1.5 MTT assay 44

4.1.6 RNA extraction and real-time quantitative PCR 45
4.1.7 Immunofluorescence analysis 45
4.1.8 Flow cytometry analysis 46
4.1.9 Monocyte adhesion assay 46
4.1.10 Statistical analysis 47
4.2 RESULTS 48
4.2.1 Determination of phenolic compounds in Picual and Changlot Real olive leaf extracts. 48
4.2.2 Effects of Picual and Changlot Real phenolic extracts on cell viability 48
4.2.3 Effects of Picual and Changlot Real phenolic extracts on *NF-kB p65* and *MCP-1* gene expression 50
4.2.4 Effects of Picual and Changlot Real phenolic extracts on NF-kB p65 phosphorylation 53
4.2.5 Effects of Picual and Changlot Real phenolic extracts on VCAM-1 protein expression 53
4.2.6 Effects of Picual and Changlot Real phenolic extracts on monocyte–HUVEC interaction 55
4.3 DISCUSSION 57
5 ANGIOGENESIS: ROLE OF AMNIOTIC MEMBRANE VIA VEGFR2/AKT/ENOS SIGNALLING PATHWAY (*AIM 2*) 60
5.1 MATERIALS AND METHODS 60
5.1.1 Amniotic Membrane collection and storage 60
5.1.2 HUVEC isolation and culture 61
5.1.3 Experimental protocol 61
5.1.4 MTT assay 62
5.1.5 RNA extraction and real-time quantitative PCR 62
5.1.6 Flow cytometry analysis 62
5.1.7 Matrigel tube formation assay 63
5.1.8 Statistical analysis 64

5.2 RESULTS 65
5.2.1 Effect of AM on *VEGFa* gene expression 65
5.2.2 Effect of AM on VEGFR2 gene and protein expression 66
5.2.3 Effect of AM on VEGFR2 activation 67
5.2.4 Effect of AM on AKT activation 69
5.2.5 Effect of AM on nitro-oxidative stress 70
5.2.6 Effect of AM on VEGFR2 activation counteracted by VEGFR2 inhibitor 72
5.2.7 Effect of AM on nitro-tyrosine levels counteracted by VEGFR2 inhibitor 73
5.2.8 Effect of AM on Matrigel vessel formation counteracted by VEGFR2 inhibitor 74
5.3 DISCUSSION 76
6 ANGIOGENESIS: ROLE OF THE INTERACTION BETWEEN ENDOTHELIAL CELLS AND DERMAL FIBROBLASTS IN DIABETES (*AIM 3*) 81
6.1 MATERIALS AND METHODS 81
6.1.1 HUVEC isolation and culture 81
6.1.2 Experimental protocol 81
6.1.3 RNA extraction and real-time quantitative PCR 82
6.1.4 Flow cytometry analysis 84
6.1.5 Immunofluorescence analysis 84
6.1.6 Zymography 85
6.1.7 Wound healing scratch assay 85
6.1.8 Presto Blue assay 86
6.1.9 PicoGreen assay 86
6.1.10 Matrigel tube formation assay 87
6.1.11 Statistical analysis 87
6.2 RESULTS 89
6.2.1 Effect of GD-HUVEC on ECM production by dermal fibroblasts 89
6.2.2 Effect of GD-HUVEC on Smad2-3 and MAPK activation by dermal fibroblasts… 90

6.2.3 Effect of GD-HUVEC on ECM degradation by dermal fibroblasts 91
6.2.4 Effect of GD-HUVEC on migration by dermal fibroblasts 94
6.2.5 Effect of GD-HUVEC on Hippo pathway and FAK expression by dermal fibroblasts 95
6.2.6 Differences between HDF and diabHDF on metabolic activity and dsDNA amount. 97
6.2.7 Differences between HDF and diabHDF on *COL1, SMAD3-3, MCP-1* and *VEGFa* gene expression 97
6.2.8 Effect of diabHDF on migration by C-HUVEC 98
6.2.9 Effect of diabHDF on Matrigel vessel formation by C-HUVEC 99
6.2.10 Effect of diabHDF on VEGFR2 gene and protein expression by C-HUVEC 101
6.2.11 Effect of diabHDF on Matrigel vessel formation by GD-HUVEC 102
6.3 DISCUSSION 104
7 CONCLUSIONS 109
8 REFERENCES 110

1 ABSTRACT

Diabetes mellitus is a severe metabolic disorder clinically characterized by hyperglycaemia. Chronic exposure to high glucose levels leads to endothelial dysfunction defined by impairment of multiple mechanisms, including increased vascular inflammation and oxidative stress, reduced nitric oxide bioavailability, and decreased angiogenesis. These altered processes result in several vascular complications including diabetic foot ulcer, which strongly impact patients' quality of life and healthcare systems. Insufficient angiogenesis, a key process that profoundly influences delayed healing of diabetic chronic wounds, is caused by different factors among which an inadequate Vascular Endothelial Growth Factor Receptor 2 (VEGFR2) mediated signalling pathway and a compromised crosstalk between the endothelium and dermal fibroblasts. Although many strategies focus on hyperglycaemia management, vascular diabetic complications remain a significant challenge.

Therefore, this thesis aims to gain insight into the mechanisms underlying the endothelial dysfunction in diabetes with a particular focus on molecular pathways associated with reduced angiogenesis, typical of chronic diabetic wounds, and on innovative therapeutic strategies ranging from phenolic extracts to perinatal derivatives such as the amniotic membrane. Specifically, this general aim was divided into three objectives: to investigate the vascular anti-inflammatory role of olive leaf phenolic extracts, to study the pro-angiogenic effects of amniotic membrane via VEGFR2/AKT/eNOS signalling pathway and to elucidate the interaction between endothelial cells and dermal fibroblasts in diabetes.

To this end, the unique *in vitro* model of human umbilical vein endothelial cells isolated from the umbilical cord vein of gestational diabetes affected mothers (GD-HUVEC) has been employed. Owing to stable epigenetic modifications induced by *in vivo* exposure to hyperglycaemia, this model faithfully reproduces the typical features of diabetic endothelial dysfunction.

Firstly, the results showed that olive leaf phenolic extracts counteract vascular inflammation by modulating the NF-kB pathway which, in turn, reduces vascular adhesion molecules expression and membrane exposure, leading to decreased monocyte adhesion to the endothelium.

Additionally, the findings demonstrated that the pro-angiogenic effect driven by amniotic membrane is mediated by VEGFR2 activation, which consequently triggers AKT signalling, leading to reduced nitro-oxidative stress and improved vessel formation.

Lastly, the results showed that GD-HUVEC promote an unbalanced extracellular matrix (ECM) remodelling by dermal fibroblasts, increasing ECM degradation and reducing collagen production, through the downregulation of the MAPK mediated signalling pathway, and induce a reduction in fibroblasts migration, indirectly contributing to insufficient angiogenesis. Furthermore, dermal fibroblasts isolated from type 2 diabetic patient induce decreased endothelial cell migration and vessel formation, further providing preliminary evidence of the mechanisms underlying reduced angiogenesis in diabetic skin.

Overall these results lay the foundation for a better understanding of the endothelial dysfunction mechanisms in diabetes, especially those related to decreased angiogenesis typical of chronic diabetic wounds and highlight the potential beneficial effects of innovative therapeutic strategies ranging from phenolic extracts to amniotic membrane. These findings support the identification of new potential therapeutic targets and the development of novel treatment strategies for clinical application.

2 INTRODUCTION

2.1 DIABETES MELLITUS

Diabetes mellitus is a class of metabolic disorders characterized by carbohydrate metabolism dysfunction leading to hyperglycaemia (Sack DB et al, 2023). In particular, the hyperglycaemic condition is the clinical outcome of glucose massive production and its scarce utilization, revealed by excessive glucose concentrations in venous plasma and high glycated haemoglobin (HbA1c) levels in the blood (American Diabetes Association, 2014; American Diabetes Association Professional Practice Committee, 2024).

The 11th edition of the Diabetes Atlas (2025) edited by the International Diabetes Federation (IDF) claims that, in 2024, 589 million people aged 20-79 were affected by diabetes in the world and its prevalence is predicted to increase by 45% in 2050 (IDF, 2025). In particular, the most representative area is the Western Pacific which accounts for around 37% of the worldwide diabetic population counting 215,4 million people affected in 2024. In Europe, 65,6 million people are affected by diabetes in 2024, and its prevalence will increase of 10%, reaching 72,4 million in 2050. Remarkably, the Middle East and North Africa diabetic population is forecasted to increase by 90% in 25 years, going from 84,7 million in 2024 to 162,6 million people affected in 2050 (IDF, 2025). Moreover, in 2024, type 1 diabetes affected people are over 9,5 million and, of these, around 1,9 million are children and teenager under 20 years old (IDF, 2025). Notably, a large high-risk population is estimated considering people with compromised glucose tolerance and altered fasting glucose and pregnant women with hyperglycaemia. Furthermore, there is an enormous percentage of people with diabetes, especially type 2 diabetes, undiagnosed (IDF, 2025).

Healthcare expenditure related to diabetes mellitus overcome 1 trillion USD (IDF, 2025). The elevated costs are caused by the handling of chronic diabetes complications which are usually categorized into microvascular, such as retinopathy, nephropathy and neuropathy, and macrovascular, like stroke and coronary artery disease (American Diabetes Association, 2018). For these reasons, diabetes mellitus is one of the most frequent causes of death worldwide, estimating around 3,4 million deaths in 2024 (Sacks DB et al, 2023; IDF, 2025).

Conventionally, diabetes mellitus can be classified in four different categories, according to genetic, metabolomic and pathophysiological features: type 1 diabetes, type 2 diabetes, other specific types and gestational diabetes (Sacks DB et al, 2023; American Diabetes Association, 2014; American Diabetes Association, 2011).

Hyperglycaemia, the most representative clinical symptom in diabetes, can be caused by different processes covering autoimmune destruction of beta pancreatic cells resulting in inadequate insulin production, typical of type 1 diabetes, and defects in target organs/tissues insulin response, peculiar of type 2 diabetes (American Diabetes Association, 2011).

Traditional symptoms of diabetes include polyuria (elevated urine production), polydipsia (excessive thirst), weight loss and vision problems. Uncontrolled hyperglycaemia can lead to severe and lethal pathological conditions such as ketoacidosis and nonketotic hyperosmolar syndrome (American Diabetes Association, 2011).

From 1997, the diabetes mellitus diagnosis, in non-pregnant patients, must meet the following criteria: fasting plasma glucose (FPG) ≥7.0 mmol/L (126 mg/dL), 2h post-load glucose >11.1 mmol/L (200 mg/dL) during an oral glucose tolerance test (OGTT), or symptoms of diabetes and a random plasma glucose ≥11.1 mmol/L (200 mg/dL) (Sacks DB et al, 2023; The Expert Committee on the Diagnosis and Classification of Diabetes Mellitus, 1997). Additionally, also the glycated haemoglobin (HbA1c) concentration above 48 mmol/mol (6·5%) can be useful to detect diabetes (DiMeglio LA et al, 2018).

2.1.1 TYPE 1 DIABETES

Type 1 diabetes mellitus (T1DM) is an heterogenous, and chronic metabolic disorder determined by pancreatic beta cells destruction by T-cells, leading to an insufficient production and secretion of insulin, resulting in hyperglycaemia (Primavera M et al, 2020; Akil AA et al, 2021).

In most cases the autoimmune T-cells mediated destruction of insulin secreting cells is the origin of the pathology (Type 1a), meanwhile in a small group of patients the causes can be the idiopathic destruction or failure of beta cells (Type 1b) (Maahs DM et al, 2010).

T1DM is the most common type of diabetes in children and young people, even if can be diagnosed at any age, with a high presentation rate between 5-7 years old and near adolescence (Maahs DM et al, 2010; Atkinson MA et al, 2014). Moreover, the pathology is slightly more frequent in men than in female (DiMeglio LA et al, 2018).

Although T1DM is considered a heritable polygenic disease, with 30-70% of twin concordance, 6-7% of sibling risk and 1-9% risk for children with diabetic parents, its onset is strictly connected to both genetic susceptibility and environmental factors (DiMeglio LA et al, 2018; Primavera M et al, 2020).

The main genetic predisposition refers to 2 different haplotypes of Human Leukocyte Antigen (HLA) class II, in particular to HLA DRB1*0301-DQA1*0501-DQ*B10201 (DR3) and HLA DRB1*0401-DQA1*0301- DQB1*0301 (DR4-DQ8), which represent around 50% chance of inheritance Indeed, HLA class II is generally involved in antigen presentation during the immune response, highlighting how these haplotypes are involved in T1DM development. HLA class I haplotypes are normally connected to small risk of disease development. Moreover, 60 non-HLA loci were detected in genome wide association studies (GWAS) as genetic variations associated with a higher T1DM development risk (Primavera M et al, 2020). However, the link between T1DM and haplotype variants are not yet completely understood (DiMeglio LA et al, 2018).

The most recognized environmental risk factors connected to T1DM are viral infections and diet. With regards to viral infections, two principal theories are identified: the hygiene hypothesis, claiming that infections can be a protective factor during childhood, and the triggering hypothesis, asserting that viruses can stimulate beta cells destruction. Enteroviruses are the more investigated meanwhile rubella infection role is controversial (Primavera M et al, 2020; Kondrashova A et al, 2014).

Moreover, some nutritional aspects are studied as possible T1DM-connected risk factors even if the results are still under debate. Indeed, although the Trial to Reduce Insulin-Dependent Diabetes Mellitus in the Genetically at Risk (TRIGR) claims no differences in T1DM risk between the nutrition with cow's milk and the nutrition with the hydrolysed infant formula, cow's milk proteins, especially Bovine Serum Albumin (BSA), seem to have a role in the immune suppression of beta cells according to different studies (Primavera M et al, 2020; Knip M et al, 2014; Writing Group of the TRIGR Study Group et al, 2018; Martin JM et al, 1991; Karjalainen J et al, 1992). Furthermore, vitamin D, that regulates innate and adaptive immune system cells, appears to be linked to a decreased risk of T1DM in children (Hypponen E et al, 2001). Concerning nutrition, also the gut microbiota is a remarkable risk factor. Indeed, an association between gut permeability, intestinal dysbiosis and immune system is relatively known even if not fully understood (Vaarala O et al, 2008; Del Chierico F et al, 2022).

The development of T1DM is normally categorized in 3 different stages. Nevertheless, all cases start with the exposure to environmental drivers that, together with genetic predisposition, trigger beta cell autoimmunity by T-cells and humoral response. The stage 1, also called "asymptomatic phase", is characterized by the presence of at least 2 different autoantibodies against GAD65 (GADA), zinc transporter 8 (ZnT8A), insulin (IAA), islet cell antibodies (ICA), insulinoma-associated proteins (IA-2A and IA-2β) in a normoglycemic condition. The stage 2,

called “early metabolic alteration with the asymptomatic state”, is determined by glucose metabolism variation named “dysglycaemia”. The stage 3 is defined by the beginning of diabetes clinical symptom among which polyuria, polydipsia, and weight loss (Primavera M et al, 2020; Atkinson MA et al, 2014).

Moreover, T1DM is dramatically linked to complications, among these ketoacidosis and hypoglycaemia are the most severe ones. However, microvascular complications like nephropathy, neuropathy and retinopathy, as well as macrovascular complications like stroke and atherosclerosis remain the major adverse effects connected to hyperglycaemia occurrence (DiMeglio LA et al, 2018).

The clinical course of the disease is characterized by progressive beta cells disruption and consequent requirement of exogenous insulin (Maahs DM et al, 2010). For this reason, although the maintenance of the endogenous insulin secretion is a crucial point for T1DM patients even though in low amounts, many strategies to improve insulin injection-based therapies are needed (Steffes MW et al, 2003; Pickup JC, 2012). Normally, long-acting insulin is administered to provide basal levels and rapid-acting insulin is provided before meals according to carbohydrate consumption (Atkinson MA et al, 2014). Moreover, in the last years, insulin infusion pumps utilization is increasing allowing better T1DM management (Steffes MW et al, 2003; Pickup JC, 2012). In addition, further therapeutic strategies gain the interest among which non-specific immunosuppressant, antigen-based therapies, stem cells transplantation and personalized medicine (Akil AA et al, 2021; Jeun R, 2025).

2.1.2 TYPE 2 DIABETES

Type 2 diabetes mellitus (T2DM) accounts around 90% of all diabetes cases. Thus, T2DM is the worldwide most severe metabolic disorder. Anyway, T2DM incidence and prevalence results to be strongly associated to ethnicity and geographical area.

It is characterized by deficient secretion of insulin by pancreatic beta cells, insulin resistance by target organs and insufficient insulin release by compensatory response, resulting in altered glucose homeostasis and consequently to hyperglycaemia (Stumvoll M et al, 2005; Weyer C et al, 1999; Galicia-Garcia U et al, 2020). At the beginning an increased amount of insulin is secreted by pancreatic beta cells attempting to overcome insulin insensitivity of target organs (muscle, liver and adipose tissue). This leads to enhanced glucose release by the liver resulting in the so called “pre-diabetes” condition. The progressive reduction of beta cells function and

mass leads to augmented hyperglycaemic condition and T2DM development (Fonseca VA et al, 2009; Zaccardi F et al, 2016; Kahn SE et al, 2014; Dendup T et al, 2018).

Importantly, hyperglycaemia in T2DM contributes to endothelial dysfunction and vascular complications, highlighting the relevance of studies on nitric oxide bioavailability, VEGFR2/AKT/eNOS signalling, and potential therapeutic interventions.

The onset of T2DM is the results of an intricated network of genetic, metabolic and environmental aspects (Mizukami H et al, 2022) (**Figure 1**).

T2DM genetic predisposition is considered a challenging aspect due to the association between different genetic variants and insulin production and secretion as highlighted from GWAS studies (Fuchsberger C et al, 2016).

Pancreatic beta cells are responsible for insulin production, maturation and storage into granules which fuse with the plasma membrane releasing insulin whenever the blood glucose concentration increases (Fu Z et al, 2013). In T2DM, beta cells dysfunction, resulting in insufficient insulin production over time, is caused by different factors which include: glucotoxicity, lipotoxicity, mitochondrial dysfunction, chronic inflammation, oxidative stress and endoplasmic reticulum stress (Galicia-Garcia U et al, 2020; Christensen AA et al, 2019; Młynarska E et al, 2025). Moreover, in addition to beta cells dysfunction, a crucial event leading to hyperglycaemia in T2DM is insulin resistance by target organs. In particular, skeletal muscle normally produce glycogen in response to glucose uptake due to insulin signalling. In T2DM, genetic variations in glucose transporter type 4 (GLUT4) and insulin receptor (INSR) and/or in their upstream and downstream molecules lead to defective response to insulin thus, determining hyperglycaemia (Petersen KF et al, 2002; Satoh T, 2014). Moreover, incorrect uptake glucose from the blood, weakened lipolysis and increased free fatty acids release are the common features of adipose tissue insulin resistance in T2DM patients (Czech MP et al, 2020). The liver, in physiological state, in reaction to insulin signalling stores glucose as glycogen and block glucose release. Due to insulin resistance, hepatic tissue inhibits glycogen storage, promotes glucose release, induce lipogenesis and promotes inflammation (Leclercq IA et al, 2007).

Diet, obesity and gut dysbiosis are environmental factors that have to be considered in T2DM development. Indeed, western countries diet includes excessive amounts of fat and carbohydrates leading to high postprandial levels of very-low-density lipoproteins (VLDLs) and triglycerides (TG) that, in turn, boost reactive oxygen species (ROS) and inflammatory mediators production affecting T2DM risk (Galicia-Garcia U et al, 2020; Dali-Youcef N et al, 2013). Obesity, enormous fat accumulation in the body, is a pathological condition strictly

connected to T2DM onset due to the elevated amount of free fatty acids released contributing inevitably to insulin resistance (Goyal R et al, 2023; Chandrasekaran P et al, 2024; Lin X et al, 2021).

A well-known correlation between T2DM and gut microbiome is established by different studies. Gurung M. et al (2020), claims that over 42 observation studies show the association between T2DM and some specific taxa (Gurung M et al, 2020). In particular, a negative correlation was identified for the genera of *Bifidobacterium, Bacteroides, Faecalibacterium, Akkermansia* and *Roseburia* meanwhile a positive correlation was revealed for the genera of *Ruminococcus, Fusobacterium,* and *Blautia* (Gurung M et al, 2020).

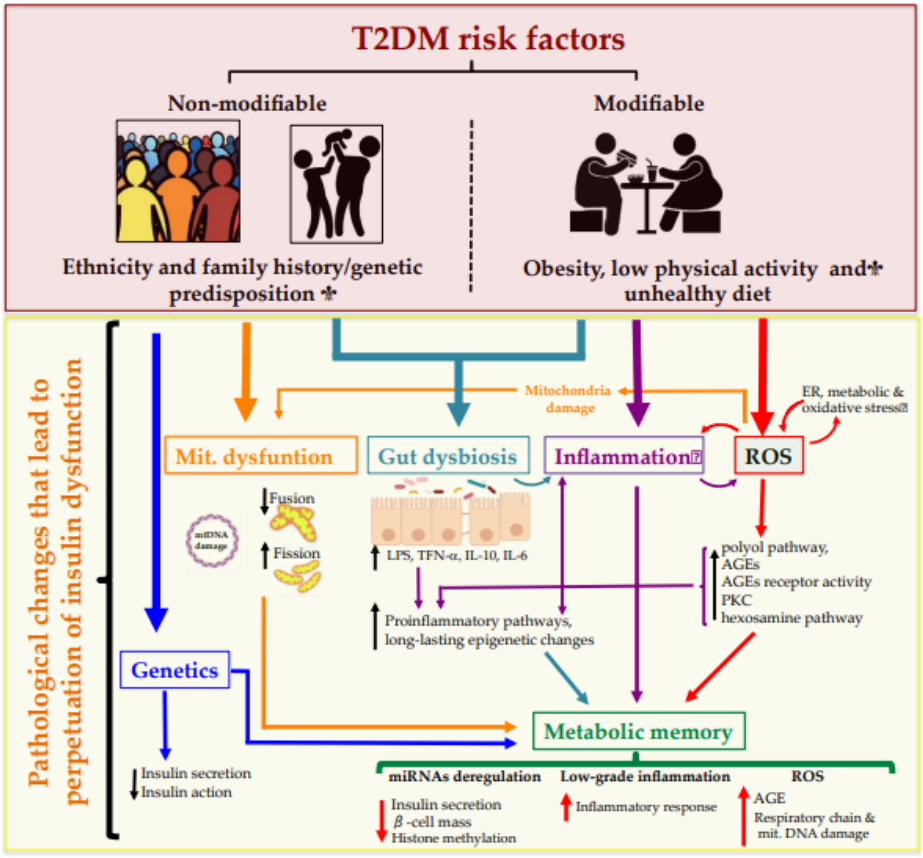


Figure 1. Genetic, metabolic and environmental factors which modulate T2DM onset (Galicia-Garcia U. et al, 2020).

Lifestyle interventions are a good non-pharmacological approach to reduce T2DM risk and symptoms even though they are not sufficient. Periodic physical exercises based on muscle resistance as well as balance diet based on low-fat and high protein consumption showed to enhance insulin sensitivity and glucose metabolism (Samsudeen H et al, 2025; Rodrigo-Carbó C et al, 2025).

On the other hand, many pharmacological approaches have been widely used to overcome the major dysfunctions associated with T2DM (Padhi S et al, 2020). Sulfonylureas are a class of drugs used to boost insulin secretion from beta pancreatic cells interacting with their sulfonylurea receptor (SUR) of ATP sensitive potassium channel (Seino S et al, 2017). Biguanides are drugs that improve endogenous insulin response and reduce liver glucose release. Among biguanides, metformin is the most used one due to its low risk of lactic acidosis development (Quillen DM et al, 1999). Insulin sensitizers are a class of drugs used to increase cells sensitivity to insulin and are also called Peroxisome Proliferator Activated Receptor agonists (PPARs). PPARs are nuclear receptors of ligand activated transcriptional factors that are able to regulate glucose metabolism, especially the isoform PPARγ (Tyagi S et al, 2011). In the last period new drugs appear to be promising in treating T2DM among which Sodium–glucose cotransporter 2 (SGLT2) inhibitors, able to reduce blood glucose concentrations, Glucagon-like peptide (GLP-1) receptor agonists, able to promote insulin secretion and beta cells regeneration, Alpha-glucosidase Inhibitors (AGIs), able to reduce post meal hyperglycaemic condition, and amylin analogues, normally deficient in T2DM (Młynarska E et al, 2025; Padhi S et al, 2020).

Anyway, unfortunately, blood glucose levels management and hyperglycaemia control, thanks to pharmaceutical and non-pharmaceutical approaches, are not sufficient to counteract diabetes complications. This concept is called “metabolic memory” (Galicia-Garcia U et al, 2020). Metabolic memory considers different processes among which: epigenetic, inflammation, oxidative stress and non-enzymatic glycation of proteins (Galicia-Garcia U et al, 2020) (**Figure 2**).

Epigenetic implies changes in gene expression profile without modification in the DNA sequence. Many epigenetic mechanisms can be involved in T2DM connected metabolic memory, among these microRNA (miRNA) seems to have a role in modulating processes involved in beta cells functioning (LaPierre MP et al, 2017).

Hyperglycaemia triggers oxidative stress inducing ROS release by mitochondria, advanced glycated end products (AGEs) formation and inflammatory response laying the foundation for the impaired and dysfunctional processes involved in diabetes complications development (Galicia-Garcia U et al, 2020; Reddy MA et al, 2015).

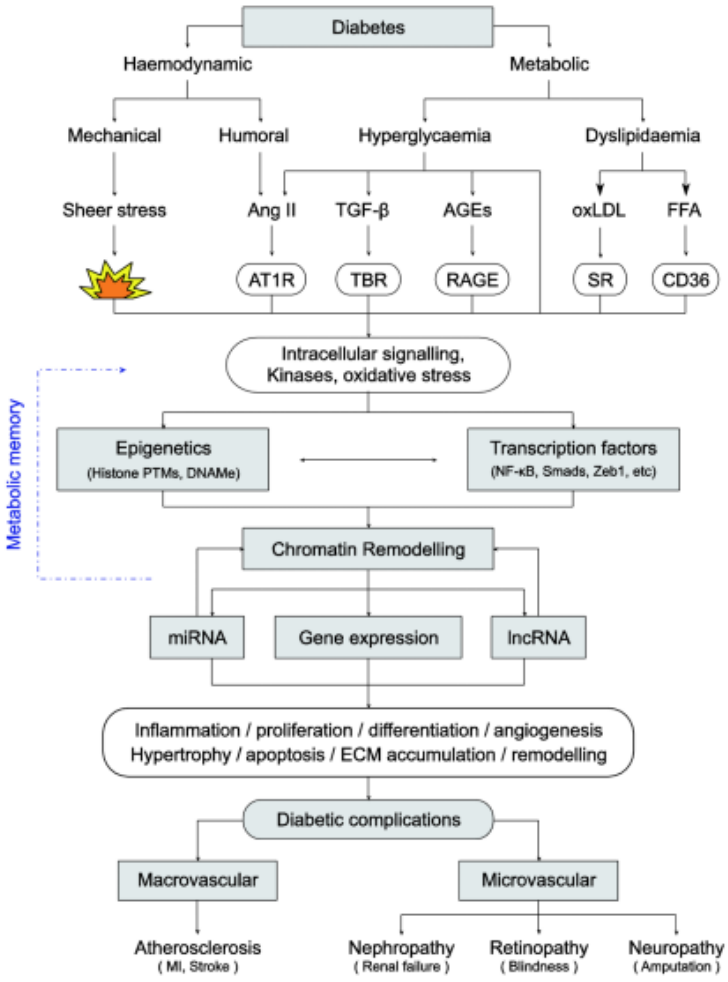


Figure 2. Diabetes complications and metabolic memory (Reddy MA et al, 2015).

2.1.3 OTHER DIABETES MELLITUS TYPES

Several types of diabetes mellitus, linked to monogenic diseases altering beta cells functioning, are categorized as “maturity-onset diabetes of the young” (MODY). MODY is inherited as autosomal dominant disease and accounts around 1-2% of all diabetes cases (Kleinberger JW et al, 2015). Moreover, they are marked by early onset of hyperglycaemia caused by defective production and secretion of insulin (American Diabetes Association Professional Practice Committee, 2024; American Diabetes Association, 2011).

The causes are attributable to alterations in at least 13 different genes in different chromosomes (American Diabetes Association Professional Practice Committee, 2024). In particular, the most common forms are linked to hepatocyte nuclear factor (HNF)-1 mutations located in chromosome 12 (called MODY3) and to glucokinase aberrations situated in chromosome 7p (named MODY2). Glucokinase is involved in the metabolic process which

trigger insulin production in response to glucose levels. Conversely, the rarest variants include aberration in several transcription factors such as HNF-4 (MODY1 form), HNF-1beta, insulin promoter factor (IPF)-1, and neurogenic differentiation 1 (NeuroD1) (American Diabetes Association Professional Practice Committee, 2024; American Diabetes Association, 2011).

Other less common diabetes mellitus types are associated with genetic variations in insulin action, specifically in insulin receptor causing symptoms ranging from mild hyperglycaemia to severe diabetes. Moreover, any diseases that lead to exocrine pancreas dysfunction, such as trauma, infections, and pancreatitis, could result in diabetes. In addition, endocrinopathies, defective production of insulin antagonist hormones, can cause hyperglycaemia which is normally resolved after hormones production restoration to normal levels (American Diabetes Association, 2011).

Furthermore, some external factors can lead to diabetes. Certain drugs can impair beta cell functioning or insulin action especially in patients with insulin resistance. Furthermore, some correlation between some viral infections such as rubella, coxsackievirus B, cytomegalovirus, adenovirus, and mumps and diabetes are known in literature (American Diabetes Association, 2011).

Genetic syndrome, including Down syndrome, Klinefelter syndrome, and Turner syndrome, as well as some autoimmune disorders, namely stiff-man syndrome, are connected to a higher risk to developing diabetes (American Diabetes Association, 2011).

A correct diagnosis is important to allow patients to have cost-effective personalized medicine. In particular, the diagnosis for monogenic diabetes is done in patients with an early onset without obesity and the following criteria: absence of typical sign of T1DM and T2DM, diagnosis of diabetes within 6 months of life, constant and mild fasting hyperglycaemia (100–150 mg/dL) and stable glycated haemoglobin (between 38 and 60 mmol/mol) (American Diabetes Association Professional Practice Committee, 2024).

2.1.4 GESTATIONAL DIABETES

Gestational diabetes mellitus (GDM) is a type of diabetes mellitus resulting in hyperglycaemia during pregnancy. According to the American Diabetes Association (ADA), GDM is considered as “diabetes first diagnosed in the second or third trimester of pregnancy that is not clearly either preexisting type 1 or type 2 diabetes” (American Diabetes Association, 2018).

The GDM prevalence worldwide is increasing over time due to influence of different factors: geographical area, higher maternal age, obesity, diet, lifestyle, physical exercise (Li Y et al, 2020; Kim SY et al, 2010).

Genetic plays an important role in GDM development as predisposition factor. Indeed, several genetic variants as well as single-nucleotide polymorphism (SNPs) are associated to increased risk of GDM development (Elliott A et al, 2024; Prasad RB et al, 2021). Particularly, some SNPs in genes coding for insulin receptor, adiponectin, and some cytokines are known to be linked with GDM. Moreover, MODY could be the cause of a small percentage of GDM cases (Mittal R et al, 2025).

GDM is normally defined by both insulin resistance mainly caused by placental hormones release and beta cells dysfunction determining impaired insulin production (Sweeting A et al, 2022; Mittal R et al, 2025).

Insulin resistance is characterized by glucose transporter type 4 (GLUT4) dysfunction. In physiological conditions, insulin interacting with its receptor induces GLUT4 translocation in the cell membrane allowing glucose uptakes, mainly in adipose tissue and in muscle. However, in insulin resistance status, target tissues do not respond to insulin due to GLUT4 impairment resulting in hyperglycaemia (De Meyts P et al, 2000; Mittal R et al, 2025). Therefore, in GDM affected women, hormones released by placenta such as human placental lactogen and human placental growth hormone can strongly contribute to insulin resistance (McIntyre HD et al, 2010).

In addition, also beta cells dysfunction and decreased insulin production are linked to GDM. In healthy pregnancies, changes are necessary to support the foetus growth and development. In particular, at the very beginning of pregnancy, insulin sensitivity increases triggering glucose storage in the adipose tissue to support higher energy consumption but, as gestation progresses, due to placental hormones release, insulin resistance is established allowing enhanced glucose production and utilization of fat (Di Cianni et al, 2003; Catalano PM et al, 1991). To overcome all these changes beta cells undergo to a hypertrophic status releasing and producing more insulin. When the compensatory process, to maintain glucose homeostasis, by beta cells do not occur GDM evolve (Plows JF et al, 2018) (**Figure 3**). In this context, pro-inflammatory cytokines release which, in turn, contributes to ER and oxidative stress leads to beta cells apoptosis and a consequent reduction in insulin production (Bo S et al, 2005; Mittal R et al, 2025).

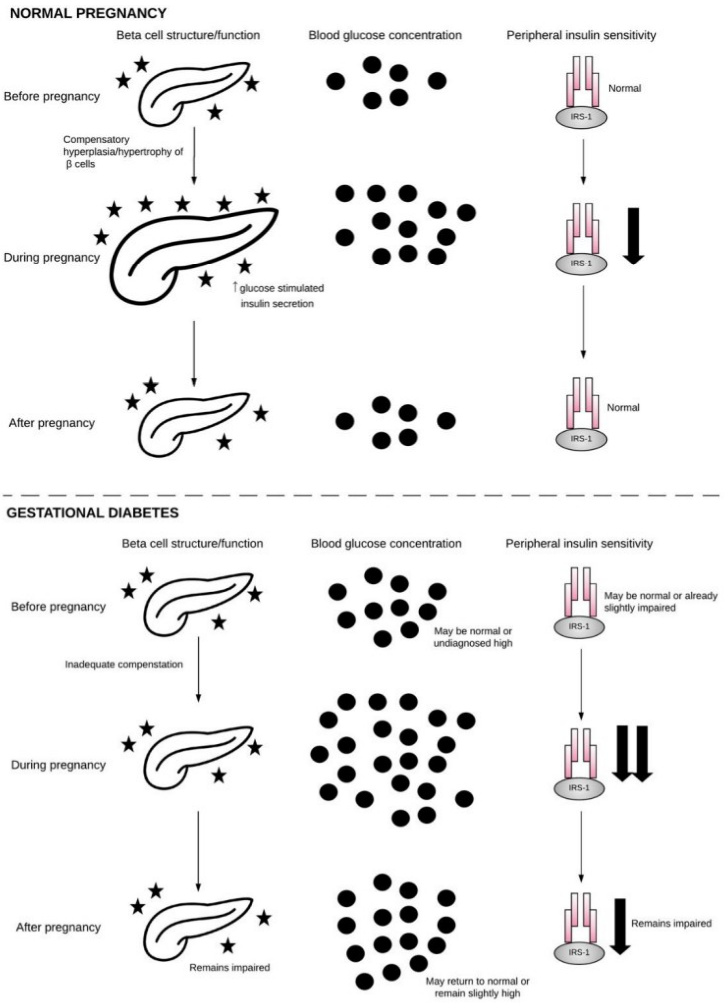


Figure 3. Beta cell structure/function, blood glucose concentration and peripheral insulin sensitivity in healthy pregnancy and in GDM pregnancy (Plows JF et al, 2018).

The above image is part of "Plows JF et al, 2018" original article. As reported in the original caption: "Pancreas image obtained from The Noun Project under the terms and conditions of the Creative Commons Attribution (CC BY) license (http://creativecommons.org/licenses/by/4.0/), by artist Arif Fajar Vulianto".

The GDM pathophysiology involves not only pancreas and placenta but also many different organs among which brain, adipose tissue, and gut microbiome.

Neural tissues, both central and peripheral, modulate glucose consumption and adiposity through the action of some regulators among which leptin and adiponectin. Leptin is an adipose tissue secreted hormone that, interacting with neurons, regulates appetite and energy expenditure. It is secreted, during pregnancy, by placenta and, in particular, in GDM women its production is enhanced leading to hyperleptinemia (Pérez-Pérez A et al, 2013). Comparable to leptin, adiponectin is secreted by adipose tissue, however its concentration decreases as fat mass increases. It positively regulates insulin secretion and signalling and reduces gluconeogenesis. Thus, GDM is correlated with low adiponectin levels (Williams MA et al, 2004).

It is well-known that gut microbiome has a correlation with diabetes and with obesity, even in pregnant women. Indeed, some studies reveal that women that were affected by GDM show low levels of the phylum *Firmicutes* and higher amounts of the family *Prevotellaceae* compared to healthy pregnancies (Fugmann M et al, 2015).

Thus, the sum of genetic factors and impaired hormonal, metabolic and cytokine-associated processes, that involve different organs, damage beta cells function and insulin secretion as well as decrease insulin sensitivity in GDM (Mittal R et al, 2025).

GDM is a pathological condition that has a great impact on both maternal and offspring health during pregnancy. Indeed, GDM is connected to many complications for the mother, among which preeclampsia, psychological stress, and caesarean delivery, and for the offspring such as macrosomia (Lee J et al, 2025; Mittal R et al, 2025).

In particular, preeclampsia, high blood pressure during pregnancy, is connected to endothelial dysfunction and inflammation contributing to long-lasting GDM consequences such as cardiovascular diseases (Khosla K et al, 2021). Moreover, sustained release of cortisol, due to psychological stress during gestation, influences negatively insulin sensitivity promoting gluconeogenesis from the liver and reduces glucose uptakes from target organs/tissues contributing to the hyperglycaemic status (Kivimäki M et al, 2023). In addition, GDM has significant implications for the foetus such as macrosomia, characterized by unusual newborn large dimensions. This condition is driven by increased placental glucose transport, favouring lipid storage and glucose uptake in the foetus determining of neonatal hypoglycaemia and metabolic problems after the delivery (Li M et al, 2020; Mittal R et al, 2025).

The prevalence of GDM changes a lot according to the geographical area due to absence of standardized criteria for diagnosis. Early screening of glucose levels is normally conducted during the 26-28 gestational weeks for pregnant women at risk. Nowadays, there are two accepted protocol-based guidelines for the diagnosis (Vounzoulaki E et al, 2020; Retnakaran R et al, 2023).

The first protocol, called “one step approach” is defined by the International Association of the Diabetes and Pregnancy Study Groups (IADPSG). This protocol requires to test blood glucose after an overnight fasting and after 1-hour and 2 hours 75g glucose administration. The diagnosis of GDM is carried out when the measurements are equal or exceed the following thresholds: 92 mg/dL (5.1 mmol/L) fasting, 180 mg/dL (10 mmol/L) at 1h, and 153 mg/dL (8.5 mmol/L) at 2h (Shepherd PR et al, 1999; Aubry EM et al, 2021).

The second protocol, called “two step approach”, is suggested by the American College of Obstetrics and Gynaecology (ACOG) and the National Institutes of Health (NIH). This protocol

requires glucose challenging test after 1h 50g glucose administration (prior to a night fasting). If the measurement is higher than 7.2 mmol/l, an Oral Glucose Tolerance Test (OGTT) is performed after 75g or 100g of glucose administration. An abnormal value of one of the following thresholds leads to GDM diagnosis: 5.3 mmol/l fasting, 10.0 mmol/l at 1 h, 8.6 mmol/l at 2 h or 7.8 mmol/l at 3 h (Shepherd PR et al, 1999; Aubry EM et al, 2021).

GDM management is primarily based on hyperglycaemia control through diet and physical exercises. Diet, based on high fibres and low sugar content, should allow correct nutritional intake for both mother and foetus and, in addition, proper foetus growth. Moreover, consistent and regular physical activities, prior consultation with a professional, during pregnancy enhances sensitivity to glucose and improve glucose management. Anyway, pharmacological treatments are required when hyperglycaemia arise for 1-2 weeks, and the foetus is above the 75th percentile. In these cases, insulin is the most common treatment due to its well-known safety, not crossing the placental barrier, and effectiveness (Mittal R et al, 2025).

Even though, after the delivery, hormonal and inflammatory impairing disappears restoring glucose levels and insulin sensitivity to a physiological status, GDM is connected to many lifelong complications for both mother and offspring. (Moyce BL et al, 2018; Vounzoulaki E et al, 2020). Indeed, many studies claim that women with a history of GDM, are linked to a moderate-high risk of T2DM progression as well as cardiovascular diseases development later in life (Vounzoulaki E et al, 2020; Wicklow B et al, 2023; Kramer CK et al, 2019). Moreover, several risk factors are associated to T2DM development in patients with GDM history, among which pre-pregnancy and after delivery body mass index (BMI), hypertension, age, and high fasting glucose levels in the blood (Chen K et al, 2024).

Additionally, exposure to maternal hyperglycaemia *in utero* leads to immediate and long-term complications and diseases in newborns (Wicklow B et al, 2023) (**Figure 4**).

Elevated blood glucose and obesity in the mother cause hyperinsulinemia, excessive foetus nutrition and growth leading also to hypoglycaemia after the delivery (Metzger BE et al, 2010). The overnutrition to whom the foetus is exposed is translated into high fat mass and risk of obesity during childhood (Wicklow B et al, 2023). Indeed, the Hyperglycaemia and Adverse Pregnancy Outcome Follow-up Study (HAPO FUS) demonstrates that newborns coming from GDM pregnancy exerts 54% of probability of infant obesity, 35% of excessive body fat, 34% of increased circumference in an age range between 10 and 14 years old. Moreover, uncontrolled glycemia in pregnancy is strongly connected to altered glucose metabolism in the offspring resulting in insulin resistance and damaged tolerance to glucose leading to higher probability to develop T2DM (Josefson JL et al, 2020; Lowe WL Jr et al, 2019).

Anyway, although the association between GDM and infant obesity/T2DM is still challenging and the pathophysiology is not yet understood, recent evidence indicate that an altered DNA methylation pattern could be the link. In addition, these epigenetic modifications can be retained also in adolescence exposed to GDM *in utero* (Ruchat SM et al, 2013; Chen P et al, 2017). These risks can be also linked to an elevated probability to develop cardiovascular diseases during life.



Figure 4. Intergenerational impact of GDM (Wicklow B et al, 2023).

2.2 DIABETES COMPLICATIONS

Diabetes is associated to a wide spectrum of complications. Among them, the most lethal ones are ketoacidosis and coma due to hypoglycaemic events.

The hyperglycaemic condition in diabetes leads to blood vessels damage resulting in microvascular complications, occurring in small blood vessels, and macrovascular complications, occurring in arteries (Forbes JM et al, 2013).

In particular microvascular complications include mainly nephropathy, retinopathy and neuropathy.

Nephropathy or diabetes kidney disease (DKD) is a pathological condition that occurs in 40% of diabetic patients and it is the major risk of mortality (Alicic RZ et al, 2017; Reidy K et al, 2014). The most representative clinical symptoms include proteinuria (excessive protein presence in urine) and a consequent impairment in glomerular filtration rate. Moreover, DKD greatly contributes to macrovascular complications onset such as stroke (Forbes JM et al, 2013).

Retinopathy is marked by different lesions in the retina causing a high probability of blindness in adult patients. It can be divided into non-proliferative and proliferative stages. At the beginning of the disease hyperglycaemia induces intra-mural pericyte death and thickening of the basement membrane altering retinal blood vessels modifying vascular permeability and the integrity of the blood-retinal barrier. Over time, ischemia can occur stimulating pro-angiogenic molecules release and promoting formation of vessels and macula oedema resulting in the proliferative stage and visual loss (Frank RN et al, 2004).

Neuropathy is a disease which involves both the autonomic and somatic peripheral nervous system and engage around 50% of total diabetic patients (Abbott CA et al, 2011). There are different types of neuropathies but the most common is the distal symmetric polyneuropathy (Albers JK et al, 2014). The clinical symptoms refer to numbness, pain, impaired sensitivity to thermal stimuli and vibration and tingling (Feldman EL et al, 2017). Because of these features it is one of the leading causes of diabetic foot ulcers formation and lower limbs amputation.

Macrovascular complications include cardiovascular disease (CVD) resulting in stroke, coronary and periphery artery disease, myocardial infarction and cerebrovascular diseases (Frobes JM et al, 2013).

Stroke is a challenging condition which exert severe acute and long-term symptoms. The acute ones refer to confusion, numbness, vertigo, problems in speaking and coordination, meanwhile long-term symptoms are anxiety and depression (Gargano JW et al, 2011; Knapp P et al, 2020). Stroke can be divided, according to the leading causes, into ischemic (insufficient perfusion of a brain region called penumbra), and haemorrhagic (blood vessels damage in the brain with consequent bleeding) (Campbell BCV et al, 2019; Chen S et al, 2014).

Coronary artery disease (CAD) is characterized by atherosclerotic plaque rupture and consequent blockage of coronary vessels bloodstream leading to myocardial infarction (Fedele F et al, 2013).

Peripheral artery disease (PAD) is a pathological condition that involve decrease in bloodstream due to atherosclerosis in the lower limb of diabetic patients. PAD is linked to pain,

delayed wound closure and development of skin chronic ulcers (McDermott MM et al, 2010; Saely CH et al, 2013).

2.3 DIABETIC FOOT ULCER

Diabetic foot ulcer (DFU) is a debilitating diabetes complication which manifest as chronic wound in the lower limb of patients. DFU is developed in 15% of diabetic patients, accounting approximately 18.6 million of people worldwide every year. Thus, it is one of the most common diabetes complications. Moreover, around 20% required hospitalization and roughly the same percentage of DFU undergo to amputation, due to incorrect healing, increasing the impact of patients' life quality and the related healthcare economics (Zhang Y et al, 2020; Armstrong DG et al, 2017; Armstrong DG et al, 2023). Indeed, only in the United Stated the cost associated to DFU treatment and management fluctuates from 9 to 13 billion annually (Rice JB et al, 2014).

The risk factors associated to DFU development are multiple and interconnected, the ones of greater interest are PAD, peripheral neuropathy, wound infections and cell dysfunction (Deng H et al, 2023) (**Figure 5**).

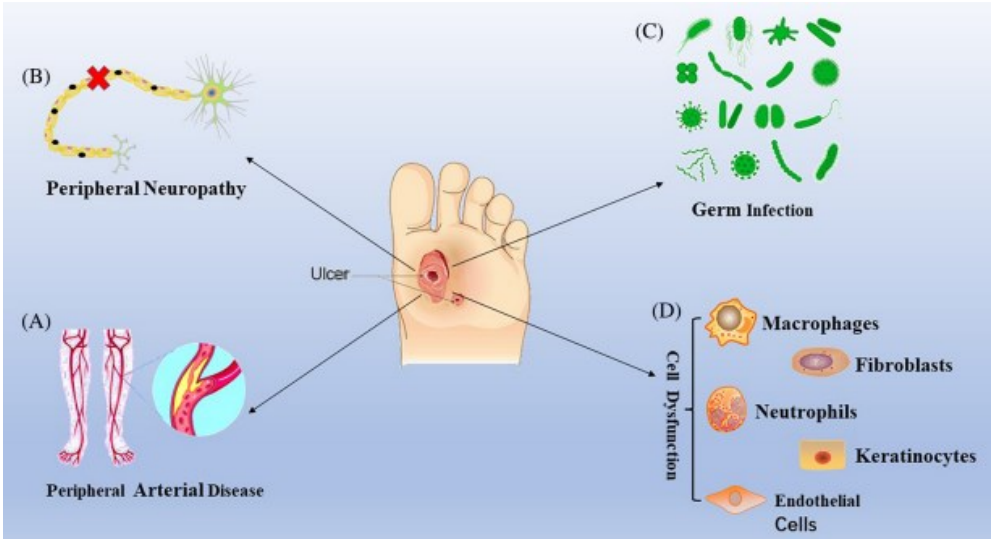


Figure 5. The major risks linked to DFU formation (Deng H et al, 2023).

Of note, many minor aspects, related to DFU development, have to be considered, such as gender, age, duration of the disease, hypertension and dyslipidaemia, obesity and physical activity (Rossboth S et al, 2020).

PAD, mentioned above as macrovascular diabetes complication, includes the diseases associated to non-cardiac and non-intracranial arteries. In particular, the most representative clinical symptom of PAD is the upper limbs and/or lower limbs peripheral arteries total or partial occlusion, due to atherosclerosis process, leading to lower blood supply resulting in reduced amount of nutrients and oxygen in the tissue (Morley RL et al, 2018).

Moreover, roughly in the half of diabetic patients, PAD is a fundamental aspect for DFU development. In addition, one third of these patients undergo to pain and cramping, in a phenomenon called claudication, that contributes to dysfunction and ischemia, strongly promoting ulcers formation and amputations (Marso SP et al, 2006; Wang N et al, 2019).

Peripheral neuropathy, which manifest as damaged of peripheral sensory or motor/vegetative nervous systems, is one of the key aspects of DFU. Indeed, hyperglycaemia which occur in diabetic patients, resulting in excessive production of inflammatory cytokines, AGEs and ROS, leads to nerve cells' structure and function damages. The result is the loss of pain perception. For this reason, ulcers can be unnoticed for long time increasing the amputation risk (Galiero R et al, 2023). Moreover, neuropathies lead also to sweat glands dysfunction causing skin drying and contributing to wounds formation (Vinik AI et al, 2003).

The third risk factor associated to DFU formation is wound infection. Indeed, PAD and neuropathies, described above, strongly contribute to bacterial and fungal infections. Bacterial infections can be caused by a single bacterium, *Staphylococcus aureus,* or by the combination of different bacteria including coagulase negative staphylococci, enterococci, gram-negative bacteria, and anaerobes. Additionally, also fungal infections can affected chronic ulceration, the most frequent are *Candida albicans, Candida subsmooth,* and *C. tropicalis.* Of note, ulcers infections as a result of microorganisms' action are strictly linked to immune cells dysfunction and strong inflammation (Yates C et al, 2009; Chellan G et al, 2010; Deng H et al, 2023).

2.3.1 WOUND HEALING MECHANISMS

Wound healing is a intricated process which involves a countless amount of mechanisms and cell types that simultaneously and synergistically results in skin repair (Wilkinson HN et al, 2020).

In physiological conditions, the wound healing is composed of four different phases: haemostasis, inflammation, proliferation and remodelling (**Figure 6**).

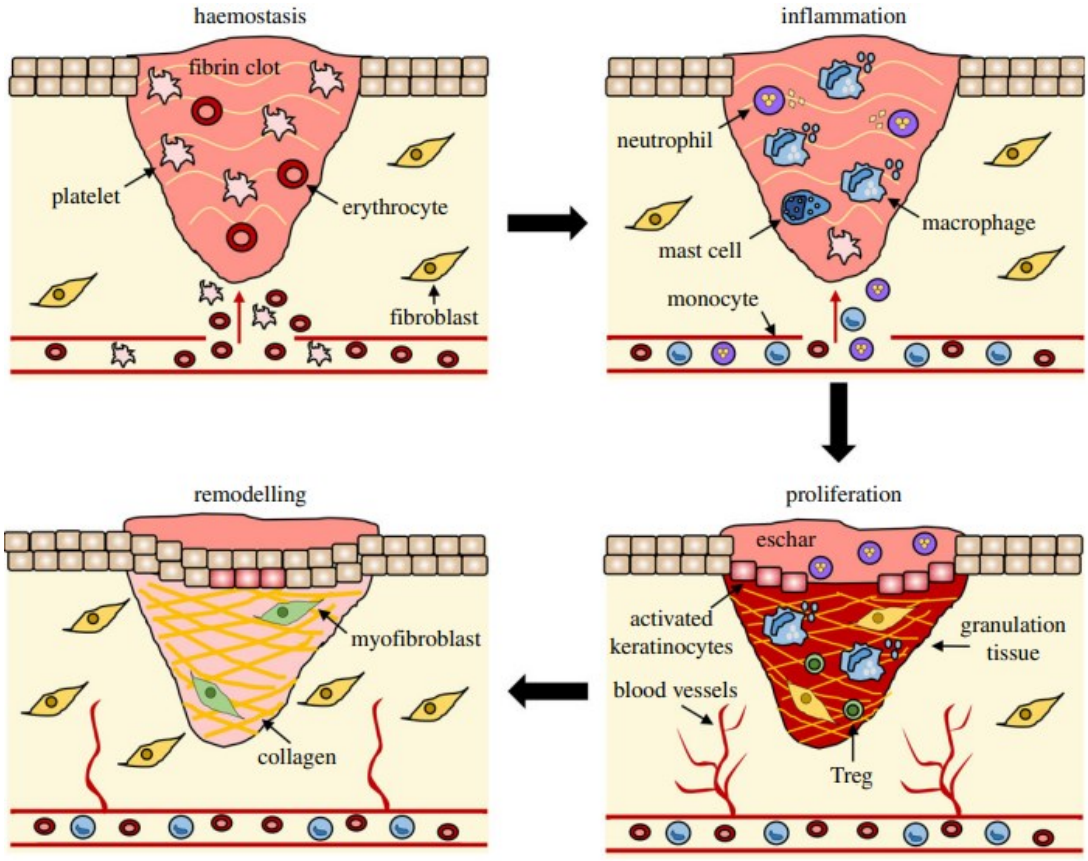


Figure 6. Wound healing phases in physiological conditions (Wilkinson HN et al, 2020).

Following skin damage, injured blood vessels contracts and platelets, the key cells involved in coagulation, are activated. Platelets receptors interact with the proteins of the extracellular matrix (ECM) and consequently, thrombin determines platelets activation inducing the formation of an insoluble clot of fibrin, fibronectin, vitronectin and thrombospondin. The clot is important also to avoid bacterial infections, recruit immune cells and release cytokines and factors which modulate the first steps of healing. Once a clot is formed the coagulation process is stopped to avoid thrombosis. Simultaneously, blood vessels start to be repair by smooth muscle cells and start to proliferate (Golebiewska EM et al, 2015; Wilkinson HN et al, 2020).

The second step is inflammation to trigger a response to pathogen invasion of the wound. Resident immunes cells are activated by damage-associated molecular patterns (DAMPs) and pathogen-associated molecular patterns (PAMPs), respectively released by cells in necrosis and microorganisms' particles. Consequently, inflammatory cytokines, such as interleukin 1 (IL-1) and tumour necrosis factor-alpha (TNF-α), are released to recruit leukocytes from the blood stream to the injured tissue. This process occurs due to vasodilatation and vascular inflammation, which activating the transcription factor Nuclear Factor kappa-light-chain-

enhancer of activated B cells (NF-kB) triggers adhesion molecules expression and exposure allowing immune cells, mainly macrophages and neutrophils, adhesion to the blood vessels and diapedesis. Neutrophils and pro-inflammatory macrophages phagocyte necrotic cells and pathogens. After that, neutrophils are cleared from the injured site with different mechanisms including also apoptosis and macrophages efferocytosis. In this way, in the late stage of inflammation, macrophages are the most prevalent immune cell type in the wound.

After complete clearance of the injured area, macrophages phenotype switch to pro-inflammatory to anti-inflammatory, due to variations in the cytokines present in the microenvironment. Anti- inflammatory macrophages release cytokines, such as IL-4, IL-10 and IL-13, which turn off inflammation and trigger the following step stimulating the repairing process (Martin P et al, 2005; Vestweber D et al, 2015; Mahdavian Delavary B et al, 2011).

Keratinocytes, fibroblasts, endothelial cells and macrophages activation is the hallmark of the third step of healing, the proliferative phase (Wilkinson HN et al, 2020).

In particular, keratinocytes start to migrate laterally to create a new epithelial layer in a mechanism defined re-epithelialization. Moreover, keratinocytes to increase their migration abilities secrete metalloproteases (MMP) and, in addition, they produce new ECM to rebuild the new basement membrane (Rousselle P et al, 2019).

Fibroblasts, both resident and derived from mesenchymal cells, replace the temporary matrix rich in fibrin to a new granulation tissue. To do this, fibroblasts respond to thousands of molecules, i.e. transforming growth factor beta (TGF-b) and platelet-derived growth factor (PDGF), coming from the cells resident in the same microenvironment, such as platelets, endothelial cells and macrophages. Indeed, fibroblasts, producing MMP, degrade the temporary matrix and, producing different types of collagens, fibronectin and proteoglycans, form the new granulation tissue that is useful for cell migration, angiogenesis and mature ECM deposition (Li J et al, 2007; Xue M et al, 2015; Wilkinson HN et al, 2020).

Endothelial cells are mainly involved in new blood vessels formation during the proliferative phase, promoting angiogenesis to support new tissue formation in terms of nutrients and oxygen. The process of angiogenesis is activated by hypoxia that trigger hypoxia-inducible factors (HIF) expression and vascular endothelial growth factor (VEGF) release. In response to these signalling pathways, endothelial cells proliferate, migrate and reduce apoptosis contributing to wound healing (Wilkinson HN et al, 2020).

Macrophages, in addition, play a part in angiogenesis, producing MMP and chemotactic molecules, like VEGF and TGF-b, to degrade the fibrin rich provisional matrix and to promote endothelial cells migration, respectively (Du Cheyne C et al, 2020).

Furthermore, during the proliferative step, also nerve regeneration occurs (Wilkinson HN et al, 2020).

The remodelling phase, the last step of wound healing, can perpetuate for months and even years and is characterized by ECM deposition, substituting progressively collagen III with collagen I, and useless vasculature regression. If cells, after tissue remodelling, not undergo to apoptosis hypertrophic scar occurs (Gurtner GC et al, 2008; Rodrigues M et al, 2019).

Wounds that for more than 12 weeks do not heal are considered chronic wounds. This condition is attributable to different diseases among which diabetes mellitus.

Indeed, delayed wound healing in diabetic patients is caused by several cellular dysregulations leading to altered cytokines, growth factors and molecules production and release impairing the finely coordinated process of healing (Patel S et al, 2019) (**Figure 7**).

Firstly, diabetic wounds show a long-lasting inflammation which contribute to abolish mature granulation tissue formation and to reduce skin tensile strength. Indeed, hyperglycaemia leads to altered macrophage polarization toward the pro-inflammatory phenotype resulting in a greater and persistent production of pro-inflammatory cytokines such as tumour necrosis factor alpha (TNF-a), IL-1β and IL-6. This aspect strongly contributes to leukocytes accumulation, thus, contributing to delayed healing. In addition, together with inflammation also elevated oxidative stress promote chronic wounds formation (Patel S et al, 2019).

ECM remodelling is an important process to achieve a correct wound healing, and it is defined by a fine balance between ECM deposition and ECM degradation by MMP. It is mediated by different factors among which the most representative ones are PDGF, VEGF and TGFβ.

PDGF, produced by macrophages, has many functions comprising collagen, proteoglycans and glycosaminoglycans production, helping the granulation tissue and provisional ECM formation, proliferation and migration of fibroblasts as well as angiogenesis improvement. Anyway, in diabetic wounds PDGF levels are strongly decreased (Li H et al, 2008; Jian K et al, 2022).

VEGF is key growth factor modulating and promoting angiogenesis in the skin interacting with its receptor 2 (VEGFR2). VEGF helps to restore the blood flow in the newly formed tissue and it is involved in granulation tissue formation, further supporting the healing process. However, diabetic wounds are defined by reduced levels of VEGF since the macrophages are blocked into the pro-inflammatory phenotype. Indeed, anti-inflammatory macrophages are one of the main sources of VEGF. Thus the interaction between VEGF and its receptor VEGFR2 is

reduced contributing to decreased angiogenesis and consequently, impaired healing (Zhou K et al, 2015; Patel S et al, 2019).

TGFβ is involved in the recruitment of leucocytes, keratinocytes and more importantly fibroblasts. The correct levels of TGFβ finely promote angiogenesis, ECM formation and inhibit ECM degradation. In particular, TGFβ1, activating the transcription factors Suppressor of Mothers against Decapentaplegic (SMAD)-2 and SMAD-3, regulates collagen production through the so-called canonical pathway. Anyway, TGFβ triggers many non-canonical pathways through several factors among which Mitogen-activated protein kinase (MAPK) (Zhang YE, 2017).

Anyway, diabetic wounds show reduced amounts of TGFβ that, coupled with an excessive production of MMP, cause decreased collagen production and increased matrix degradation further contributing to delayed wound healing in diabetic patients. Particularly, hyperglycaemia induces elevated pro-inflammatory cytokines and AGEs production resulting in increased MMP and decreased tissue inhibitor of metalloproteinase (TIMP) expression, supporting chronic ulcers formation (Patel S et al, 2019).

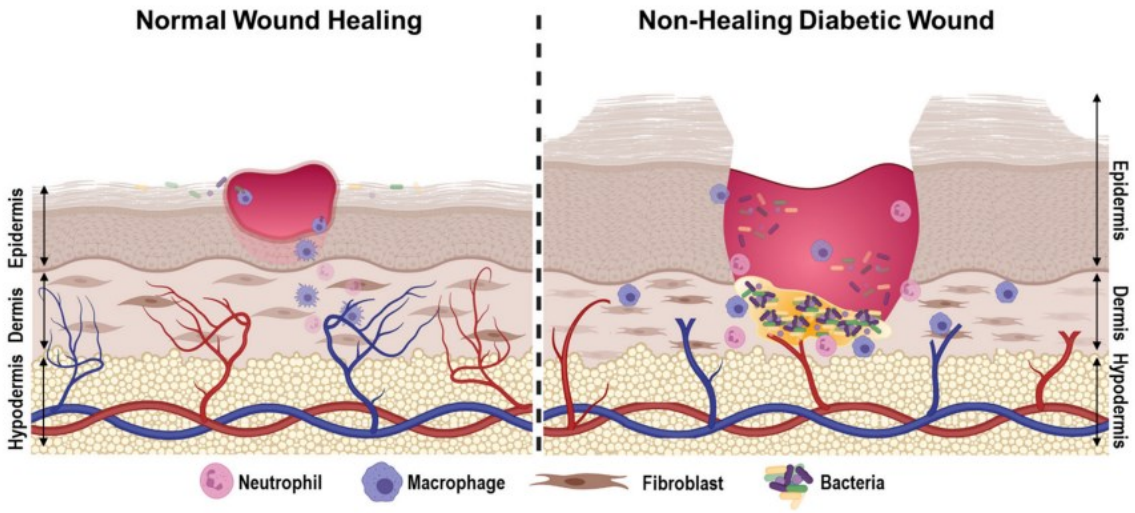


Figure 7. Altered pathophysiology of chronic wounds in diabetic condition (Burgess JL et al, 2021).

2.3.2 WOUND ANGIOGENESIS

Before injury, vessels are in a quiescent state, to support the correct amount of nutrients and oxygen to the tissue, guaranteed by a balance between pro-angiogenic factors, such as VEGF

and fibroblast growth factor (FGF), and anti-angiogenic molecules, including angiopoietin 1 (Ang-1) and pigment epithelium derived factor (PEDF) (Demidova-Rice TN et al, 2012; Tonnesen MG et al, 2000).

When a wound occurs, a hypoxic status is established disrupting the equilibrium. Hypoxia triggers leukocytes (neutrophils and macrophages) recruitment and, through the activation of the transcription factor hypoxia-inducible factor-1 (HIF-1), upregulates pro-angiogenic factors release (Tandara AA et al, 2004; Koh TJ et al, 2011).

The most important molecule is VEGFa, the main VEGF isoform in the wound site. It upregulates vascular growth by interacting with its receptor VEGFR2. VEGFR2 is the key tyrosine kinase receptor that, binding to its ligand, trigger its homo or heterodimerization and subsequent autophosphorylation of different tyrosine residues activating multiple downstream pathways that control endothelial cells proliferation, migration, survival and permeability (Shah FH et al, 2025) (**Figure 8**).

Phosphoinositide 3-kinase (PI3K) is a crucial molecule in angiogenesis. PI3K is activated by VEGFa through different molecular signaling comprising TSAd/Src/Axl axis. Indeed, VEGFR2, activated by VEGFa binding, autophosphorylates on Tyr 951 and, in turn, activates Src via the SH2 domain-containing T cell-specific adaptor (TSAd). Src attracts the tyrosine kinase receptor Axl to further induce the association with PI3K and the consequent activation of Protein Kinase B (PKB), also called AKT.

AKT modulates different pathways, mainly contributing to endothelial cells survival, regulating apoptosis, and to endothelial function, activating endothelial Nitrix Oxide Synthase (eNOS) and thus, releasing Nitric Oxide (NO), a crucial molecule for vasodilatation (Claesson-Welsh L et al, 2013; Wang X et al, 2020; Ruan GX et al, 2012; Shah FH et al, 2025; Clegg LW et al, 2015; Gazzini S et al, 2024).

Indeed, Ahmad S et al, in 2006, demonstrated that a loss of Tyr951 residue results in a reduction of around 50% of NO production, highlighting the role of this phosphorylation site in NO synthesis. At the same time, the partial reduction identified in their study underlies that VEGFR2 mediated NO release is mediated by many and different downstream pathways (Ahmad S et al, 2006). Indeed, phosphorylation on Tyr1175 directly activates PI3K/AKT/eNOS signalling pathway (Claesson-Welsh L et al, 2013).

Moreover, Src, activated by VEGFR2 on Tyr951, modulates and increases vascular permeability phosphorylating vascular endothelial cadherin (VE-cadherin) in vessels adherend junctions (Claesson-Welsh L et al, 2013).

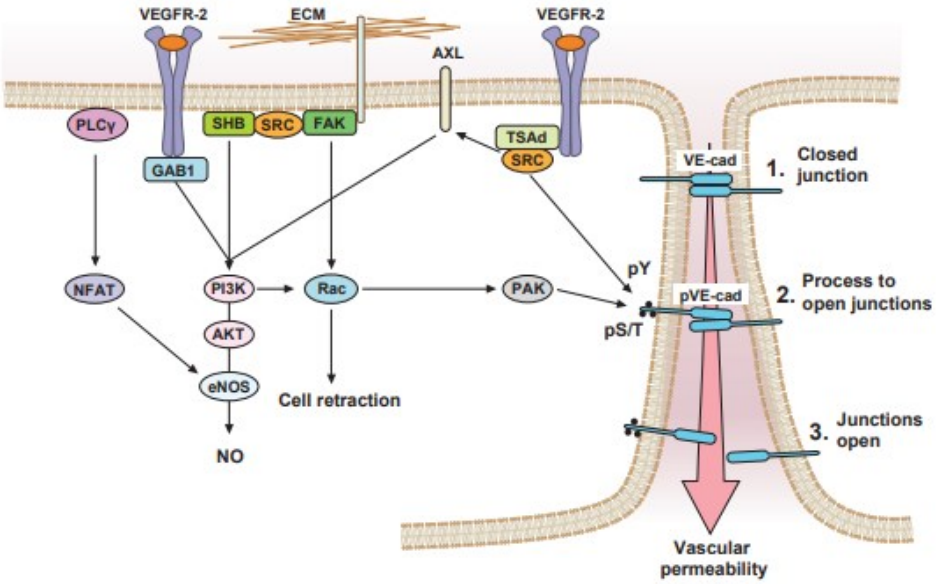


Figure 8. VEGFR2 mediated signaling pathway involved in vascular permeability and NO production (Claesson-Welsh L et al, 2013).

The angiogenesis in wound healing starts with strong disorganized vessels formation with loops and blind-ended sprouting. Thus, the proliferative phase of wound healing is characterized by intense and chaotic angiogenesis. After that, pro-angiogenic factors are replaced by anti-angiogenic ones leading to vessels regression due to apoptosis, selecting competent vasculature that undergo to a stabilization process by pericytes to become pre-injured vasculature (Dimmeler S et al, 2000; Chen RR et al, 2007; Fukumura D et al, 2008). In this context, Ang-1 and Ang-2 together with Tie2 receptor modulates vascular remodelling. Particularly, Ang1 is involved in vessels stabilization, while Ang-2 exerts destabilize vessels (Staton CA et al, 2010).

The end of vessels remodelling process restore the correct vascular function and permeability (Carmeliet P et al, 2005).

During wound healing, angiogenesis interacts with plenty of different processes that occur during the proliferative phase. Indeed, ECM production and degradation by fibroblasts as well as fibroblasts migration and proliferation to achieve wound closure take place in the same timeframe of angiogenesis highlighting how these processes simultaneously support one another (Okonkwo UA et al, 2017).

Indeed, endothelial cells interaction with ECM, due to integrins, is fundamental for migration, proliferation and assembly in blood vessels. Anyway, also fibroblasts presence is

necessary for angiogenesis due to the greater amount of signalling molecules released among which VEGF, FGF, Ang-1, Ang-2 and IL-8. Moreover, ECM proteins like fibronectin, perlecan and trombospondin-1 and -2 are important modulator of vessel formation (Stunova A et al, 2018; Berthod F et al, 2006).

Anyway, even endothelial cells exert influence on fibroblasts modulating alpha-smooth muscle actin (αSMA) expression, which is involved in collagen production and contraction as well as in fibroblasts differentiation into myofibroblasts through the action of an endothelial cells derived protein, endothelin-1 (Villaschi S et al, 1994; Stunova A et al, 2018) (**Figure 9**).

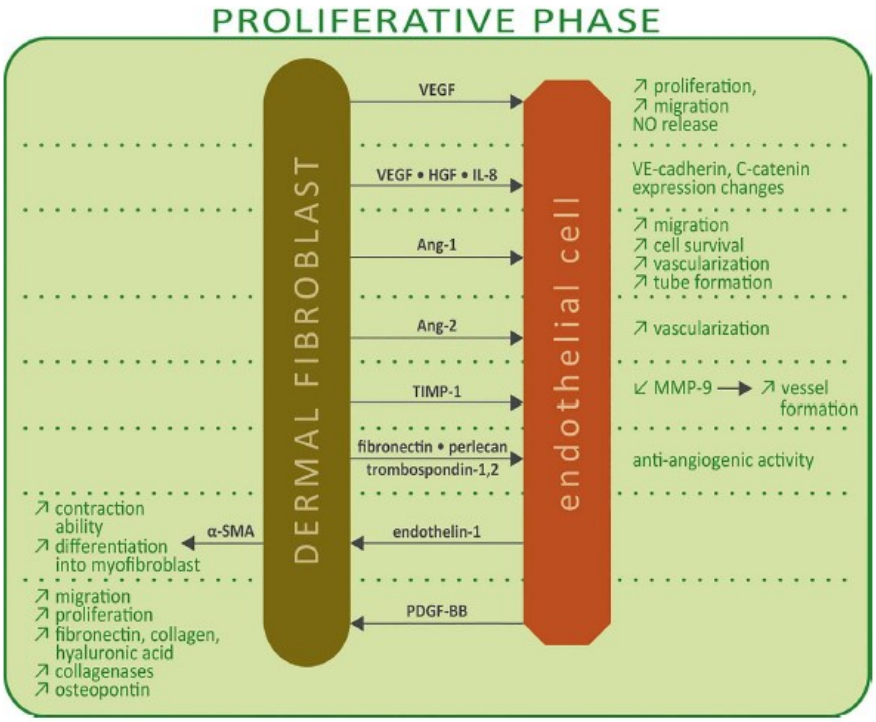


Figure 9. Molecular crosstalk between dermal fibroblasts and endothelial cells during the proliferative phase of wound healing in physiological conditions (Stunova A et al, 2018).

Diabetic wounds show extremely reduced angiogenesis powerfully reinforcing delayed healing mechanisms. The reasons linked to this deficit can be multiple and intricated (Okonkwo UA et al, 2017).

As mentioned above, macrophages in diabetic patients fail to switch from pro-inflammatory phenotype to anti-inflammatory one. This deficit not only determine persistent inflammation but also contributes to reduced VEGFa levels in diabetic wounds, since macrophages are the main source of VEGF.

Moreover, studies reveal elevated anti-angiogenic factors levels, dysregulated ratio of Ang-1 to Ang-2 and decreased expression of platelet derived growth factor (PDGF) evidencing an impaired ability to produce mature vasculature in diabetic wound tissues.

In addition, many microRNAs (miRNAs) levels, small non-coding RNA involved in gene silencing and pro-translational modifications, are altered in diabetic ulcers.

Moreover, diabetes induces an important depletion of bone marrow derived endothelial progenitor cells limiting basal vascularity and negatively impacting wound angiogenesis (Mirza R et al, 2011; Qi W et al, 2015; Kämpfer H et al, 2001; Xu J et al, 2014; Drela E et al, 2012).

Thus, diabetes affects both early and late steps of the angiogenic process impairing both vascular formation and maturation.

2.4 ENDOTHELIAL DYSFUNCTION

The endothelium, the continuous cell monolayer inside the vascular system, is involved in many functions that include not only angiogenesis but also the preservation of vascular tone and homeostasis. Thus, in pathological conditions, such as diabetes, endothelium undergoes to several dysfunctions, including enhanced inflammation and oxidative stress as well as decreased activity of vasodilation factors, leading to the completely loss of homeostasis (**Figure 10**).

In addition, endothelial dysfunction is a crucial hallmark for atherosclerosis development and thus, it is strictly connected to vascular damage and diabetes micro and macro vascular complications, among which also diabetic foot ulcer (Yang DR et al, 2024).

Vascular inflammation is a critical aspect in diabetes associated endothelial dysfunction. Indeed, endothelial cells, in response to injuries and hyperglycaemia, get activated producing cytokines, chemokines, monocyte chemoattractant protein-1 (MCP-1), intercellular adhesion molecule-1 (ICAM-1), vascular adhesion molecule-1 (VCAM-1), P-selectin, E-selectin and many other pro-inflammatory mediators. All these molecules attract monocytes from the blood stream to the inflamed tissue underneath through the vascular wall (Chistiakov DA et al, 2018; Xu S et al, 2021).

In this context, the transcription factor NF-kB is a critical controller of vascular inflammation. Inflammation induces the phosphorylation of IκB, the inhibitory subunit of NF-kB, that gets inactivated. Thus, this event promotes the translocation of two NF-kB regulatory subunits, p50 and p65, inside the nucleus where they activate gene expression of inflammatory

mediators (Magenta A et al, 2014) among which VCAM-1 and ICAM-1 that, positioning on cell membrane, attract monocytes modulating their diapedesis.

In addition, also insulin resistance impairs mechanisms mediate by PI3K/AKT and MAPK/extracellular signal-regulated kinases (ERK) abolishing vascular homeostasis (Janus A det al, 2016).

Moreover, the elevated AGEs production promotes a higher interaction with its receptor (RAGE) activating the expression of VCAM-1, MMP-9, IL-1β, and TNFα strongly contributing to atherosclerotic plaque formation (Bongarzone S et al, 2019).

Oxidative stress is defined as a condition in which intracellular pro-oxidant and antioxidant systems undergo to a severe unbalance. In diabetes, high amounts of ROS in endothelial cells are produced by different processes such as xanthine oxidase, nicotinamide adenine dinucleotide phosphate (NAPDH) oxidases, uncoupled eNOS and mitochondrial dysfunction (Schulz E et al, 2014; Yang DR et al, 2024).

Elevated ROS levels oxidize nucleic acids, proteins and lipids contributing to vascular dysfunction.

In particular, NAPDH oxidase (NOX) is a multi-subunit complex that produces superoxide anion (O_2^-) due to a one-electron reduction of oxygen by NAPDH. In diabetes, both NOX and O_2^- levels are enhanced (Gao L et al, 2009).

Furthermore, ROS and eNOS have a strong connection due to the mechanism of eNOS uncoupling that results in O_2^- production instead of NO. Normally, eNOS catalyse NO production using L-arginine as substrate and many co-factors among which BH4 and NADH. Afterwards, NO diffuses into the nearby compartment toward vascular smooth muscle cells activating cyclic guanosine monophosphate (cGMP) dependent vasodilation.

The process of uncoupling is defined by the switch of eNOS from generating NO to producing O_2^- aggravating oxidative stress. In addition, high levels of O_2^- reacts with NO producing peroxynitrite ($ONOO^-$) which magnify oxidative stress, consume NO reducing also its bioavailability to promote vasodilation, and greatly contribute to endothelial dysfunction (Förstermann U et al, 2006; Karbach S et al, 2014; Daiber A et al, 2020; Magenta A et al, 2014; Xu S et al, 2021).

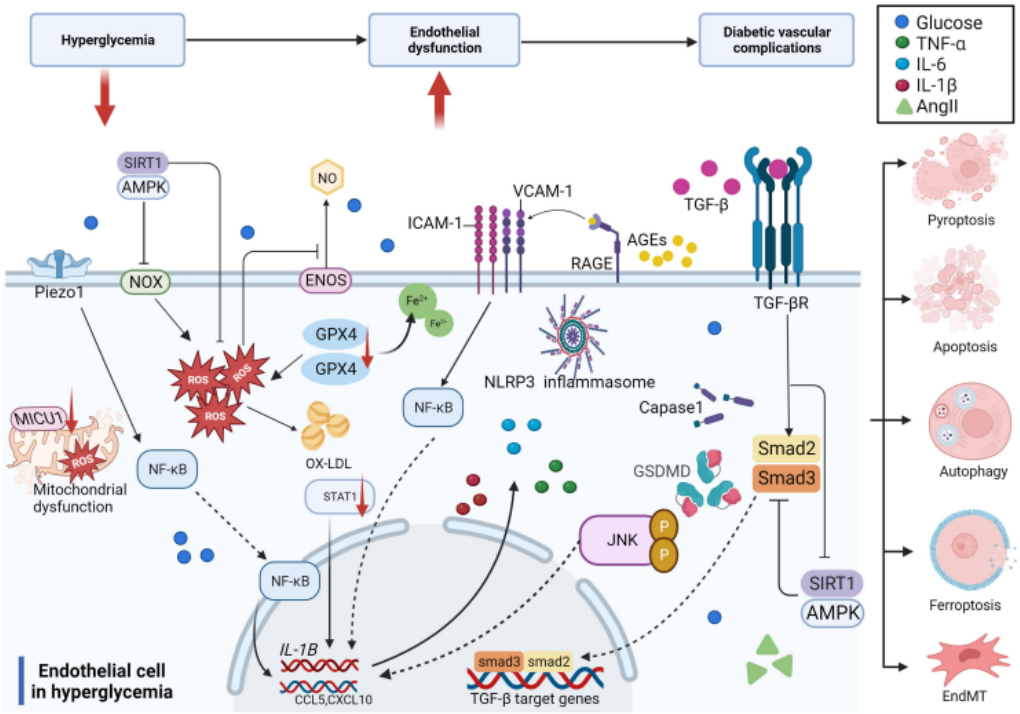


Figure 10. Molecular mechanisms that characterize endothelial dysfunction in diabetes (Yang DR et al, 2024).

2.5 HUMAN UMBILICAL VEIN ENDOTHELIAL CELLS OF GESTATIONAL DIABETIC MOTHERS

GDM, as fully discussed above, is a high incidence pathological condition that is severely correlated to lifelong complications in both the mother and the offspring. Indeed, an elevated predisposition to T2DM, obesity and atherosclerotic cardiovascular diseases are critical hallmark of GDM. This predisposition is linked to the so called "metabolic or glycaemic memory" according to which cells undergo to changes when they are exposed to hyperglycaemia that persist even after the restoration of physiological conditions (Wicklow B et al, 2023; Josefson JL et al, 2020; Lowe WL Jr et al, 2019; Dong H et al, 2024).

Human umbilical vein endothelial cells isolated from the umbilical cord vein of gestational diabetes affected mothers (GD-HUVEC), due to chronic *in vivo* exposure to high glucose levels, show pro-inflammatory and pro-oxidative phenotype even when they are cultured in normoglycemic conditions *in vitro* (Di Fulvio P et al, 2014; Di Tomo P et al, 2021).

Indeed, it was previously demonstrated that GD-HUVEC, compared to HUVEC isolated from control women (C-HUVEC), show enhanced O_2^- and ROS levels as well as decreased antioxidant enzymatic defense showcasing their pro-oxidative phenotype.

In addition, GD-HUVEC show an inflammatory disequilibrium, linked to insulin resistance, as demonstrated by elevated VCAM-1 expression as well as higher adhesion of monocytes to the endothelial monolayer, compared to control cells, highlighting their pro-inflammatory phenotype (Di Fulvio P et al, 2014; Di Tomo P et al, 2021; Ucci M et al, 2019). Moreover, Pipino C et al (2022) demonstrated that GD-HUVEC showed reduced angiogenesis compared to control cells (Pipino C et al, 2022).

Epigenetic plays a crucial role in the endothelial dysfunction representing an important part of the "glycaemic memory" phenomenon. Indeed, it is known that hyperglycaemia leads to epigenetic modifications, such as DNA methylation, post-translational modifications of histones, and miRNA. *In utero* exposure to elevated glucose levels due to GDM development during pregnancy, could contribute to the T2DM and cardiovascular diseases development higher risk in the offspring.

In particular, Mixed Lineage Leukaemia 1 (MLL1), one of the histone 3 lysine 4 methyltransferase, drives the transcriptional activation of multiple genes involved in inflammatory and oxidative stress. For the first time, Di Pietrantonio N et al, in 2024 demonstrated that MLL1 leads H3K4me3, boosting gene expression of inflammatory and oxidative markers, in GDM women and their offspring highlighting its role on GDM-associated T2DM and cardiovascular diseases elevated risk. Specifically, H3K4me3, led by MLL1, in the NF-kBp65 promoter region activates downstream gene expression, such as *VCAM-1, ICAM-1, MCP-1,* and *IL-6* in Peripheral Blood Mononuclear Cells (PBMC) from GDM women and in Cord Blood Mononuclear Cells (CBMC) and HUVEC from their newborns. Moreover, H3K4me3 in NF-kBp65 promoter region is detected also in PBMC from teenagers born to women with GDM history. Furthermore, H3K4me3 drives also NOX4 expression as well as O_2^- levels in GD-HUVEC (Di Pietrantonio N et al, 2024).

For all these reasons, GD-HUVEC, showing stable epigenetic modifications acquired during *in vivo* exposure to hyperglycaemia, reproduce the endothelial dysfunction typical of diabetes, and thus, represent an innovative *in vitro* platform to deeply investigate diabetic endothelial dysfunction associated mechanisms and to study novel potential therapeutic strategies among which natural bioactive compounds and perinatal derivatives, such as amniotic membrane.

2.6 NATURAL BIOACTIVE COMPOUNDS

Natural bioactive compounds are categorized in 4 different groups: macronutrients, micronutrients, phytonutrients and regulators of the gut microbiome.

Macronutrients include carbohydrates, lipids and proteins meanwhile micronutrients comprise minerals and vitamins. Phytochemicals includes a variety of minor components such as terpenes, alkaloids, phenolic compounds and organosulfur compounds. Gut microbiome regulators comprises probiotics, prebiotics, symbiotics and postbiotics (Kussmann M et al, 2024).

Many bioactive natural molecules show beneficial effects toward the vascular component to counteract the endothelial dysfunction associated to the diabetic condition.

Among terpenes, oleanolic acid (OA), a pentacyclic triterpenoid part of the human diet due its presence in plants and herbs, show several positive properties in different contexts as demonstrated by thousands of publications in the time frame from 2010 to 2021 (Castellano JM et al, 2022).

Indeed, in a collaborative study we previously demonstrated OA potential therapeutic role on vascular dysfunction typical of the diabetic milieu. GD-HUVEC, as *in vitro* model of diabetic endothelial dysfunction, pre-treated with OA and then, stimulated with TNFα, a pro-inflammatory cytokine, showed reduced *VCAM-1* and *E-selectin* gene expression as well as decreased VCAM-1 protein expression and lower number of monocytes adherent to HUVEC monolayer, further confirming OA anti-inflammatory effect on vascular endothelium. Moreover, OA demonstrated additional positive effects on migration and angiogenesis. Particularly, OA treatment promoted cell migration in both C- and GD-HUVEC and significantly enhanced vessels formation improving several angiogenic parameters further suggesting its beneficial properties on endothelium (Stelling-Férez J et al, 2023).

Among phytochemicals, carotenoids, such as β-carotene and lycopene, are well characterized for their antioxidant properties and they are investigated as innovative protective therapeutics for diabetes associated persistent inflammation and oxidative stress (Ucci M et al, 2019; Di Tomo P et al, 2012).

Particularly, Ucci M at al. in 2019, demonstrated that GD-HUVEC treated with β-carotene and lycopene, at concentrations similar to their circulating levels subsequent to oral administration, showed reduced amounts of VCAM-1 and ICAM-1 membrane exposure and NF-kB nuclear translocation as well as decreased monocytes-endothelial cells interaction, suggesting their anti-inflammatory effects. In addition, GD-HUVEC treated with β-carotene

and lycopene showed enhanced NO bioavailability and, contextually, reduced peroxynitrite production (Ucci et al, 2019).

Furthermore, also plants derived essential oils (EO) show many biological activities among which anti-inflammatory and antioxidant (Pandur E et al, 2022). EO are a variegated mix of different volatile compounds. Monoterpenes, sesquiterpenes and oxygenated derivatives are the most important ones together with some aliphatic and aromatic compounds coming from phenylpropane. Moreover, EO and some of their derived compounds are able to reduce cardiovascular disease risk factors (Long Y et al, 2022).

Schiavone V and Romasco T et al (2023) demonstrated the anti-inflammatory potential of anise and laurel EO using the *in vitro* model of GD-HUVEC. Indeed, GD-HUVEC treated with anise and laurel OE showed reduced levels of VCAM-1 gene and protein expression as well as NF-kB nuclear translocation and monocyte-endothelial cells interaction (Schiavone V and Romasco T et al, 2023).

Among phytochemicals, polyphenols, in the last decades, have gained attention due to their beneficial properties.

2.6.1 POLYPHENOLS

Polyphenols are natural bioactive compounds which belong to the class of phytochemicals. They can assume many different structures, from basic monomers to intricated polymers. Moreover, polyphenols can be classified in different groups comprising phenolic acids, flavonoids, stilbenes, lignans, tannins, lignins, xanthones, chromones, and anthraquinones (Iqbal I et al, 2023).

They are present in many plants and fruits in variable quantities and proportions. For this reason, diet composition strongly affects the amount of polyphenols. Certainly, fruits and vegetables rich diets are linked to an elevated content of flavonoids as well as diets with a frequent consumption of extra-virgin olive oil (EVOO) and wine leads to a high intake of tyrosols and stilbenes. Of note, polyphenols bioavailability is relatively low since they are badly absorbed in the small intestine while they are absorbed in the colon after transformation by the colonic flora (Godos J et al, 2017; Gross G et al, 2022).

Polyphenols anti-diabetic effect and anti-inflammatory and antioxidative properties in vascular health have been widely established in the last decades. Indeed, flavonoids improve NO bioavailability by activating eNOS through different pathways mediated by PI3K/AKT (Neyrinck AM et al, 2019; Li j et al, 2019). Moreover, the regulation of the vascular tone is

exerted by many other polyphenols, such as luteolin and caffeic acid, acting directly or indirectly on smooth muscle cells that surround vessels (Li W et al, 2019; de Alencar Silva A et al, 2020). In addition, flavonoids showed a strong activity to scavenge free radicals counteracting vascular oxidative stress (Ciumărnean L et al, 2020; Chen X et al, 2020). Indeed, polyphenols antioxidant activity is one of the most studied and well-characterized. Furthermore, many polyphenols exert also anti-inflammatory action preventing the early phases of the atherosclerotic process (Sha W et al, 2021).

Thus, polyphenols, derived from natural sources, which show anti-inflammatory and antioxidant properties against diabetes-associated endothelial dysfunction, as well as cardioprotective effects, have attracted considerable research interest.

In particular, olive tree (*Olea europaea L.*), a fundamental part of the Mediterranean diet, is an essential source of polyphenolic compounds. Although many studies focus on the beneficial properties of EVOO, olive leaves, a discarded product of the olive supply-chain, represents an underestimated resource of bioactive compounds (Somova LI et al, 2003; Andreadou I et al, 2007; Soni MG et al, 2006; Stelling-Férez J et al, 2023).

Olive leaf extract (OLE), containing important polyphenols such as oleuropein, hydroxytyrosol, luteolin, and apigenin reveals potent effects such as antioxidant, anti-inflammatory, cardioprotective, and neuroprotective. Indeed, in preclinical studies, OLE supplementation improves antioxidant enzymes activities, counteracting oxidative stress, and reduces inflammation. In addition, OLE promotes pancreatic islet integrity, decreases metabolic problems and improve glycaemia (Jemai H et al, 2009; Jemai H et al, 2008; Manna C et al, 2004; Lins PG et al, 2018; Romani A et al, 2019).

Although, all these findings suggest that OLE could help in diabetes management by improving vascular function and becoming a new potential perspective for addressing diabetes complications, further studies are still necessary.

2.7 AMNIOTIC MEMBRANE

Perinatal derivatives are tissues associated with birth including placenta and its components such as human amniotic membrane (AM), chorion, decidua basalis and umbilical cord, and amniotic fluid. Moreover, perinatal derivatives include birth associated tissues derived cells and secretome (Deus IA et al, 2020).

Among these, AM is the birth-associated tissue studied for the longest time for tissue engineering and regenerative medicine.

AM is the innermost placental layer more in contact with the fetus and amniotic fluid. It derives from epiblasts cells, the same cells that form the embryo. AM is a translucent, strong and flexible biological structure with a variable thickness ranging from 0.02 mm to 0.5 mm, according to interindividual variability, without nerves, vessels, lymphatic system and muscles. It takes nutrients and oxygen from the chorionic fluid, amniotic fluid and surface vessels of the fetus (Favaron PO et al, 2015; Mamede AC et al, 2012).

AM, due to its elasticity and robustness, protects the embryo from traumas and pressure changes and it adapts to embryo growth. Furthermore, AM exerts several metabolic functions including water and soluble molecules transport, and produces different growth factors, cytokines and vasoactive peptides (Favaron PO et al, 2015; Mamede AC et al, 2012).

AM has a complex structure compartmentalized in five different strata, from the most internal to the most external: the epithelial layer, the basement membrane, the compact layer, the fibroblast layer and the spongy layer (Mamede AC et al, 2012).

The epithelial layer contains amniotic cuboidal epithelial cells that create a homogenous sheet. These cells, characterized by a big nucleus and nucleolus and villi con the apical surface, produce and release several growth factors and cytokines, such as VEGF, TGFβ, TGFα, FGF and IL-8, and also glycoproteins, collagen and hyaluronic acid that promotes cellular migration as well as exerts anti-inflammatory and immunosuppressive activities (Favaron PO et al, 2015; Mamede AC et al, 2012).

The basement membrane is a permeable barrier involved in many functions and contains proteoglycans rich in heparan sulphate (Mamede AC et al, 2012)..

The third layer is the acellular compact layer, composed of connective tissue mainly consisting of collagen type I, II and V, which provides structural support and ensures the mechanical cohesion of AM (Favaron PO et al, 2015).

The second last layer contains mesenchymal fibroblast-like cells deriving from the mesodermal embryonic plate. This layer contributes to membrane tensile strength due to its high amount of collagen and represents the thickest stratum of the AM.

The outermost layer, in contact with the chorion, is the spongy layer, also called zona spongiosa due to its histological appearance caused by the abundant presence of proteoglycans, glycoproteins and collagen III (Mamede AC et al, 2012)..

AM includes two different multipotent stem cells: amniotic epithelial cells and amniotic stromal cells.

Of note, the isolation and collection of these cells, as well as of the human amniotic membrane, overcome any ethical issue considering that placenta is a waste product of the delivery.

Amniotic epithelial cells have a cuboidal shape, and they cover completely the innermost layer thus, they are directly in contact with amniotic fluid. From one amniotic membrane it is possible to isolate, through enzymatic digestion, more than 100 million cells (Farhadihosseinabadi B et al, 2018). These cells express embryonic stem cells markers among which stage specific embryonic antigen 3 (SSEA-3), SSEA-4, T cell receptor alpha-1-60 (TRA-1-60), TRA-1-81, octamer-binding transcription factor 4 (OCT4) and NANOG. These last two gene are normally expressed by pluripotent stem cells deriving from the epiblast (Farhadihosseinabadi B et al, 2018).

Amniotic epithelial cells produce and secrete some growth factors with important biological activities such as TNFα, nerve growth factor (NGF), brain-derived neurotrophic factor (BDNF), noggin and activin. Moreover, these cells produce secretory leukocyte proteinase inhibitor (SLPI) and elafin, supporting its anti-inflammatory activity, and β-defensin and cathelicidin LL-37, responsible for infections safeguard (Pipino C et al, 2013).

Moreover, they can differentiate in the three germ layers cell types and form 3D systems such as spheroids. They do not originate teratomas in immunodeficient mice and, in contrast with embryonic stem cells, they do not require additional layers to support *in vitro* cultures growth.

Amniotic stromal cells occupy the fourth layer of the amniotic membrane and, as epithelial cells, differentiate into the three germ layers cell types. These cells express typical mesenchymal surface markers, such as CD44, CD73, CD29, CD105 and CD90, and some pluripotent stem cells markers including SSEA4, SSEA4, OCT4, NANOG, TRA-1-60 and TRA-1-81 (Pipino C et al, 2013).

Amniotic stromal cells, producing several molecules and growth factors, exerts anti-inflammatory action modulated by prostaglandin E2 (PGE2), indoleamine 2,3-dioxygenase (IDO), hepatocyte growth factor (HGF) and TGFβ release. At the same time, these cells, producing VEGF and PDGF, has also pro-angiogenic activity (Farhadihosseinabadi B et al, 2018).

Human amniotic membrane, as well as all perinatal derivatives, has immune tolerance ability. This crucial biological property is guaranteed by the absence of Human Leukocyte Antigen (HLA) -A, -B, and -C (corresponding to major histocompatibility complex (MHC) class I surface antigens) and HLA-DR (corresponding to MHC class II antigens). Indeed, both amniotic epithelial and stromal cells express HLA-G, typically expressed by immunocompetent

tissues, which abrogates T-cells, B-cells, natural killer (NK) and dendritic cells activation. Particularly, amniotic epithelial and stromal cells abolish the conversion of monocytes into dendritic cells varying the expression of the following markers, CD1a, CD80, CD86, CD83 and HLA-DR, to block NK activation and PBMC proliferation (Insausti CL et al, 2014).

The use of placenta dates to the 16th century in China where the *Compendium of Materia Medica* included an entire paragraph to the medical use of human placenta (Young SM et al, 2010). Anyway, the first published report regarding the beneficial properties of amniotic membrane dates back to 1910 as skin graft (Davis J, 1910). Indeed, in 1913, other studies reported the use of AM as skin dressing to treat burns and ulcers of the skin describing absence of infections, reduction in pain and enhanced epithelialization (Stern M, 1913; Sabella N, 1913). Many years later, around late 1930s and 1940s, AM has been used for different applications such as vaginal reconstruction but more successfully, in ophthalmology to repair conjunctiva defects and burns (Brindeau A, 1934; Burger K, 1937; De Rotth A, 1940; Sorsby A and Symons HM, 1946). Nowadays, ophthalmology remains one of the most popular fields of application. Anyway, from 1940s many clinical trials were published highlighting the beneficial effects of human amniotic membrane to treat skin injuries. Indeed, AM improves the healing process by decreasing pain, infections, fluid loss and exerting anti-inflammatory effects and promoting the epithelialization of the injured area (Silini AR et al, 2015; Tenenhaus M, 2017).

Rodríguez-Valiente M et al, in 2018, used amniotic membrane processed to have a medicinal product to treat 14 diabetic patients with DFU. The AM patches were applied every 7-10 days until the achievement of total epithelialization of the wound. Diabetic patients obtained from 4 to 40 AM applications according to wound dimensions and epithelialization timing. At the end of the study, total epithelialization of all wounds was obtained with no adverse effects underling the effectiveness of AM as wound dressing (Rodríguez-Valiente M et al, 2018).

Moreover, in 2024, Rodríguez-Valiente M et al applied once a week AM patches in five different patients affected by DFU that were non-healed, even if they were treated with multiple strategies, for at least six weeks. Complete epithelialization was achieved by four out of five patients. The fifth patient reached 40% reduction in wound area after the treatment period. Anyway, they also achieved reduction in pain and infections suggesting the potential effects of AM (Rodríguez-Valiente M et al, 2024).

Although, the effectiveness of AM as a wound dressing, mainly for compassionate use, has been well recognized for many decades, the molecular mechanisms behind its positive effects are not yet completely understood. For these reasons, many studies in the last years investigated the signaling pathways associated to AM properties.

In particular, Bernabé-García Á et al, in 2017, demonstrated, in Mv1Lu and HaCaT cells, the ability of AM to increase cell migration modulating the rearrangement of focal structures by Paxillin and focal adhesion kinase (FAK) regulation. They determined that AM driven focal adhesion regulation is mediated by c-Jun N-terminal kinases (JNK) and MEK MAP kinase signalling pathways (Bernabé-García Á et al, 2017).

Additionally, Liarte S et al (2023) demonstrated that AM treatment improved migration and proliferation, at early and late stages of wound healing respectively, and the gene expression profile of keratinocytes chronically exposed to TGF-β, as an *in vitro* model of dysfunctional keratinocytes typical of chronic wounds (Liarte S et al, 2023).

Furthermore, in 2022, we previously investigated in a collaborative study the potential anti-inflammatory and pro-angiogenic role of AM on diabetic endothelium using the *in vitro* model of GD-HUVEC (**Figure 11**). We demonstrated that AM treatment reduced TNFα-induced *VCAM-1, ICAM-1, CCL2* and *E-selectin* gene expression as well as VCAM-1 and ICAM-1 protein expression. Contextually, AM treatment reduced NF-kB phosphorylation and nuclear translocation and it decreased monocytes-endothelial cells interaction suggesting its potent anti-inflammatory effect on diabetic endothelium. In addition, AM treatment increased NO bioavailability by up-regulating the levels of cGMP in GD-HUVEC. Moreover, AM treatment improved GD-HUVEC migration as evidenced by scratch assay and Paxillin focal adhesion remodelling and enhanced vessels formation. All these results lay the foundation for a better understanding of the AM driven mechanisms especially regarding its anti-inflammatory and pro-angiogenic role as possible therapeutic strategy for the treatment of DFU (Pipino C et al, 2022). Anyway, further studies are still necessary to further investigate the molecular pathways involved in AM associated effects, in particular the pro-angiogenic property, to support AM clinical utilization.

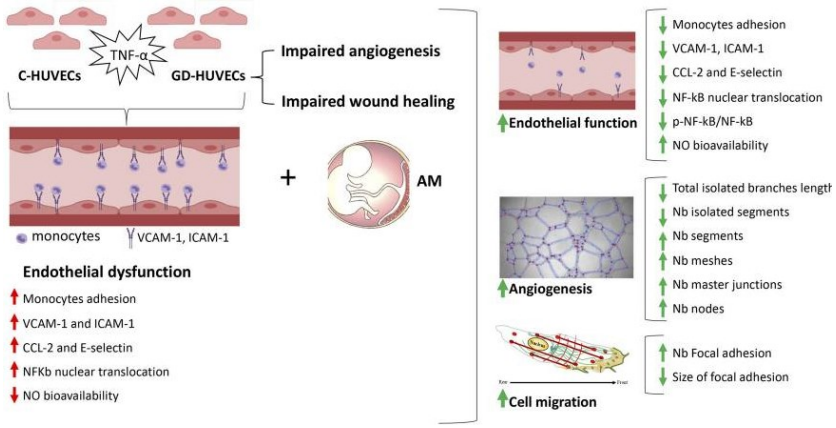


Figure 11. Graphical abstract representing the anti-inflammatory and pro-angiogenic effects of AM on GD-HUVEC (Pipino C et al, 2022).

3 AIMS

This thesis aims to deeply investigate the mechanisms underlying endothelial dysfunction in diabetes with a particular focus on molecular pathways associated with reduced angiogenesis, typical of chronic diabetic wounds, and on innovative therapeutic strategies ranging from phenolic extracts to perinatal derivatives such as the amniotic membrane. To this end, the unique *in vitro* model of GD-HUVEC has been employed. Owing to stable epigenetic modifications acquired following *in vivo* exposure to hyperglycaemia, this model faithfully reproduces the typical features of diabetic endothelial dysfunction.

The overall objective can be further divided into three specific aims:

1. *AIM 1* – **VASCULAR INFLAMMATION: ROLE OF OLIVE LEAF PHENOLIC EXTRACTS**

   New strategies to improve diabetes endothelial dysfunction are still necessary. In this context, phenolic extracts derived from olive leaf, a byproduct of the EVOO supply-chain, may exert beneficial properties in counteracting vascular inflammation. For these reasons, the anti-inflammatory potential of phenolic extracts obtained from Picual and Changlot Real olive leaf, two Spanish monocultivars, was investigated using the *in vitro* model of GD-HUVEC.

2. *AIM 2* – **ANGIOGENESIS: ROLE OF AMNIOTIC MEMBRANE VIA VEGFR2/AKT/eNOS SIGNALLING PATHWAY**

   The effectiveness of amniotic membrane in diabetic wound healing has been well-established from many decades. However, although it is mainly used as a compassionate therapy, the mechanisms behind its positive effects are not yet completely understood. We previously demonstrated the anti-inflammatory property of amniotic membrane on diabetic vascular endothelium using GD-HUVEC with a limited attention to its pro-angiogenic effects, which showed enhanced vessel formation and improved NO bioavailability. In this context, the VEGFR2/AKT/eNOS signalling pathway was investigated to further elucidate the pro-angiogenic role of amniotic membrane on diabetic vascular endothelium.

3. *AIM 3* – ANGIOGENESIS: ROLE OF THE INTERACTION BETWEEN ENDOTHELIAL CELLS AND DERMAL FIBROBLASTS IN DIABETES

During the proliferative phase of wound healing, in physiological conditions, the interaction between endothelial cells and dermal fibroblasts is crucial to achieve a correct ulcer closure. In particular, dermal fibroblasts, thanks to a continuous ECM remodelling and factors secretion, have a great direct impact on angiogenesis promoting vessel formation. On the other hand, endothelial cells, releasing molecules and growth factors, influence the migration ability as well as the ECM production and degradation by fibroblasts, indirectly regulating angiogenesis. However, these interactions and their impact on the delayed wound healing, typical of diabetic patients, are largely unknown. For this reason, to gain deeper insight into endothelium-fibroblast interaction in diabetes, the role of GD-HUVEC on migration and ECM remodelling by dermal fibroblasts as well as the impact of diabetic fibroblasts on vessel formation and endothelial cells migration were investigated.

4 VASCULAR INFLAMMATION: ROLE OF OLIVE LEAF PHENOLIC EXTRACTS (*AIM 1)*

From ***Cappellacci I****, Di Pietrantonio N****, Viola D, Formoso G, Zujko ME, Martín-García B, Gomez-Caravaca AM, Verardo V, Pandolfi A, Pipino C.* ***Unveiling the anti-inflammatory potential of olive leaf phenolic extracts in diabetes-related endothelial dysfunction.*** *Front Endocrinol (Lausanne). 2025 Oct 14;16:1671932. doi: 10.3389/fendo.2025.1671932.* **Contributed equally*

4.1 MATERIALS AND METHODS

4.1.1 Olive leaf samples

Olive leaf samples from Changlot Real and Picual monocultivars were supplied by "IFAPA, Centro Alameda del Obispo" in Córdoba, Spain (37°51′36.5″ N 4°47′53.7″W). Both samples were grown under the identical agronomic and environmental conditions in the same olive orchards. The olive leaves were collected in July.

4.1.2 Extraction of phenolic compounds and their analysis by HPLC-ESI-TOF-MS

According to Talhaoui N et al (2015), 0.5 g of dried olive leaves were extracted with methanol/water 80/20 v/v. The extracts were reconstituted with methanol/water 50/50 v/v and analysed by HPLC-TOF-MS. The determination of targeted compounds was performed employing an Agilent 1200 HPLC system coupled to a QTOF Agilent 6520 B mass spectrometer using the column and the chromatographic condition reported by Talhaoui N et al (2015).

4.1.3 Clinical characteristics of umbilical cords donors and newborns

Umbilical cords were obtained from randomly recruited healthy Caucasian mothers (Control, C) and women affected by Gestational Diabetes (GD) in the third trimester of pregnancy followed by 'Diabetes and Pregnancy Clinic' until the delivery at the Hospital Santo Spirito of Pescara (Italy). GD women were treated with diet only. Women with pre-gestational diabetes

were excluded. All procedures agreed with the Declaration of Helsinki principles and with the ethical standards of the Institutional Committee on Human Experimentation (the studies involving humans were approved by COMITATO ETICO territoriale REGIONE ABRUZZO C.Et.R.A reference number 123821/25). Following protocol approval by the Institutional Review Board, signed informed consent was obtained from each participating subject. The characteristics of donors' Control (n=4) and GD (n=4) women together with the newborns are detailed in **Table 1**.

Women matched by age and body mass index (BMI) were separated into two groups, one normoglycemic/healthy controls (basal glycaemia < 5.1 mmol/L, oral glucose tolerance test (OGTT) 1h < 10 mmol/L and OGTT 2h < 8.5 mmol/L, n=4) and the other diagnosed with gestational diabetes (basal glycaemia ≥ 5.1 mmol/L, OGTT 1h ≥ 10 mmol/L, and OGTT 2h ≥ 8.5 mmol/L, GD, n=4) according to the criteria of the American Diabetes Association (American Diabetes Association Professional Practice Committee, 2022).

Pregnant women	Control	GD	*p*
women (n)	4	4	
age (years)	35 ± 2	35 ± 6	0.9
OGTT (gestational week)	26 ± 2	26 ± 1	0.6
basal glycaemia (mmol/L)	4.4 ± 0.4	5.1 ± 0.2	0.01
1 h glycaemia (mmol/L)	5.8 ± 1	10.4 ± 0.9	0.001
2 h glycaemia (mmol/L)	4.4 ± 0.7	9 ± 1	0.001
height (cm)	162 ± 8	161 ± 6	0.8
pre-gestational weight (kg)	60 ± 7	67 ± 17	0.4
post-gestational weight (kg)	71 ± 8	76 ± 15	0.5
gestational weight gain (kg)	11 ± 3	9 ± 3	0.3
pre-gestational BMI (kg/m^2)	23 ± 1	26 ± 5	0.3
post-gestational BMI (kg/m^2)	27 ± 2	29 ± 4	0.4
SBP (mmHg)	112 ± 13	112 ± 5	1
DBP (mmHg)	72 ± 12	65 ± 4	0.3
GA at delivery	40 ± 0.5	38 ± 1	0.1
Newborns	**Control**	**GD**	***p***
Newborns (n)	4	4	
Sex (female/male)	3/1	2/2	
Birth Height (cm)	51 ± 1.5	50 ± 0.5	0.2
Birth Weight (kg)	3.4 ± 0.4	3 ± 0.2	0.2

Table 1. Anthropometric and biochemical characteristics of control women, women with gestational diabetes and newborns. Data are expressed as mean ± SD. GD: gestational diabetes; BMI:

body mass index; OGTT oral glucose tolerance test; SBP: systolic blood pressure; DBP: diastolic blood pressure; GA: gestational age.

4.1.4 HUVEC isolation and culture

Primary human umbilical vein endothelial cells (HUVEC) were isolated from umbilical cords of newborns delivered between the 37th and 40th gestational weeks at the hospitals of Chieti and Pescara (Italy).

Donors were randomly selected Caucasian mothers, either diagnosed with gestational diabetes (GD) or serving as healthy controls (C), following previously established protocols (Di Fulvio P et al, 2014; Ucci M et al, 2019).

Briefly, umbilical cords were collected immediately after delivery. The veins were cannulated and enzymatically digested with 1 mg/mL collagenase 1A at 37 °C. The resulting HUVEC were isolated and cultured in a basal medium consisting of DMEM/M199 (1:1), supplemented with 1% L-glutamine, 1% penicillin/streptomycin, and 20% foetal bovine serum (FBS) (ThermoFisher; Waltham, MA, USA). Following centrifugation at 1200 rpm for 10 minutes, the cell pellet was resuspended in the same medium and plated onto 1.5% gelatine-coated culture flasks (Sigma-Aldrich, Germany).

Phenotypic characterization of HUVEC was confirmed by the expression of endothelial markers such as von Willebrand factor, CD31, and CD34, along with inducible expression of adhesion molecules (ICAM-1, VCAM-1, and E-selectin) and cytokines (IL-6 and IL-8) upon pro-inflammatory stimulation (Di Fulvio P et al, 2014; Ucci M et al, 2019; Stelling-Férez J et al, 2023; Pipino C et al, 2022).

Functional validation confirmed their capacity to create capillary-like structures on Matrigel. Notably, GD-HUVEC formed less interconnected tubes with fewer segments, meshes, junctions, and nodes compared to control cells, confirming impaired angiogenic ability (Pipino C et al, 2022; Zheng L et al, 2024).

In addition, GD-HUVEC showed a stable pro-inflammatory phenotype induced by epigenetic modifications acquired during *in vivo* exposure to hyperglycaemia (Di Pietrantonio N et al, 2024). Accordingly, in this study, GD-HUVEC demonstrated a significant upregulation of NF-kB p65 gene expression and VCAM-1 protein expression compared to C-HUVEC (**Figure 12**).

Cells used for assays were cultured between passages 3 and 5, with passage 5 never exceeded. For experiments, HUVEC were maintained on 1.5% gelatine coated plates in complete endothelial growth medium composed of low-glucose (1 g/L) DMEM and M199 (1:1),

supplemented with 10 µg/mL heparin, 50 µg/mL endothelial cell growth factor (ECGF), 20% FBS, 1% penicillin/streptomycin, and 1% L-glutamine (all from Sigma-Aldrich, Germany).

All experiments were performed in technical triplicates using HUVEC from at least three independent donors per group (control and GD, n ≥ 3).

TNFα exposure times were selected to reflect the temporal dynamics of the NF-kB cascade: 1-hour to identify early p65 phosphorylation, 6-hours to evaluate transcriptional activation, and 16-hours to monitor late functional effects including VCAM-1 surface expression and leukocyte adhesion (Ucci M et al, 2019; Di Pietrantonio N et al, 2024; Kim JH et al, 2025) (**Figure 13**).

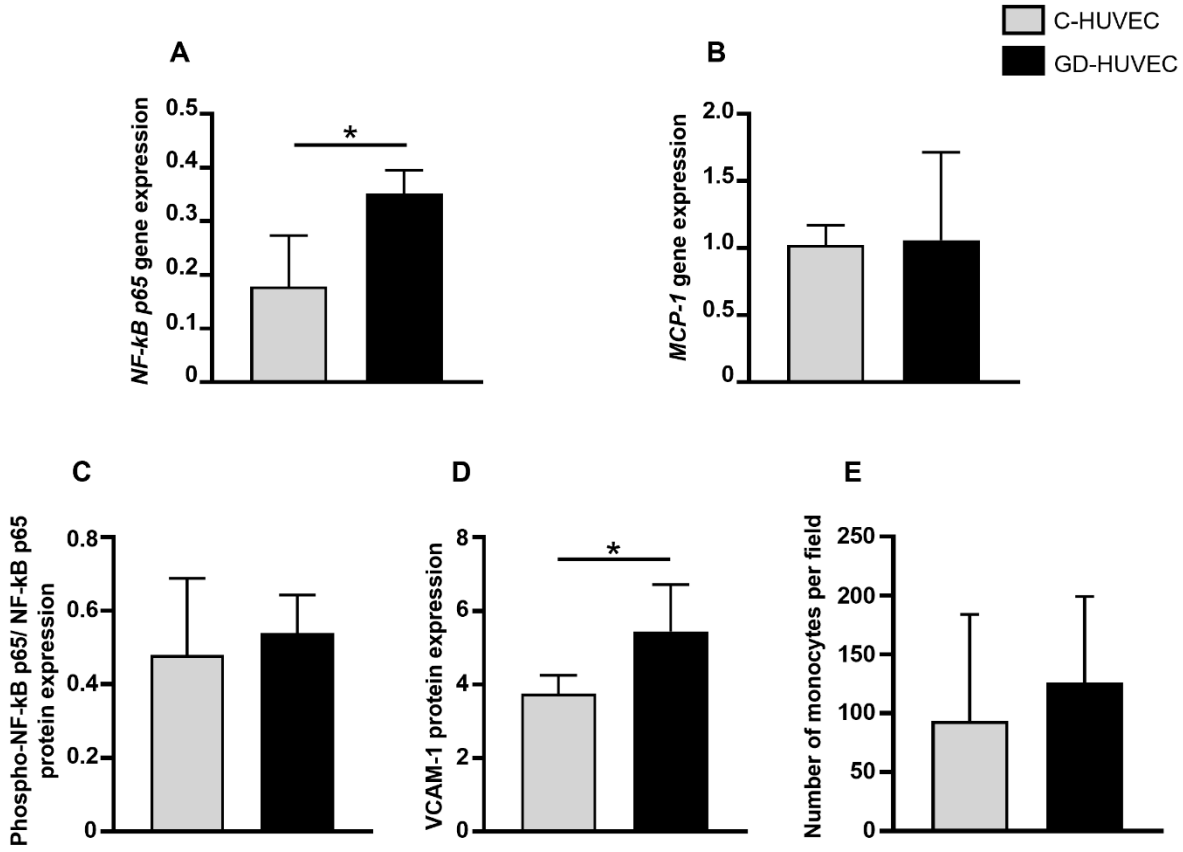


Figure 12. *Basal differences between C- and GD-HUVEC.* Relative mRNA expression of *NF-κB p65* (A) and *MCP-1* (B), NF-κB p65 phosphorylation (C), VCAM-1 protein levels (D) and monocytes adhesion (E) in C- and GD-HUVEC in basal conditions. Results are expressed as the mean ± SD (n≥3). Asterisks point out statistically significant differences between the selected conditions (*p<0.05).

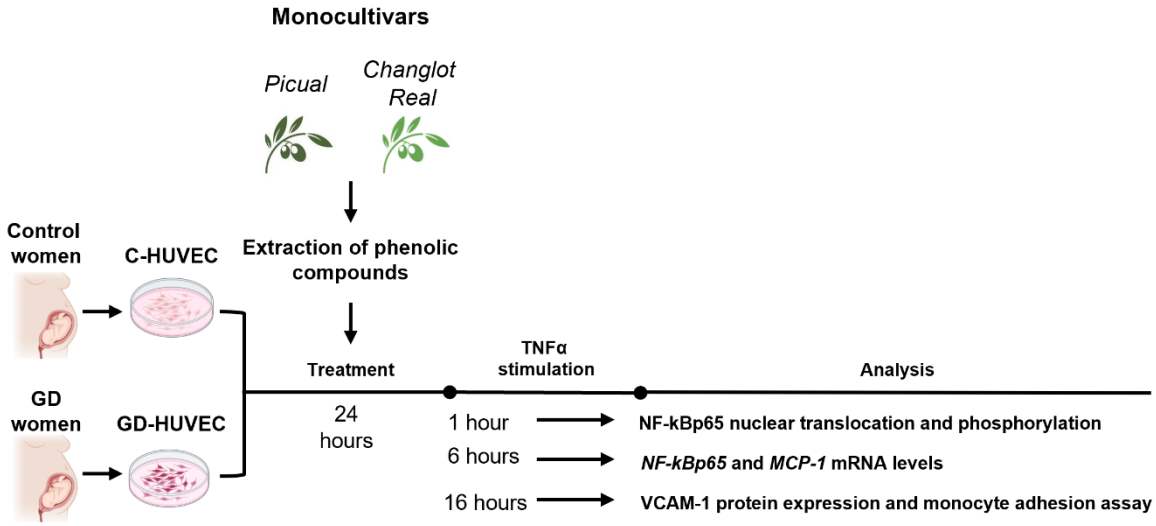


Figure 13. *Experimental protocol.* Briefly, C- and GD-HUVEC were pre-treated with Picual and Changlot Real phenolic extracts for 24-hours (10 µg/mL) and then, cells were stimulated with TNFα (10 ng/mL) at different timing (1-hour, 6-hours and 24-hours) according to the experiment performed.

4.1.5 MTT assay

To determine the effect of Picual and Changlot Real polyphenol extracts on C- and GD-HUVEC viability, the 3-(4,5-dimethylthiazolyl-2)-2,5-diphenyltetrazolium bromide (MTT) assay (cat # M2128, Sigma- Aldrich, Germany) was carried out according to manufacturer's instructions.

HUVEC were seeded in 96-well plates at a density of 5600 cells/cm^2. After 24 hours treatment with increasing extracts concentration (0.1-100 µg/mL), cells were incubated for 3 hours at 37°C with 5 mg/mL of MTT dissolved in PBS. Thereafter, MTT crystals were dissolved by DMSO addition (200 mL/well) and gentle shaking for 30 minutes. Finally, the absorbance of each sample was recorded at 540 nm using a microplate spectrophotometer system (Multimode Microplate Reader, BioTek Synergy H1, Agilent).

4.1.6 RNA extraction and real-time quantitative PCR

The total RNA was isolated and extracted from HUVEC treated with Picual and Changlot Real polyphenol extracts (10 µg/mL), using the TRIzol reagent (Sigma-Aldrich, Germany) protocol. Quantification of obtained RNA was performed using NanoDrop 2000 spectrophotometer (Thermo Scientific; Waltham, MA, USA). The High-Capacity cDNA Reverse Transcription Kit was employed to synthesize cDNA. The TaqMan Universal Master Mix II and TaqMan Gene Expression Assay probes for human NF-kB p65 (Hs01042014_m1), MCP-1 (Hs00234140_m1) and RPLP0 (Hs00420895_gH) were used according to the manufacturer's instructions.

All samples were analysed in technical duplicate. The relative expression of the target genes was calculated using the $2^{-\Delta Ct}$ method using RPLP0 as housekeeping gene (Applied Biosystems QuantStudio 7 Pro Real-Time PCR System, Thermo Fisher Scientific).

4.1.7 Immunofluorescence analysis

HUVEC were fixed with 3% formaldehyde for 20 minutes at room temperature. Formaldehyde was removed, and then cells were washed with PBS for 5 minutes twice and permeabilized with 0.1% Triton X-100 (SigmaAldrich, Germany) in PBS for 10 minutes. Cells were blocked with 1% bovine serum (cat # A4503, Sigma-Aldrich, Germany) in PBS for 1-hour at room temperature. Subsequently, cells were incubated 1-hour with primary antibody NF-kB p65 (cat # C22B4, Cell Signaling Technology, 1:50). After washing with PBS, cells were incubated with Alexa Fluor 488-conjugated secondary antibody (cat #A-11034, Thermo Fisher Scientific, 1:50) and Phalloidin (cat #A12379, Thermo Fisher Scientific, Karlsruhe, Germany) at room temperature for 1-hour. Nuclei were stained with DAPI mounting medium (4′6′-diamidino-2-phenylindole; Thermo Fisher Scientific, Karlsruhe, Germany). Finally, cells were washed with PBS and mounted with Fluorescence Mounting Medium (cat # S3023, Agilent Dako, USA).

For the acquisition of the immunofluorescence signals, slides were observed under a confocal microscope (Zeiss LSM-800; Carl Zeiss Meditec AG, Oberkochen, Germany).

4.1.8 Flow cytometry analysis

Flow cytometry analysis was performed using BD FACS Canto II flow cytometer. Specifically, 1×10^4 events for each sample were analysed using FACSDiva v 6.1.3, IDEAS software (BD Biosciences). Cells were pre-treated 24-hours with Picual and Changlot Real polyphenolic extracts (10 μg/mL) and, subsequently, incubated with or without TNFα (10 ng/mL) for 16hours to evaluate VCAM-1 protein expression, and for 1-hour to assess NF-kB p65 and its phosphorylated form (46hosphor-NF-kB p65 S536). To determine protein levels, cells were permeabilized using the Intrasure kit (cat # 641778, BD Biosciences, Sweden), processed, and incubated with primary antibodies: anti-VCAM-1 PE conjugate (cat # 12-1069-42, Invitrogen, 1:100), anti-NF-kB p65 (cat # C22B4, Cell Signaling Technology, 1:100), and anti-phospho-NF-kB p65 S536 (cat #3033, Cell Signaling Technology, 1:750) for 30 minutes at 4°C. A following incubation with Alexa Fluor 488-conjugated secondary antibody (cat #A-11034, Thermo Fisher Scientific, 1:100) was performed for 30 minutes at 4°C to assess NF-kB p65 and 46hosphor-NF-kB p65 expression.

All results are expressed as the Mean Fluorescence Intensity (M.F.I.) Ratio, calculated by dividing the M.F.I. of positive events by the M.F.I. of negative events (M.F.I. of the secondary antibody).

4.1.9 Monocyte adhesion assay

C- and GD-HUVEC were pre-treated for 24-hours with Picual and Changlot Real polyphenol extracts (10 μg/mL) in six-well tissue culture plates, starved for 2-hours with 0.1% FBS, and treated with or without TNFα (10 ng/mL for 16-hours) as inflammatory stimulus. Briefly, 1×10^6 U937 cells [European Collection of Authenticated Cell Cultures (ECACC)], grown in RPMI 1640, were co-cultured with HUVEC under rotating conditions at room temperature. After 20 minutes, non-adhering cells were removed with PBS, and monolayers were fixed with 1% paraformaldehyde. Images were obtained from high power fields taken at half-radius distance from the centre of the wells using an inverted optical microscope PAULA cell imager (Leica, Wetzlar, Germany). The number of adherent monocytes was evaluated using ImageJ software.

4.1.10 Statistical analysis

All experimental data are expressed as mean ± Standard Deviation (SD). Each experiment was performed in technical triplicates using at least 3 independent donors of C- and GD-HUVEC. The normal distribution of quantitative data was assessed by the Shapiro–Wilk test. One-way ANOVA test followed by Tukey's test was used for multiple comparisons. Probability values were calculated considering a 95% compatibility interval. All analyses were performed with GraphPad Prism (version 9, GraphPad Software).

4.2 RESULTS

4.2.1 Determination of phenolic compounds in Picual and Changlot Real olive leaf extracts

Picual and Changlot Real olive leaf extracts Phenolic content is detailed in **Table 2**.

Secoiridoids, flavonoids, simple phenols, oleosides and elenolic acids, for a total of 36 phenolic compounds, were distinguished and quantified by HPLC-ESI-TOF-MS in both analysed samples. Changlot Real exhibited higher total amount of phenolic compounds than Picual.

Secoiridoids was the principal phenolic group in both samples (65.7-79.5%) and, in particular, oleuropein is the first compound that represent more than 53.5% of the total phenolic content. Flavonoids varied from 6 to 12% of phenolic compounds in Changlot Real and Picual, respectively. Tyrosol and hydroxytyrosol derivatives accounted from lower than 1.6% in both monocultivars. Oleosides ranged from 10 to 15% and, lastly, elenolic acids varied from 3.5 to 6% of total phenolic compounds.

These data are compatible with the data presented by Talhaoui N et al. (2015).

4.2.2 Effects of Picual and Changlot Real phenolic extracts on cell viability

To evaluate the potential cytotoxicity, Picual and Changlot Real monocultivar olive leaf polyphenol extracts were tested using the MTT assay on C- and GD-HUVEC (**Figure 14A,B**). Five different extracts concentrations (0.1, 1, 10, 50 and 100 µg/mL) were prepared in DMSO (at a final DMSO concentration in the culture medium of 0.05%) and used to treat both C- and GD-HUVEC for 24-hours. Vehicle matched controls were added in all experiments.

The results exhibited no significant modifications in cell viability at any tested concentration, suggesting that both extracts are well tolerated and non-cytotoxic under the evaluated conditions.

N.	Name	Changlot Real (%)	Changlot Real (mg/g)	Picual (%)	Picual (mg/g)
1	Hydroxytyrosol-hexose isomer a	0,01	0.001 ± 0.0002	0,01	0.001 ± 0.0001
2	Oleoside	1,16	0.17 ± 0.2	0,82	0.07 ± 0.1
3	Hydroxytyrosol-hexose isomer b	0,66	0.10 ± 0.1	1,03	0.09 ± 0.05
4	Hydroxytyrosol	0,11	0.02 ± 0.001	0,36	0.03 ± 0.001
5	Secologanoside isomer a	7,96	1.17 ± 0.2	7,55	0.66 ± 0.1
6	Tyrosol glucoside	0,35	0.05 ± 0.002	0,07	0.01 ± 0.002
7	Caffeoyl glucoside	0,26	0.04 ± 0.003	0,06	0.01 ± 0.001
8	Tyrosol	0,04	0.01 ± 0.001	0,06	0.01 ± 0.001
9	Elenolic acid glucoside isomer a	0,10	0.01 ± 0.001	0,22	0.02 ± 0.001
10	Secologanoside isomer b	1,16	0.17 ± 0.1	6,93	0.60 ± 0.005
11	Elenolic acid glucoside isomer b	1,31	0.19 ± 0.2	2,59	0.23 ± 0.1
12	Oleuropein aglycon	2,55	0.37 ± 0.1	4,00	0.35 ± 0.2
13	Elenolic acid glucoside isomer c	1,96	0.29 ± 0.2	2,82	0.25 ± 0.1
14	Luteolin diglucoside	0,05	0.01 ± 0.002	0,16	0.01 ± 0.002
15	Elenolic acid glucoside isomer d	0,15	0.02 ± 0.001	0,38	0.03 ± 0.001
16	Demethyloleuropein	0,37	0.05 ± 0.002	1,66	0.14 ± 0.1
17	Hydroxyoleuropein isomer a	0,36	0.05 ± 0.002	1,08	0.09 ± 0.001
18	Rutin	0,43	0.06 ± 0.002	0,58	0.05 ± 0.002
19	Luteolin rutinoside	0,05	0.01 ± 0.001	0,18	0.02 ± 0.001
20	Luteolin glucoside isomer a	2,84	0.42 ± 0.2	4,90	0.43 ± 0.1
21	Verbascoside	0,04	0.01 ± 0.001	0,03	0.003 ± 0.001
22	Hydroxyoleuropein isomer b	0,27	0.04 ± 0.001	0,27	0.02 ± 0.001
23	Apigenin rutinoside	0,08	0.01 ± 0.001	0,13	0.01 ± 0.001
24	Oleuropein diglucoside isomer a	0,07	0.01 ± 0.001	0,10	0.01 ± 0.001
25	Apigenin-7-glucoside	0,59	0.09 ± 0.002	0,40	0.03 ± 0.001
26	Oleuropein diglucoside isomer b	0,07	0.01 ± 0.001	0,12	0.01 ± 0.001
27	Luteolin glucoside isomer b	1,34	0.20 ± 0.01	3,17	0.28 ± 0.02
28	Oleuropein diglucoside isomer c	0,29	0.04 ± 0.003	0,17	0.01 ± 0.001
29	Chrysoeriol-7-O-glucoside	0,45	0.07 ± 0.002	1,00	0.09 ± 0.003
30	Luteolin glucoside isomer c	0,24	0.04 ± 0.001	0,90	0.08 ± 0.001
31	Oleuropein isomer a	67,35	9.90 ± 0.13	52,55	4.57 ± 0.19
32	Oleuropein isomer b	1,63	0.24 ± 0.03	1,10	0.10 ± 0.01
33	Oleuropein/Oleuroside2	4,29	0.63 ± 0.04	2,76	0.24 ± 0.01
34	Ligstroside aglycone	0,29	0.04 ± 0.003	1,21	0.11 ± 0.01
35	Ligstroside	1,96	0.29 ± 0.03	0,66	0.06 ± 0.003
36	Luteolin	0,02	0.003 ± 0.001	0,16	0.01 ± 0.001

Table 2. Phenolic compounds in Changlot Real and Picual olive leaf extracts quantified by HPLC-ESI-TOF-MS and displayed in the table as percentage (%) and as concentration (mg/g).

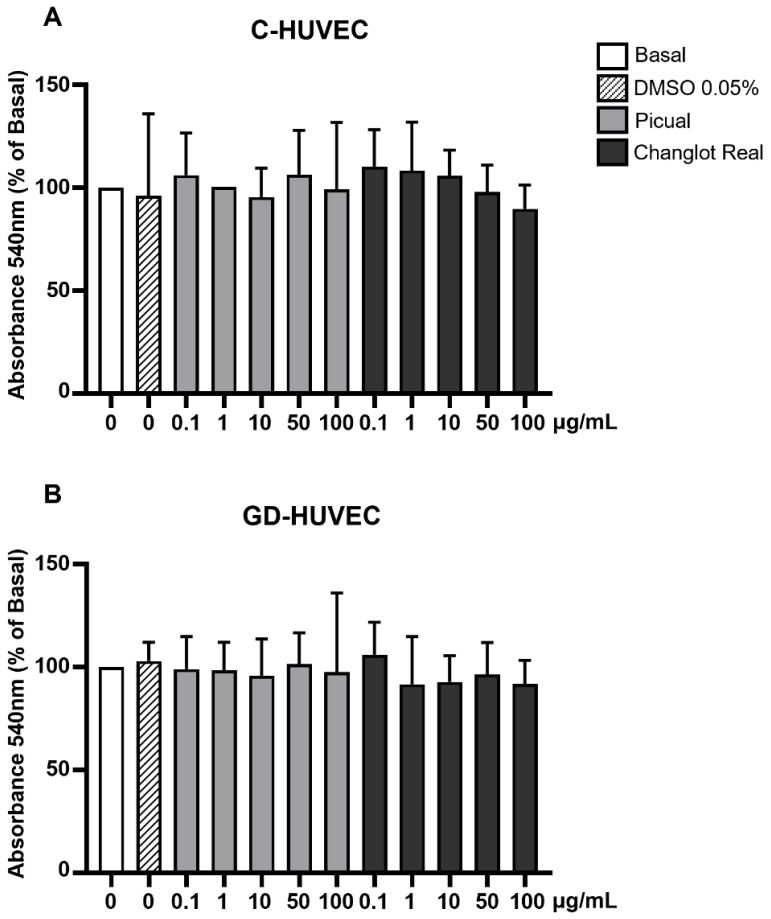


Figure 14. *Picual and Changlot Real phenolic extracts treatment do not induce significant variations in cell viability.* Cell viability of C- (A) and GD-HUVEC (B) following 24-hours treatment with Picual and Changlot Real phenolic extracts at different concentrations (0.1–100 µg/mL) analysed by MTT assay. Data are expressed as mean ± SD (n = 3).

4.2.3 Effects of Picual and Changlot Real phenolic extracts on *NF-kB p65* and *MCP-1* gene expression

To assess and compare the potential anti-inflammatory property of Picual and Changlot Real polyphenol extracts, the mRNA levels of *NF-kB p65* and *MCP-1* pro-inflammatory genes were investigated in both C- and GD-HUVEC under several conditions (**Figure 15**).

Predictably, *NF-kB p65* and *MCP-1* basal gene expression was slightly increased in GD-HUVEC compared to control cells. Following the identification of the most effective concentration by using vehicle-matched controls (**Figure 16**), both cells were pre-treated with Picual and Changlot Real polyphenol extracts at a concentration of 10 µg/mL.

The results indicated that both Picual and Changlot Real phenolic extracts induced a decrease in *NF-kB p65* and *MCP-1* gene expression, with a more evident effect in GD-HUVEC.

In GD-HUVEC, a reduction, even though not statistically significant, was also identified in the absence of the pro-inflammatory stimulus TNFα (**Figure 15B,D**).

As expected, following 6-hours TNFα stimulation (10 ng/mL) *NF-kB p65* and *MCP-1* mRNA levels were significantly upregulated in both cell types, indicating a strong inflammatory response. Nevertheless, Changlot Real polyphenol extract treatment significantly decreased the expression of both genes in C- and GD-HUVEC, counteracting the TNFα effect (**Figure 15A-D**). Comparably, Picual polyphenol extract treatment downregulated both *NF-kB p65* and *MCP-1* expression; however, its effect was more remarkable reaching statistical significance only in GD-HUVEC (**Figure 15B,D**). These results suggest that both phenolic extracts may have anti-inflammatory role, with Changlot Real showing a wider impact across the tested conditions, whereas Picual seems to have a more pronounced effect mainly in GD-HUVEC.

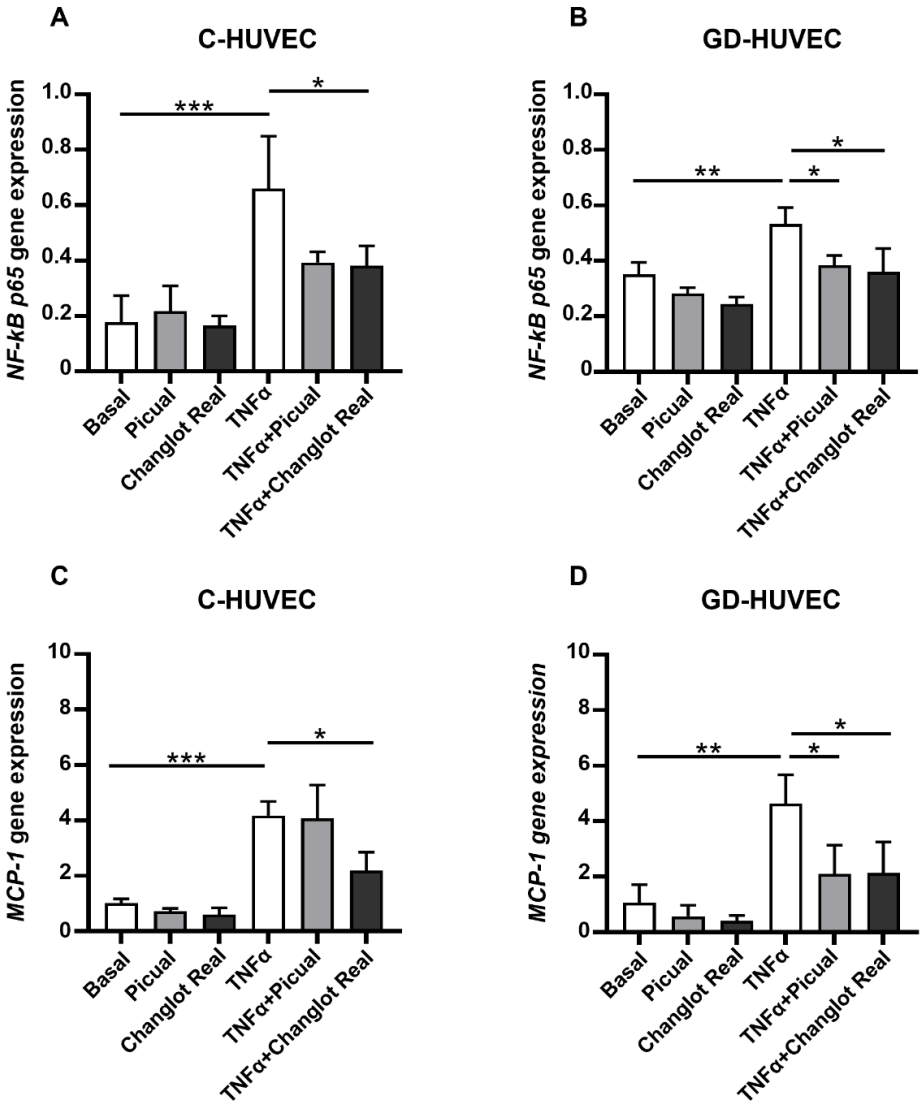


Figure 15. *Picual and Changlot Real phenolic extracts treatment decreases NF-kB p65 and MCP-1 gene expression, with a marked effect in GD-HUVEC.* Relative mRNA expression of *NF-kB p65* (A, B) and *MCP-1* (C, D) in C- and GD-HUVEC following 24-hours treatment with Picual and Changlot Real phenolic extracts (10 µg/mL), with or without 6-hours stimulation with TNFα (10 ng/mL) analysed by RT-PCR. Data are expressed as mean ± SD (n=3). Asterisks point out statistically significant differences between the selected conditions (*p<0.05; **p<0.01; ***p<0.001).

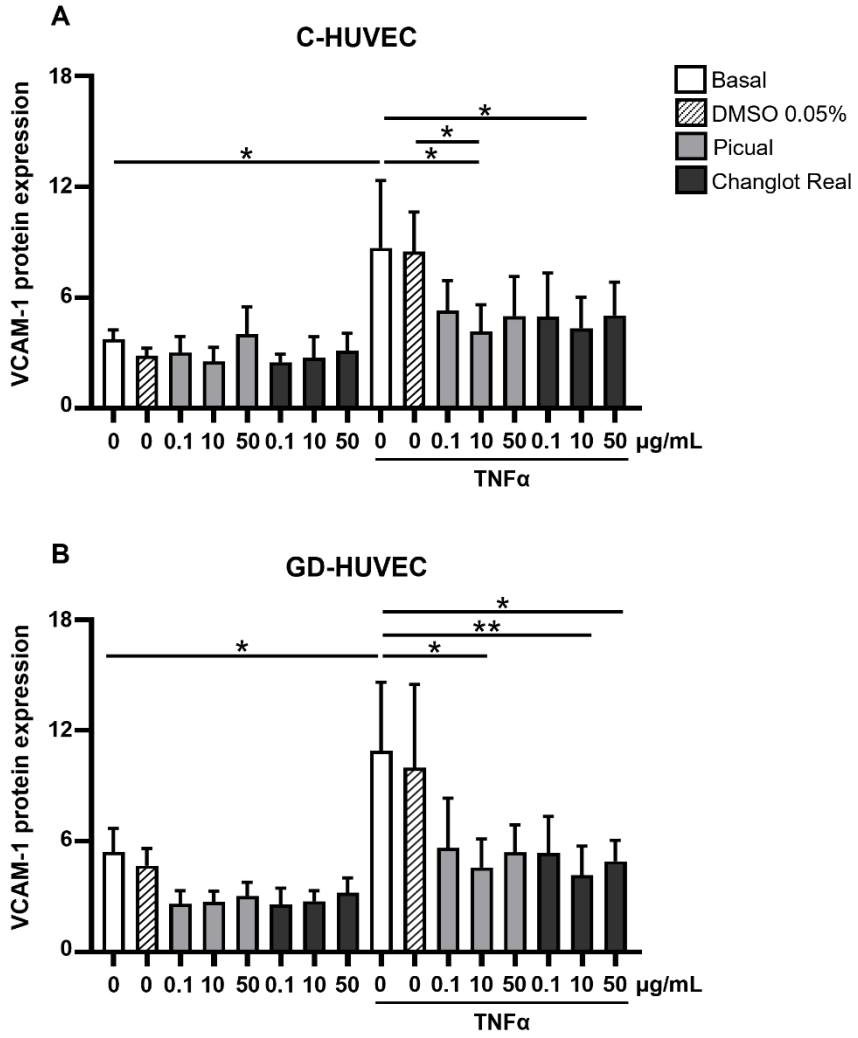


Figure 16. *Picual and Changlot Real phenolic extracts treatment at different concentrations reduces VCAM-1 protein expression in both cell types.* VCAM-1 protein expression in C- (A) and GD-HUVEC (B) following 24-hours treatment with Picual and Changlot Real phenolic extracts at different concentrations (0.1-50 µg/mL) with or without 16-hours stimulation with TNFα (10 ng/mL). Data are expressed as mean ± SD (n=4). Asterisks point out statistically significant differences between the selected conditions (*p<0.05; **p<0.01).

4.2.4 Effects of Picual and Changlot Real phenolic extracts on NF-kB p65 phosphorylation

To deeply elucidate the anti-inflammatory effect of Picual and Changlot Real phenolic extracts, NF-kB p65 phosphorylation on Ser536 was investigated in both C- and GD-HUVEC (**Figure 17**). In basal conditions, NF-kB p65 phosphorylation appeared slightly higher, even though not statistically significant, in GD-HUVEC compared to C-HUVEC.

A significant upregulation in NF-kB p65 phosphorylation, following TNFα stimulation, was identified in both C- and GD-HUVEC. Pre-treatment with Picual phenolic extract promoted an evident reduction trend in NF-kB p65 phosphorylation in both TNFα-stimulated cell types. Comparably, Changlot Real polyphenol extract pre-treatment effectively counteracted TNFα-promoted NF-kB p65 phosphorylation in both cell types, with a more statistically significant effect in GD-HUVEC (**Figure 17A,B**).

These results are consistent with NF-kB p65 nuclear translocation (**Figure 17C**) and previous findings, indicating that the anti-inflammatory property of Picual and Changlot Real phenolic extracts may be regulated through NF-kB pathway downregulation.

4.2.5 Effects of Picual and Changlot Real phenolic extracts on VCAM-1 protein expression

To deeply investigate the signalling pathway mediated by NF-kB p65, VCAM-1 protein expression, a key downstream adhesion molecule which greatly regulates endothelial inflammation, was studied in C- and GD-HUVEC treated with Picual and Changlot Real phenolic extracts with or without TNFα stimulation (**Figure 18**).

GD-HUVEC showed a significantly upregulation of VCAM-1 protein expression compared to control cells in basal conditions, further confirming their pro-inflammatory phenotype. Notably, GD-HUVEC treated with Picual and Changlot Real extracts exhibited decreased VCAM-1 expression, although not statistically significant (**Figure 18B**). Predictably, TNFα stimulation significantly upregulated VCAM-1 protein levels in both cell types, with a more marked effect in GD-HUVEC. Additionally, Picual and Changlot Real phenolic extracts pre-treatment induced a significant reduction in VCAM-1 expression caused by TNFα in both C- and GD-HUVEC, mainly in the latter one (**Figure 18A,B**). These data provide further confirmation of the potential ability of Picual and Changlot Real polyphenol extracts in counteracting vascular inflammation.

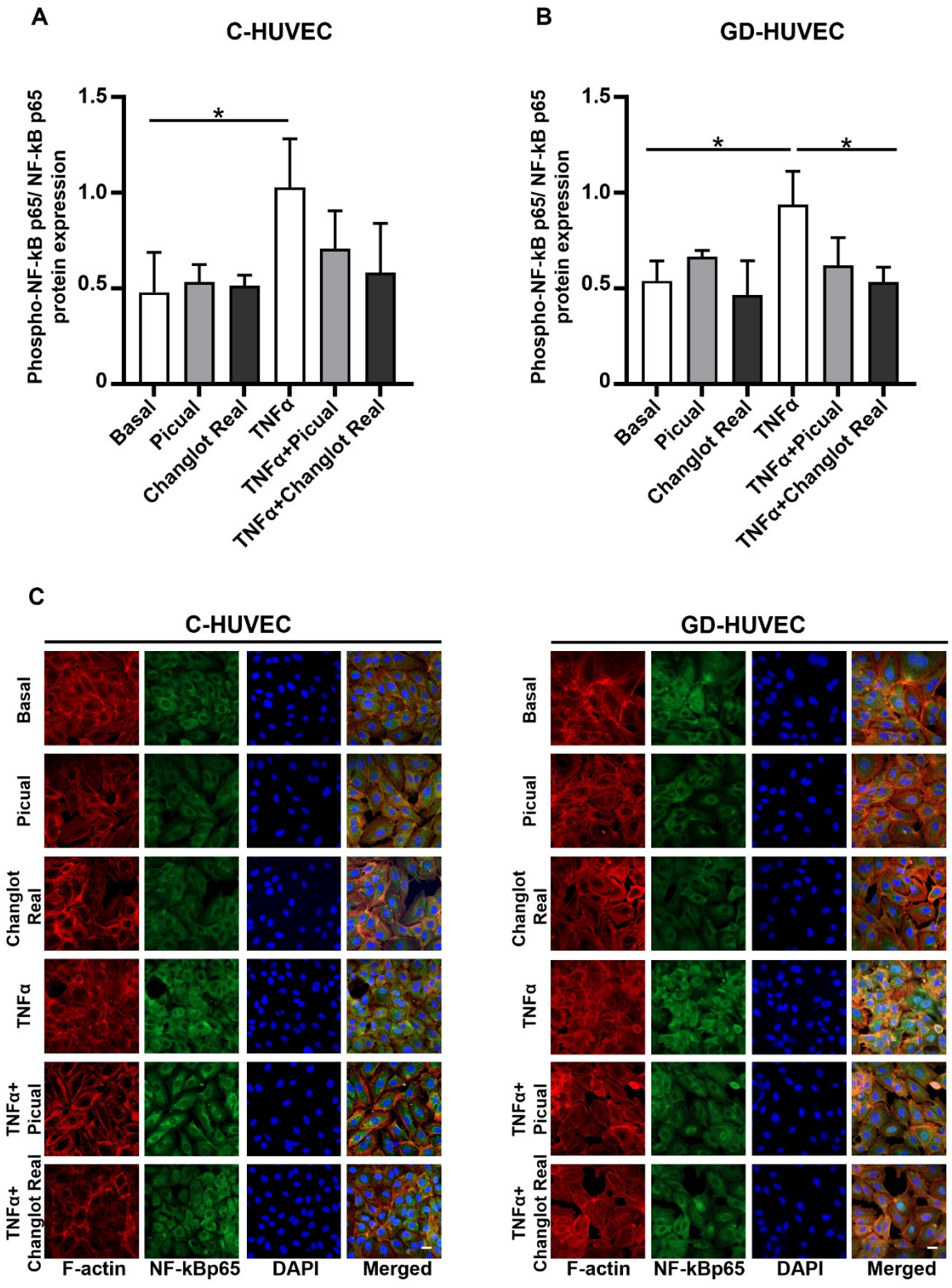


Figure 17. *Picual and Changlot Real phenolic extract treatment decreases NF-kB p65 phosphorylation and nuclear translocation*. Phosphorylated NF-kB p65 (Ser536) to total NF-kB p65 ratio in C- (A) and GD-HUVEC (B). NF-kB p65 nuclear translocation representative figures (C). Cells were treated for 24-hours with Picual and Changlot Real phenolic extracts

(10 µg/mL), with or without 1-hour TNFα stimulation (10 ng/mL). Histograms data are presented as mean ± SD (n=3). Asterisks point out statistically significant differences between the selected conditions (*p<0.05). Scale bar 20 µm.

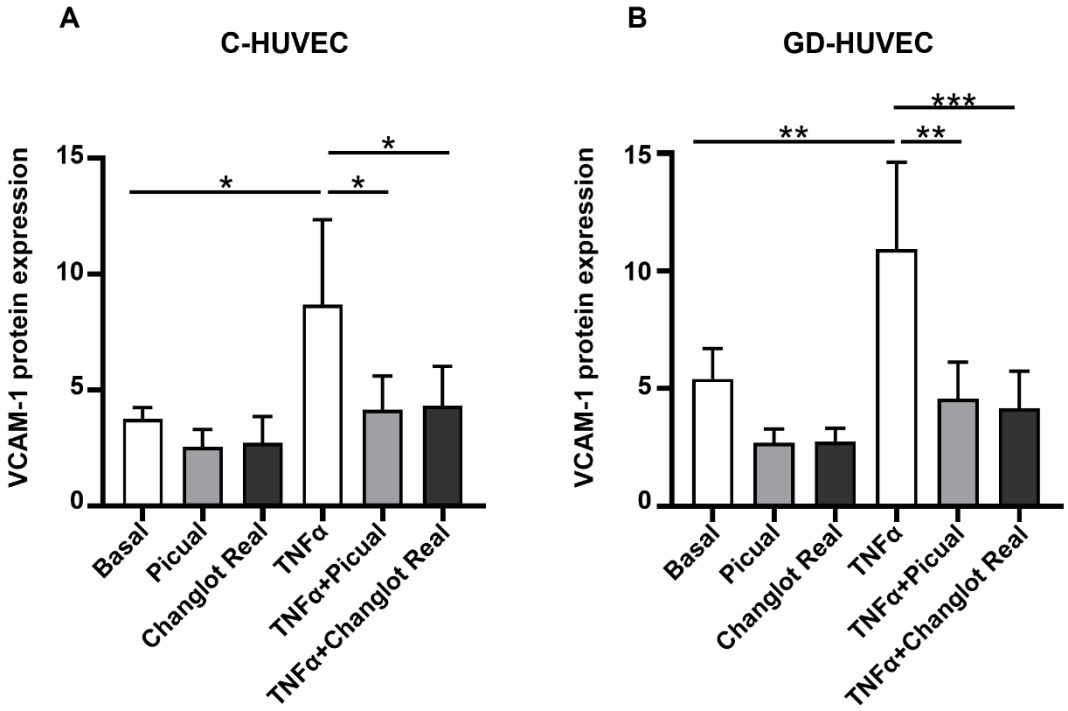


Figure 18. *Changlot Real and Picual phenolic extracts treatment reduces VCAM-1 protein expression in TNFα-stimulated HUVEC.* VCAM-1 protein expression in C- (A) and GD-HUVEC (B) following 24-hours treatment with Changlot Real and Picual phenolic extracts (10 µg/mL) with or without a 16-hours stimulation with TNFα (10 ng/mL) analysed by flow cytometry. Results are presented as mean ± SD (n=4). Asterisks point out statistically significant differences between the selected conditions (*p<0.05;**p<0.01;***p<0.001).

4.2.6 Effects of Picual and Changlot Real phenolic extracts on monocyte–HUVEC interaction

To deeply investigate Picual and Changlot Real phenolic extracts *in vitro* anti-inflammatory effect in a functionally relevant condition, a monocyte adhesion assay was performed. Of note, this experiment closely mimics the early stages of endothelial inflammation in pathological conditions including atherosclerosis. Interestingly, C- and GD-HUVEC pre-treated for 24-hours with Changlot Real phenolic extract showed a significant reduction of TNFα-stimulated monocyte adhesion, strongly confirming its anti-inflammatory role on the endothelium (**Figure 19**).

Additionally, Picual phenolic extract pre-treatment for 24-hours promoted a reduction in TNFα-stimulated monocyte adhesion in both cell types. Anyway, this reduction was statistically significant only in GD-HUVEC, highlighting its selective effect in the diabetic-like endothelial model.

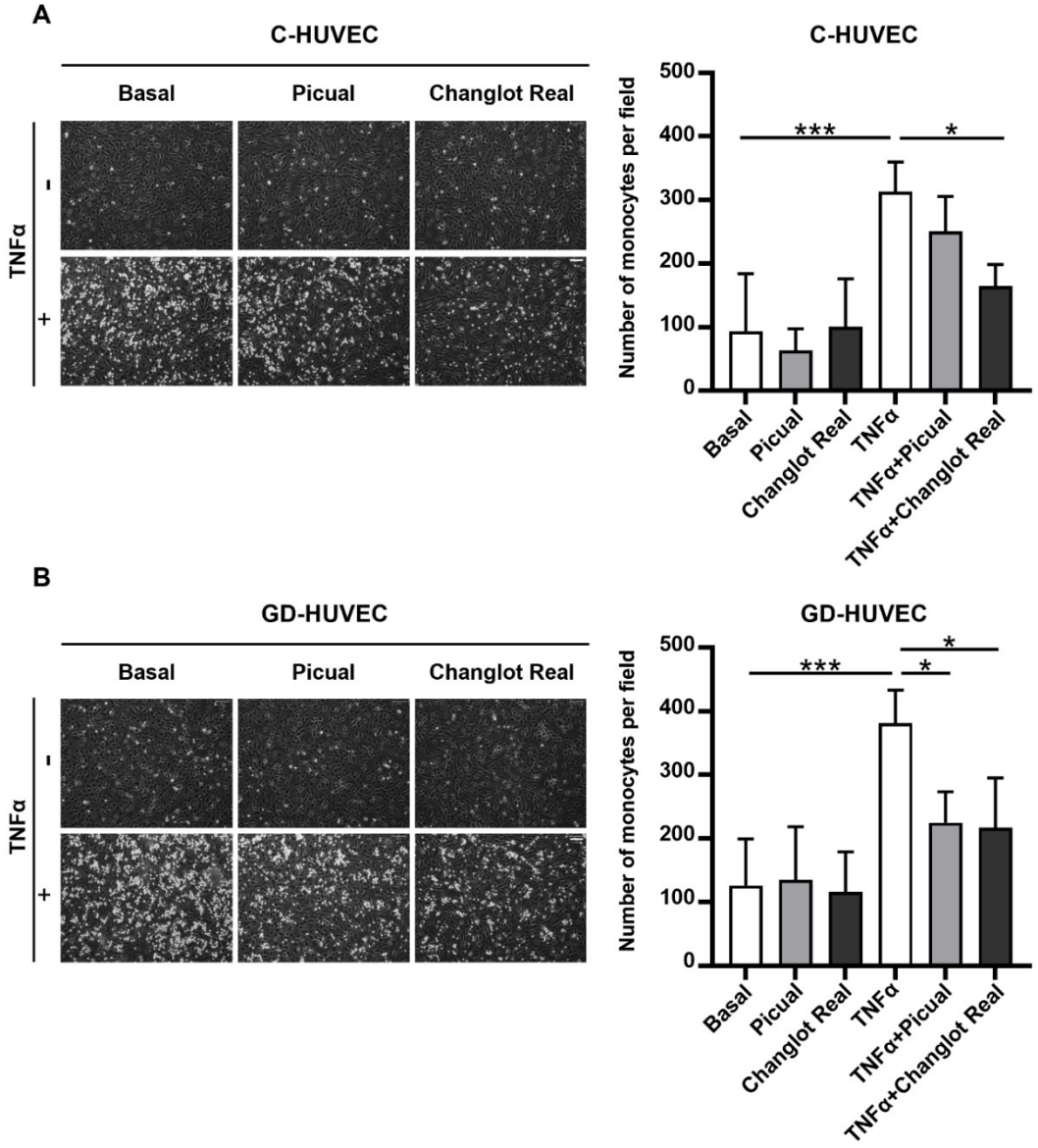


Figure 19. *Picual and Changlot Real phenolic extracts treatment reduces monocytes adhesion in both cell types, with a more marked effect on GD-HUVEC pre-treated with Changlot Real and stimulated with TNFα.* HUVEC–monocyte adhesion assay and relative quantification of adherent monocytes to C- (A) and GD-HUVEC (B) following 24-hours treatment with Changlot Real and Picual phenolic extracts (10 µg/mL), with or without 16-hours stimulation with TNFα (10 ng/mL). Data are expressed as mean ± SD (n = 4). Asterisks point out statistically significant differences between the selected conditions (*$p<0.05$; ***$p<0.001$). Scale bar 100 µm.

4.3 DISCUSSION

This study demonstrated the anti-inflammatory effect of two phenolic extracts, obtained from the olive leaves of Picual and Changlot Real monocultivars, on diabetic endothelium reproduced by the *in vitro* model of GD-HUVEC. These cells, having being exposed to hyperglycaemia *in vivo*, acquired epigenetic modifications that recapitulate key features of endothelial dysfunction, including persistent inflammation. Therefore, GD-HUVEC represent a unique *in vitro* system for investigating the anti-inflammatory properties mediated by olive leaf phenolic compounds (Di Pietrantonio N et al, 2024; Di Tomo P et al, 2012).

Consistent with our previous findings, differences between C- and GD-HUVEC, in basal conditions, were confirmed. In particular, *NF-kB p 65* mRNA levels as well as VCAM-1 protein expression, crucial regulators of endothelial inflammation, were upregulated in GD-HUVEC compared to control cells. These results highlight the pro-inflammatory phenotype of GD-HUVEC and further support their role as a unique *in vitro* model of diabetic vascular dysfunction (Di Pietrantonio N et al, 2024; Di Fulvio P et al, 2014; Di Tomo P et al, 2021).

Picual and Changlot Real extracts were characterized by HPLC-ESI-TOF-MS analysis, revealing an elevated and variegated amount of polyphenols. Changlot Real extract exhibited a higher content of total phenolic compounds, mainly in secoiridoids known for their potent bioactivity, compared to Picual. These data are in line with Talhaoui N et al (2015) that claims oleuropein as the prevalent constituent of olive leaf extracts (Talhaoui N et al, 2015).

Both phenolic extracts not induced cytotoxicity to endothelial cells in all tested concentrations, ranging from 0.1 µg/mL to 100 µg/mL, suggesting that the extracts, not altering cell integrity and viability, could be used as potential therapeutic strategy.

From a molecular perspective, the anti-inflammatory effect of the extracts were evidenced by the downregulation of crucial vascular inflammatory markers. Specifically, Picual and Changlot Real pre-treatment, with or without TNFα stimulation, induced a significant reduction in *NF-kB p65* and *MCP-1* gene expression. Of note, Changlot Real showed a wider effect, being effective in both C- and GD-HUVEC, while Picual exhibited a stronger effect exclusively in GD-HUVEC. These differences may be attributable to variations in phenolic prolife or bioavailability between the two monocultivars, suggesting that the broader effect of Changlot Real could be linked to its elevated total phenolic content.

Moreover, NF-kB p65 phosphorylation at Ser536, a key activation step in its signalling pathway, was attenuated by both extracts, especially in GD-HUVEC upon TNFα stimulation,

supporting the hypothesis that polyphenols treatment was more effective in pathological conditions associated with endothelial dysfunction.

In addition, VCAM-1 protein expression, one of the direct NF-kB downstream molecules strongly involved in monocytes recruitment during vascular inflammation, was significantly downregulated following extract treatment, mainly in GD-HUVEC.

Contextually, Changlot Real treatment induced a significant reduction in TNFα induced monocytes-endothelial cells interaction in both cell types, a critical early event in the atherosclerosis process. In contrast, Picual exerted a comparable effect only in GD-HUVEC.

Collectively, these findings demonstrate the anti-inflammatory effect of both Picual and Changlot Real phenolic extracts via NF-kB pathway, positively modulating transcriptional and post-translational activations of the main inflammatory markers and thus, reducing monocytes recruitment. A wider and stronger effect was identified for Changlot Real extract, probably due to its high content of total phenolic compounds and in particular, due to its elevated amount of secoiridoids, known as potent regulators of inflammation and oxidative stress.

These results are further supported by evidence from the literature. Indeed, our recent work on oleanolic acid, a triterpenes isolated also from olive trees, showed anti-inflammatory effects on GD-HUVEC by modulating gene and protein expression as well as activation of the main vascular inflammatory markers supporting its role in counteracting hyperglycaemia induced endothelial dysfunction (Stelling-Férez J et al, 2023).

In addition, many *in vivo* studies results corroborate our findings. Specifically, OLE supplementation in aged rats enhanced endothelial function and improved metabolic parameters, including the reduction in pro-inflammatory cytokines such as TNFα and IL-6. Moreover, these studies demonstrated that OLE supplementation upregulated antioxidant gene expression, suggesting its potential protective role in age-related vascular dysfunction (González-Hedström D et al, 2021). Several clinical trials reported better insulin sensitivity upon OLE supplementation and additional studies confirmed the safety of *Olea Europaea* leaf extracts (de Bock M et al, 2013; Clewell AE et al, 2016).

Overall, these results are fully consistent with our findings, suggesting that polyphenols from olive leaf monocultivar extracts, in particular Changlot Real, may represent a promising natural strategy to mitigate endothelial inflammation in the context of diabetes-associated vascular complications.

Nevertheless, a clear limitation of this study is the inability to assess potential sex-specific differences, which are known to influence metabolic responses and long-term health outcomes, especially in gestational diabetes. Moreover, it should be noted that these

observations are limited to an *in vitro* model and additional *in vivo* studies are required to further validate our data. Finally, further research is necessary to better delineate the specific active components responsible for the anti-inflammatory effects and to elucidate the underlying mechanisms of action.

5 ANGIOGENESIS: ROLE OF AMNIOTIC MEMBRANE VIA VEGFR2/AKT/ENOS SIGNALLING PATHWAY (*AIM 2*)

5.1 MATERIALS AND METHODS

5.1.1 Amniotic Membrane collection and storage

The amniotic membrane was processed as previously described by Ruiz-Cañada C et al (2018) and Pipino C et al (2022).

Briefly, the placenta from healthy donors was obtained from uncomplicated caesarean section. After the delivery, the foetal membranes were rapidly transferred to the laboratory under sterile conditions. Under a laminar flow cabinet, the amniotic membrane was mechanically peeled from the chorion starting with an incision near to the umbilical cord base, washed three times with 200 mL of PBS, and flattened onto the sterile nitrocellulose paper (cat n. 88018, Thermo Fisher Scientific) with the epithelial layer surfaced up, and the spongy layer facing to the nitrocellulose paper. Then, the amniotic membrane adhered to the nitrocellulose paper was cut with a scalpel into 2cm×2cm pieces. Hence, AM fragments were separated from nitrocellulose paper using forceps and placed in sterile cryovials containing Foetal Bovine Serum (FBS, Gibco, Thermo Fisher Scientific) with 10% of dimethyl sulfoxide (DMSO) (Sigma-Aldrich, Germany). Cryovials were initially frozen at −80°C and later preserved in liquid nitrogen (-196°C) until further use.

On the day of the experiment, AM pieces were thawed at 37°C, the pieces were washed three times with DMEM supplemented with 1% penicillin/streptomycin (Sigma-Aldrich, Germany) and placed at 37°C in a 7.5% CO2 incubator for 2-hours for the re-vitalization of the amniotic membrane cells. Then, for amniotic membrane treatment, a ratio of number of pieces of amniotic membrane per cultivated cell surface was established according to the following rationale: one pieces of AM (4 cm^2) in a well of a 6-well plate.

For the experiment replicates, a different AM donor was employed each time.

5.1.2 HUVEC isolation and culture

Umbilical cords were obtained from randomly recruited healthy Caucasian mothers (Control, C) and women affected by Gestational Diabetes (GD) in the third trimester of pregnancy followed by 'Diabetes and Pregnancy Clinic' until delivery at the Hospital Santo Spirito of Pescara (Italy). GD women were treated with diet only and women with pre-gestational diabetes were excluded.

Women matched by age and body mass index (BMI) were divided into two groups, one normoglycemic/healthy controls (basal glycaemia < 5.1 mmol/L, oral glucose tolerance test (OGTT) 1h < 10 mmol/L and OGTT 2h < 8.5 mmol/L, n=4) and the other diagnosed with gestational diabetes (basal glycaemia ≥ 5.1 mmol/L, OGTT 1h ≥ 10 mmol/L, and OGTT 2h ≥ 8.5 mmol/L, GD, n=4) according to the criteria of the American Diabetes Association (American Diabetes Association Professional Practice Committee, 2022).

All procedures agreed with the Declaration of Helsinki principles and with the ethical standards of the Institutional Committee on Human Experimentation (*details in the paragraph 4.1.3*).

HUVEC isolation and culture protocol is detailed in the *paragraph 4.1.4*.

5.1.3 Experimental protocol

C- and GD-HUVEC were plated in different multi-well plates, according to the specific experiment, until 80% confluence is reached. Cells were starved for 2-hours with 0.1% FBS. Then, cells were treated with AM or $VEGFa_{165}$ (cat #100-20-10UG, Peprotech, 20 ng/mL) for 1- or 6- or 24-hours, according to the specific experimental protocol, and the FBS concentration was raised to 1%. In some experiments, a selective VEGFR2 inhibitor, Ki8751 (ab141266, Abcam, 100 nM) was used 30 minutes before the AM or $VEGFa_{165}$ treatment (**Figure 20**).

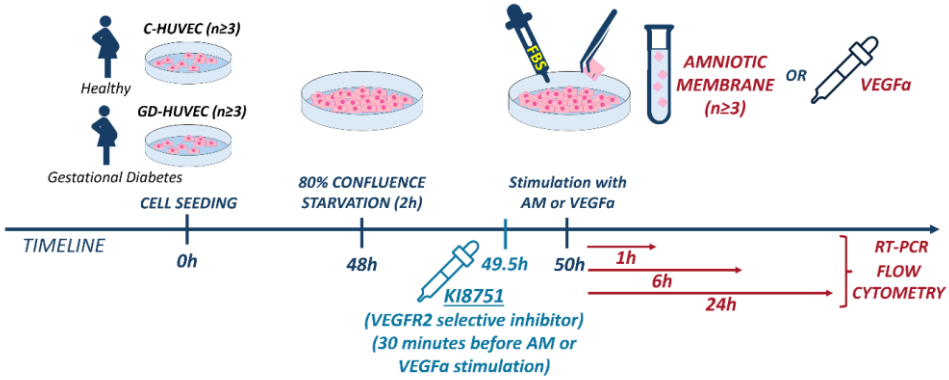


Figure 20. *Experimental plan.* Briefly, C- and GD-HUVEC were starved for 2-hours with 0.1% FBS and then, treated with AM or $VEGFa_{165}$ (20 ng/mL) for different timing. For some experiments, Ki8751 (100 nM) was pre-incubated 30 minutes before the treatment.

5.1.4 MTT assay

To determine the effect of $VEGFa_{165}$ and Ki8751 on C- and GD-HUVEC viability, the MTT assay was carried out *(detailed protocol in the paragraph 4.1.5).*

In particular, HUVEC were treated for 24-hours with increasing concentrations of $VEGFa_{165}$, ranging from 1 ng/mL to 100 ng/mL, and of Ki8751, ranging from 0.1 nM to 100 nM. Vehicle matched controls (DMSO 0.1%) were used exclusively for Ki8751.

5.1.5 RNA extraction and real-time quantitative PCR

The total RNA was isolated, extracted, quantified, retrotranscribed and amplified from HUVEC in basal conditions and following 6-hours AM treatment, according to the detailed protocol in the *paragraph 4.1.6.* The following TaqMan Gene Expression Assay probes for human VEGFa (Hs00900025_m1, Thermo Fisher Scientific), VEGFR2 (Hs00911700_m1, Thermo Fisher Scientific) and GAPDH (Hs02786624_g1, Thermo Fisher Scientific) were used according to the manufacturer's instructions.

All samples were analysed in technical duplicate. The relative expression of the target genes was calculated using the $2^{-\Delta Ct}$ (for the comparison between C- and GD-HUVEC in basal conditions) and the $2^{-\Delta\Delta Ct}$ method (for the comparison between the basal condition and the AM treatment) using GAPDH as housekeeping (Applied Biosystems QuantStudio 7 Pro Real-Time PCR System, Thermo Fisher Scientific).

5.1.6 Flow cytometry analysis

See flow cytometry analysis detailed protocol in the *paragraph 4.1.8*.

Cells were treated with AM or $VEGFa_{165}$ for 1-hour to evaluate VEGFR2 and AKT activation, identified as the phosphorylated to total ratio, and for 24-hours to evaluate VEGFR2 total protein expression, nitro-tyrosine and superoxide anion production. Exclusively for

VEGFR2 activation and nitro-tyrosine levels, cells were also pre-incubated 30 minutes with or without Ki8751.

To determine VEGFR2 total protein expression, VEGFR2 and AKT activation and nitro-tyrosine production cells were fixed, permeabilized (according to the protocol detailed in the *paragraph 4.1.8*) and incubated with primary antibodies: anti-VEGFR2 (ab2349, Abcam, 1:200), anti-phospho-VEGFR2 Tyr951 (ab38473, Abcam, 1:50), anti-AKT (cat #92725, Cell Signaling Technology, 1:100), anti-phospho-AKT Ser473 (cat #92715, Cell Signaling Technology, 1:25) and, anti-nitrotyrosine (39B6) Alexa Fluor 488 conjugated (cat NB110-96877AF488, NOVUSBIO, 1:100) for 30 minutes at 4°C. A subsequent incubation with PE-conjugated secondary antibody (cat 111-116-144, Jackson Immuno Research laboratories, 1:100) and Alexa Fluor 488-conjugated secondary antibody (cat #A-11034, Thermo Fisher Scientific, 1:100) was performed for 30 minutes at 4°C.

To evaluate superoxide anion levels, cells were treated with AM or $VEGFa_{165}$ for 24-hours. After that, cells were detached, centrifuged and incubated with hydroethidine (D1168, Thermo Fisher Scientific, 5µm) for 30 minutes at 37°C in a 7.5% CO^2 incubator.

All results are expressed as the Mean Fluorescence Intensity (M.F.I.) Ratio, calculated by dividing the M.F.I. of positive events by the M.F.I. of negative events (M.F.I. of the secondary antibody).

5.1.7 Matrigel tube formation assay

C- and GD-HUVECs were plated 2.5×10^4 cells/well in the growth factor–reduced basement membrane matrix gel (Matrigel, BD Biosciences) coated 96-well plates using 1% FBS HUVEC culture medium, consistent with the experimental protocol detailed in the *paragraph 5.1.3*. After plating, the cells were incubated 20 minutes at 37°C to allow cellular adhesion to Matrigel and then, in the respective wells, Ki8751 (100 nM) was added for 30 minutes. Subsequently, AM floating pieces or VEGFa (20 ng/mL) were added in the culture medium. 6-hours later representative photographs were acquired using EVOS M5000 Cell Imaging Systems (Thermo Fisher Scientific). Images were processed using ImageJ software (Angiogenesis analyser tool) to analyse angiogenic parameters (i.e., number of segments, meshes, and master junctions) in all the tested conditions.

5.1.8 Statistical analysis

All experimental data are expressed as mean ± Standard Deviation (SD). Each experiment was conducted in technical triplicates using at least 3 independent donors of C- and GD-HUVEC and of AM. The normal distribution of quantitative data was assessed by the Shapiro–Wilk test. T-test or Mann-Whitney test, according to data normal distribution, were used to compare two data sets. One-way ANOVA test or Kruskal-Wallis's test, according to data normal distribution, followed by Dunnett's or Dunn's or Tukey's test were used for multiple comparisons. Probability values were calculated considering a 95% compatibility interval. All analyses were performed with GraphPad Prism (version 9, GraphPad Software).

5.2 RESULTS

5.2.1 Effect of AM on *VEGFa* gene expression

To investigate the AM pro-angiogenic effect mediated by the VEGFR2 signalling pathway, *VEGFa* gene expression was evaluated in both C- and GD-HUVEC in basal conditions and following 6-hours AM treatment (**Figure 21**).

In basal conditions, GD-HUVEC showed a trend of enhanced *VEGFa* gene expression compared to control cells (**Figure 21A**). Cells were, then, treated with AM for 6-hours. The results showed that AM treatment induced an upregulation of *VEGFa* mRNA levels, even if not significant, in both cell types (**Figure 21B,C**).

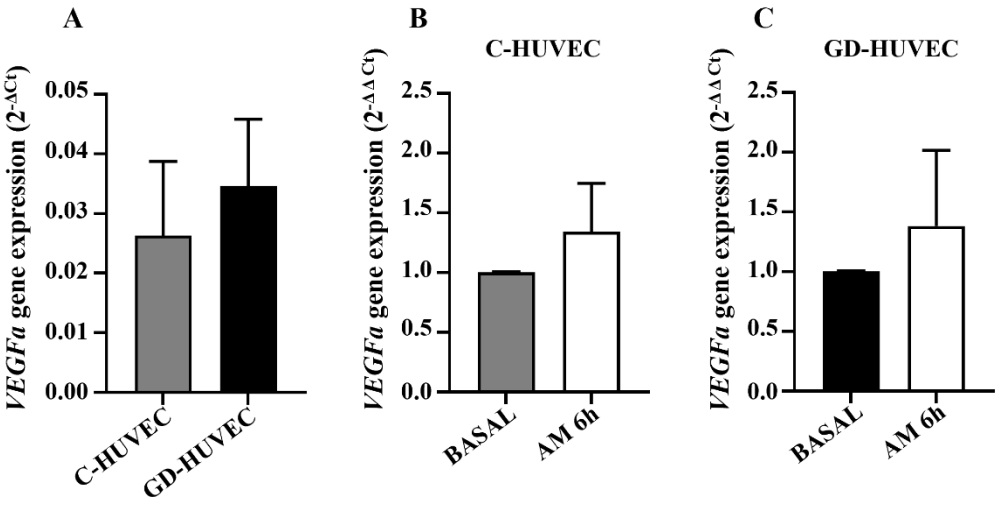


Figure 21. *GD-HUVEC show an upregulated trend of VEGFa mRNA levels compared to control cells. AM treatment induces a trend of increased VEGFa gene expression in both cell types.* Relative mRNA expression of *VEGFa* in basal conditions (A) and in C- (B) and GD-HUVEC (C) following 6hours treatment with AM analysed by RT-PCR. Data are expressed as mean ± SD ($n \geq 3$).

5.2.2 Effect of AM on VEGFR2 gene and protein expression

To further investigate the AM pro-angiogenic effect mediated by VEGFR2 signalling pathway, VEGFR2 gene and total protein expression were evaluated in basal conditions and following 6- and 24-hours AM incubation, respectively (**Figure 22**).

In basal conditions, GD-HUVEC showed an increased trend of *VEGFR2* gene and protein expression compared to C-HUVEC (**Figure 22A,D**).

Interestingly, AM treatment for 6-hours induced a significant upregulation of *VEGFR2* mRNA levels in both cell types (**Figure 22 B,C**). In addition, AM treatment for 24-hours induced a non-significant increasing trend of VEGFR2 total protein expression in control cells, while no differences were detected in GD-HUVEC (**Figure 22 E,F**).

These results suggest that AM treatment more markedly modulates the mRNA levels of early mediators involved in the VEGFR2-associated signalling pathway.

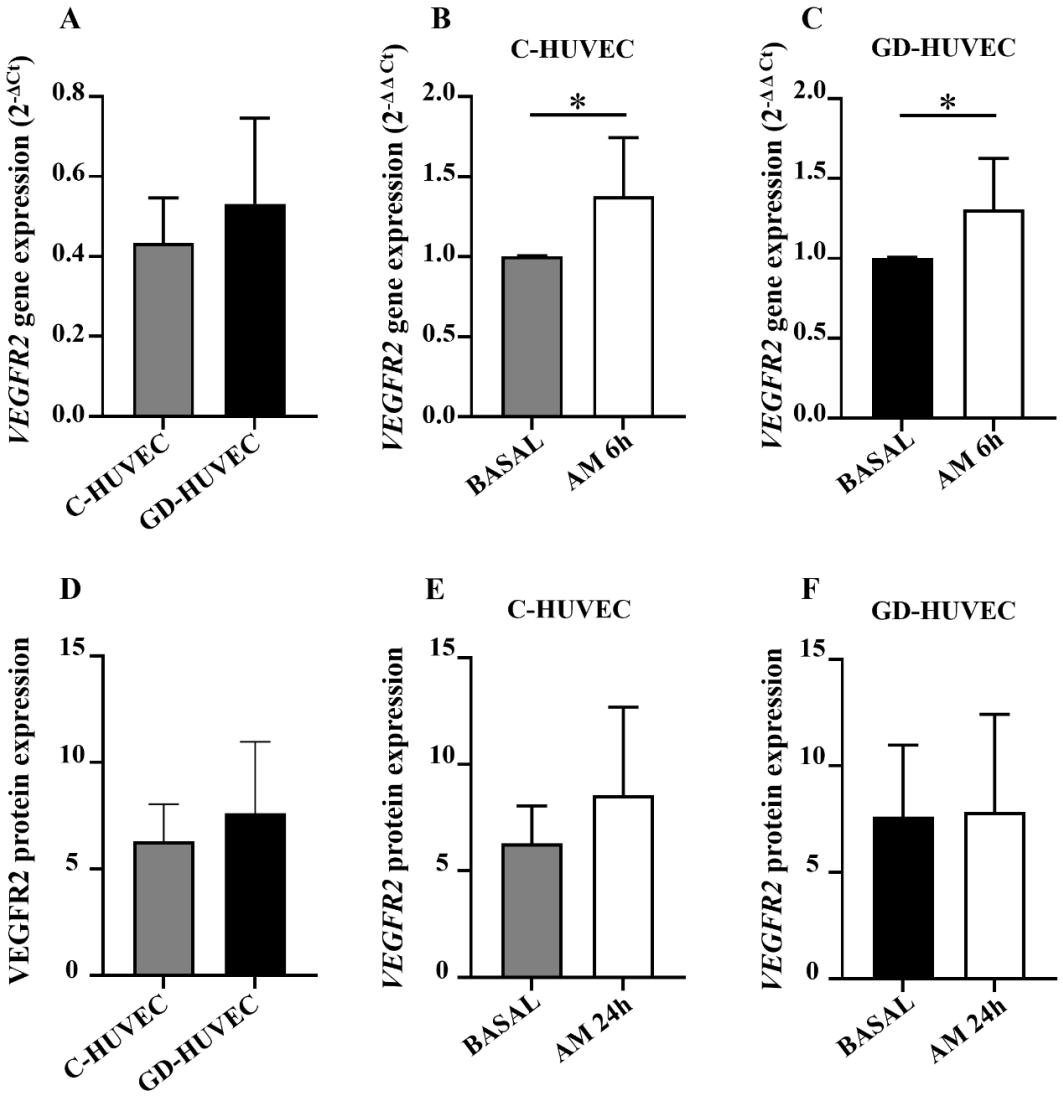


Figure 22. *GD-HUVEC show an increased trend of VEGFR2 mRNA and protein levels compared to control cells in basal conditions. AM incubation promotes a significant increase of VEGFR2 gene expression in both cell types, while no differences were detected for VEGFR2 total protein levels.* Relative mRNA expression (A-C) and total protein expression (D-F) of VEGFR2 in C- and GD-HUVEC in basal conditions and following 6- and 24-hours treatment with AM analysed by RT-PCR and flow cytometry, respectively. Data are expressed as mean ± SD ($n \geq 3$). Asterisks point out statistically significant differences between the selected conditions (*$p<0.05$).

5.2.3 Effect of AM on VEGFR2 activation

To deeply investigate the potential pro-angiogenic effect of AM via the VEGFR2 mediated signalling pathway its activation was evaluated. In particular, the VEGFR2 phosphorylated (at Tyr 951) to total ratio, in basal conditions and following 1-hour AM or $VEGFa_{165}$ (positive control, 20 ng/mL) treatment was quantified (**Figure 23**).

Different $VEGFa_{165}$ concentrations, ranging from 1 ng/mL to 100 ng/mL, were tested for cytotoxicity in C- and GD-HUVEC treated for 24-hours. The MTT results showed non-significant changes in cell viability in both cell types for all tested concentrations. Thus, the most effective $VEGFa_{165}$ concentration (20 ng/mL) was chosen according to the literature (**Figure 24**).

Interestingly, GD-HUVEC showed a decreasing trend of VEGFR2 activation compared to control cells in basal conditions (**Figure 23A**).

Of note, a significant increase in VEGFR2 activation following 1-hour $VEGFa_{165}$ stimulation was detected in GD-HUVEC while only an increasing trend was detected in control cells, further confirming the role of $VEGFa_{165}$ as positive control (**Figure 23 B,C**).

In addition, 1-hour AM treatment enhanced VEGFR2 activation, reaching statistical significance in GD-HUVEC (**Figure 23 B,C**).

These findings suggest that AM promotes VEGFR2 activation, potentially triggering its downstream signalling cascade, with a similar extend to the positive control $VEGFa_{165}$ in GD-HUVEC.

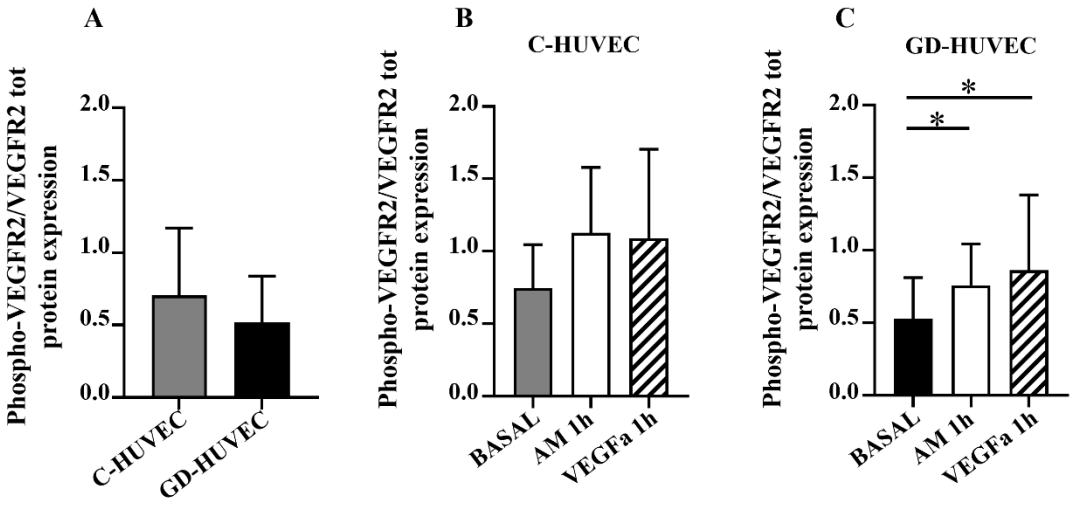


Figure 23. *GD-HUVEC show a trend of decrease in VEGFR2 activation compared to control cells. AM, as well as VEGFa$_{165}$, 1-hour treatment promotes a significant VEGFR2 activation in GD-HUVEC while control cells show a trend of upregulation*. VEGFR2 phosphorylated (Tyr951) to total ratio in C- and GD-HUVEC in basal conditions (A) and following 1-hour AM or VEGFa$_{165}$ stimulation (B,C) analysed by flow cytometry. Data are expressed as mean ± SD (n ≥ 3). Asterisks point out statistically significant differences between the selected conditions (*p<0.05).

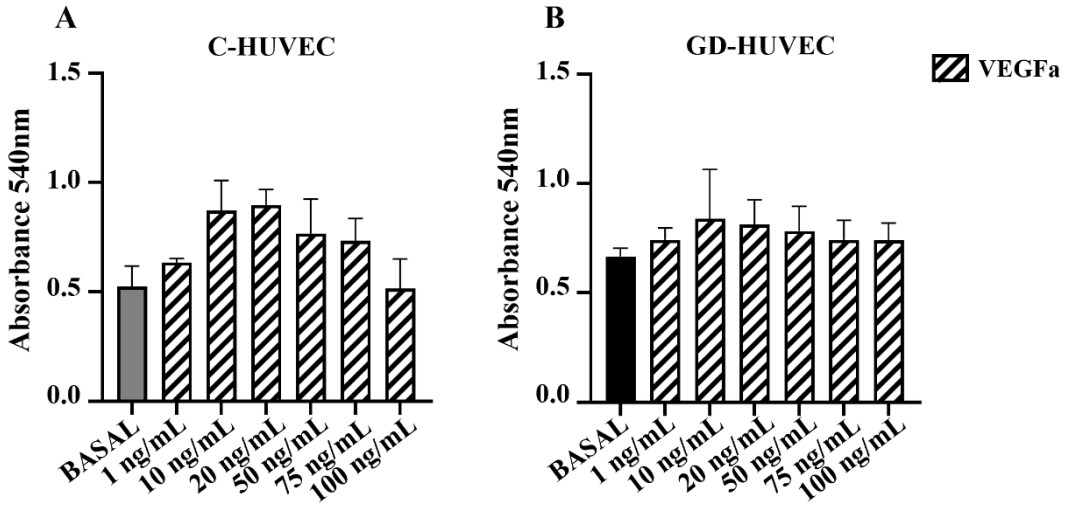


Figure 24. *VEGFa$_{165}$ treatment do not induce changes in cell viability*. Cell viability of C- (A) and GD-HUVEC (B) following 24-hours treatment with VEGFa$_{165}$ at different concentrations (1–100 ng/mL) analysed by MTT assay. Data are expressed as mean ± SD (n = 3).

5.2.4 Effect of AM on AKT activation

To unravel the signalling pathway activated by VEGFR2, AKT activation was also evaluated. In particular, the AKT phosphorylated (at Ser473) to total ratio in basal conditions and following 1-hour incubation with AM or $VEGFa_{165}$ was quantified (**Figure 25**).

Interestingly, GD-HUVEC showed, in basal conditions, a significant reduction in AKT activation compared to control cells (**Figure 25A**). AM and $VEGFa_{165}$ 1-hour stimulation do not induce significant differences in AKT activation in C-HUVEC (**Figure 25B**). Of note, GD-HUVEC showed a significant increase in AKT activation, compared to the basal condition, following 1-hour AM incubation. $VEGFa_{165}$ treatment in GD-HUVEC induced a trend of enhancement, even if not significant (**Figure 25C**).

These findings demonstrate that AM activates AKT, through Ser473 phosphorylation, only in GD-HUVEC which show, in basal conditions, a significant reduction in its activation compared to control cells. Thus, these results highlight the ability of AM to restore AKT activation in GD-HUVEC to levels comparable to the basal condition of control cells.

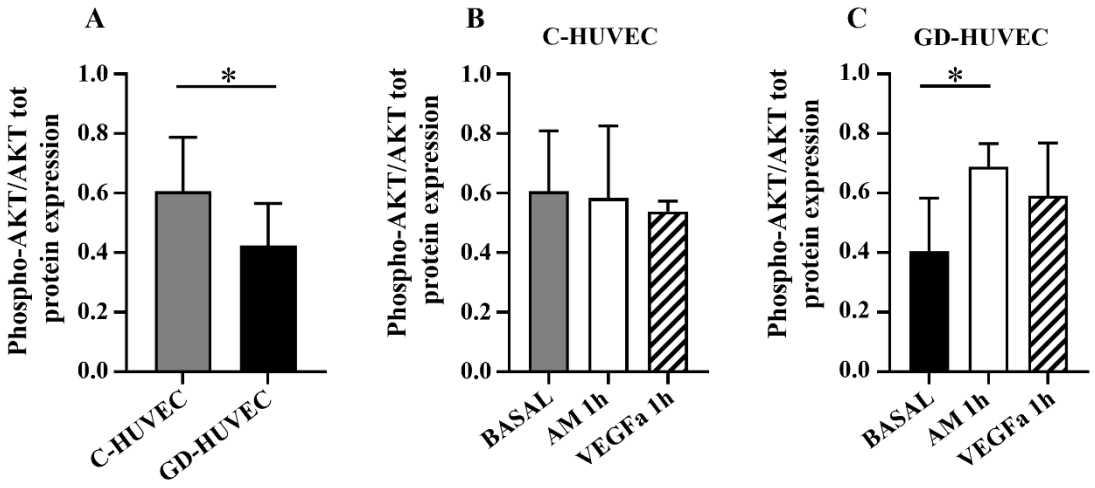


Figure 25. *GD-HUVEC show a significant downregulation of AKT activation compared to control cells in basal conditions. AM treatment induce a significant increase of AKT activation in GD-HUVEC, while C-HUVEC show no changes.* AKT phosphorylated (Ser473) to total ratio in C- and GD-HUVEC in basal conditions (A) and following 1-hour AM or $VEGFa_{165}$ stimulation (B,C) analysed by flow cytometry. Data are expressed as mean ± SD ($n \geq 3$). Asterisks point out statistically significant differences between the selected conditions (*$p<0.05$).

5.2.5 Effect of AM on nitro-oxidative stress

To further investigate the role of AM in VEGFR2 mediated signalling pathway, nitro-tyrosine and superoxide anion levels were quantified. Activation of AKT leads to eNOS induction which, in turn, produces nitric oxide (NO). Under pathological conditions such as diabetes, NO interacts with superoxide anion resulting in peroxy-nitrite formation, which contributes to increased nitro-tyrosine levels and supports diabetic nitro-oxidative stress.

GD-HUVEC showed significantly increased levels of both nitro-tyrosine and superoxide anion compared to C-HUVEC, confirming the pro-oxidative phenotype of this *in vitro* model (**Figure 26A,D**).

In particular, 24-hours treatment with AM or $VEGFa_{165}$, do not induced any changes in both nitro-tyrosine and superoxide anion levels in C-HUVEC (**Figure 26B,E**).

Interestingly, GD-HUVEC showed significant reduction in both nitro-tyrosine expression and superoxide anion levels following 24-hour AM treatment (**Figure 26C,F**).

Notably, $VEGFa_{165}$ treatment for 24-hours promoted a significant decrease in nitro-tyrosine levels and a non-significant downregulation of superoxide anion in GD-HUVEC (**Figure 26C,F**).

These findings suggest that GD-HUVEC, showing a pro-oxidative phenotype characterized by increased levels of both nitro-tyrosine and superoxide anions, positively respond to AM treatment, as well as to $VEGFa_{165}$, reducing nitro-oxidative stress. On the contrary, control cells, characterized by lower levels of both nitro-tyrosine and superoxide anion, do not respond to AM treatment.

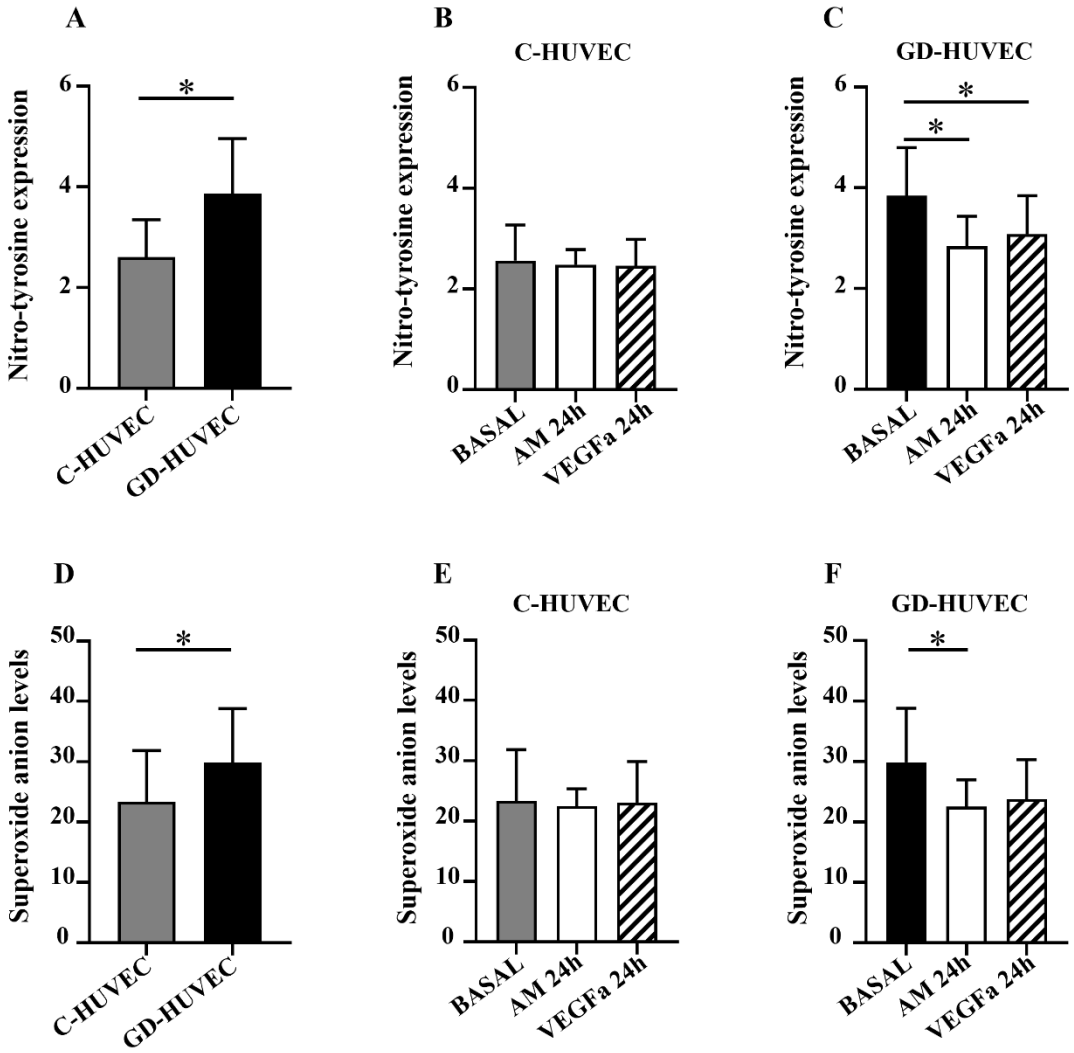


Figure 26. *GD-HUVEC show a significant increase in both nitro-tyrosine and superoxide anion levels compared to control cells in basal conditions. AM treatment promotes a significant reduction of both oxidative markers in GD-HUVEC.* Nitro-tyrosine and superoxide anion levels in C- and GD-HUVEC in basal conditions (A,D) and following 1-hour AM or $VEGFa_{165}$ stimulation (B,C,E,F) analysed by flow cytometry. Data are expressed as mean ± SD ($n \geq 3$). Asterisks point out statistically significant differences between the selected conditions (*$p<0.05$).

5.2.6 Effect of AM on VEGFR2 activation counteracted by VEGFR2 inhibitor

To deeply investigate the AM-promoted activation of the VEGFR2 downstream signalling cascade, cells were pre-treated with Ki8751, a selective VEGFR2 inhibitor, and then incubated with AM or $VEGFa_{165}$ (**Figure 27**).

Different Ki8751 concentrations, ranging from 0.1 nM to 100 nM, were tested for cytotoxicity in C- and GD-HUVEC treated for 24-hours. The MTT results showed non-significant changes in cell viability in both cell types for all tested concentrations. Thus, the most effective Ki8751 concentration (100nM) was chosen according to the literature (**Figure 28**).

Control cells showed an increased trend of VEGFR2 activation when treated 1-hour with AM or $VEGFa_{165}$, as previously demonstrated in **Figure 23B**. This trend was reverted, not significantly, when C-HUVEC were pre-incubated with VEGFR2 inhibitor **(Figure 27A**).

In addition, GD-HUVEC showed a significant upregulation of VEGFR2 phosphorylated to total ratio when incubated with AM or $VEGFa_{165}$, as previously mentioned in **Figure 23C**. Interestingly, AM or $VEGFa_{165}$ promoted upregulation in GD-HUVEC was significantly abolished following Ki8751 pre-treatment. Of note, VEGFR2 activation was downregulated to levels comparable to the basal condition (**Figure 27B**).

These results demonstrate that the AM driven VEGFR2 activation is comparable to the one trigger by $VEGFa_{165}$ treatment and that, this activation is completely abolished in the presence of a selective VEGFR2 inhibitor in GD-HUVEC. These findings suggest a possible release of VEGFa from AM as a possible driver of the VEGFR2 signalling pathway activation.

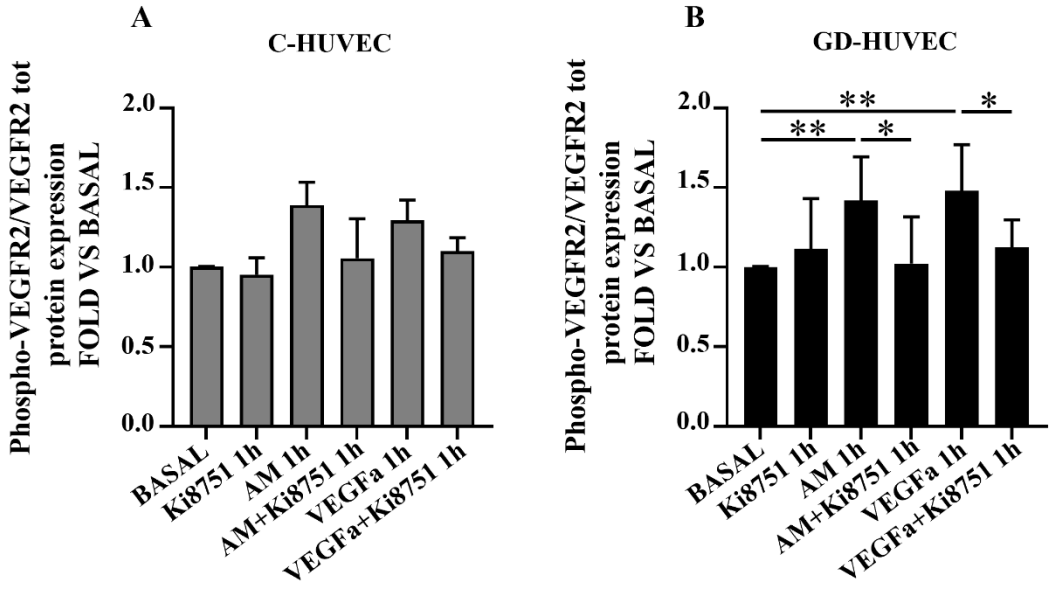


Figure 27. *AM and VEGFa$_{165}$ induces a significant upregulation of VEGFR2 activation in GD-HUVEC, significantly reverted following Ki8751 stimulation.* VEGFR2 phosphorylated (Tyr951) to total ratio in C- (A) and GD-HUVEC (B) following 1-hour AM or VEGFa$_{165}$ stimulation with or without Ki8751 treatment, analysed by flow cytometry. Data are expressed as mean ± SD (n ≥ 3). Asterisks point out statistically significant differences between the selected conditions (*p<0.05; **p<0.01).

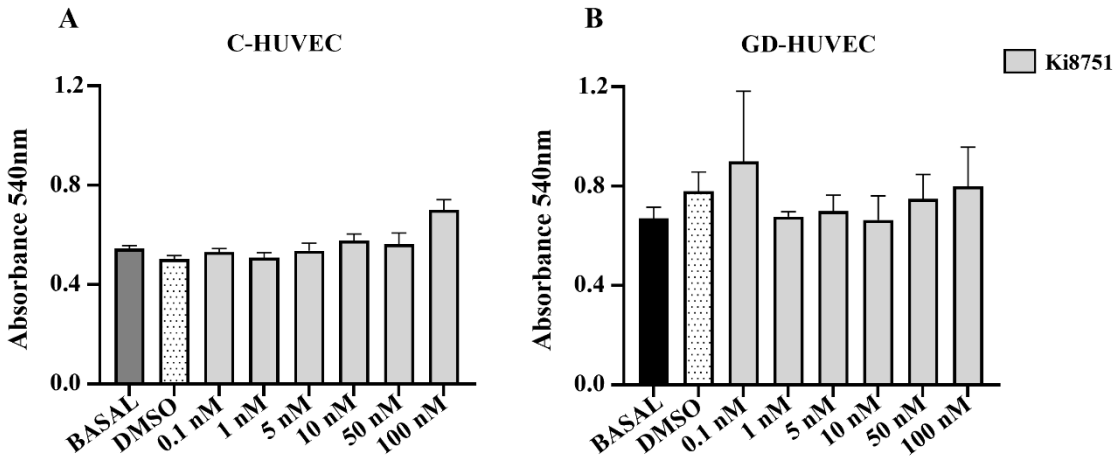


Figure 28. *Ki8751 treatment do not induce changes in cell viability*. Cell viability of C- (A) and GD-HUVEC (B) following 24-hours treatment with Ki8751 at different concentrations (0.1–100 nM) analysed by MTT assay. Data are expressed as mean ± SD (n = 3).

5.2.7 Effect of AM on nitro-tyrosine levels counteracted by VEGFR2 inhibitor

To further investigate if the VEGFR2 signalling cascade activated by the AM influences nitro-oxidative stress, nitro-tyrosine production was evaluated in presence of VEGFR2 inhibitor. In particular, to evaluate nitro-tyrosine expression cells were pre-treated with Ki8751 for 30 minutes and then, incubated 24-hours with AM or VEGFa$_{165}$ (**Figure 29**).

As already shown in **Figure 26B**, C-HUVEC showed no significant changes of nitro-tyrosine production following 24-hours AM or VEGFa$_{165}$ treatment, probably owing to already low basal nitro-tyrosine levels. In addition, the pre-treatment with Ki8751 did not induce significant variations in control cells (**Figure 29A**). In contrast, GD-HUVEC showed a significant reduction of nitro-tyrosine levels following 24-hours AM or VEGFa$_{165}$ stimulation, as already mentioned in **Figure 26C**, and interestingly, the pre-treatment with Ki8751 restored nitro-

tyrosine expression to levels comparable to the basal condition, although the effect was not statistically significant (**Figure 29B**).

These findings suggest a possible involvement of nitro-oxidative stress in the VEGFR2 mediated pathway activated by AM as one of the putative mediators of the AM pro-angiogenic effect.

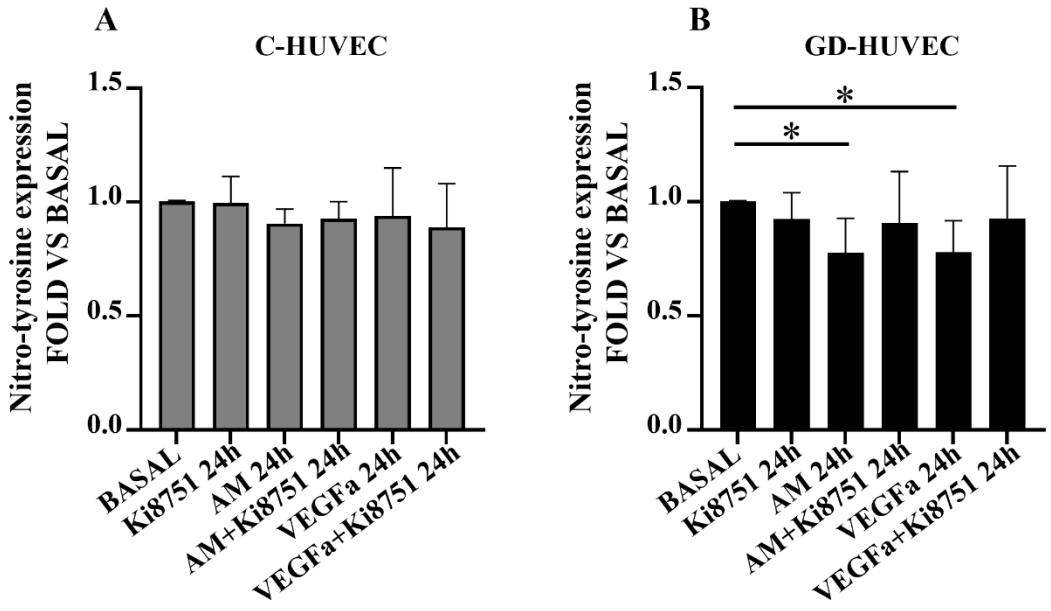


Figure 29. *GD-HUVEC show a significant downregulation of nitro-tyrosine levels following 24-hours incubation with AM or VEGFa$_{165}$ which is reverted to basal levels by pre-incubation with Ki8751.* Nitro-tyrosine expression in C- (A) and GD-HUVEC (B) following 24-hours AM or VEGFa$_{165}$ stimulation with or without Ki8751 pre-treatment, analysed by flow cytometry. Data are expressed as mean ± SD ($n \geq 3$). Asterisks point out statistically significant differences between the selected conditions (*$p<0.05$).

5.2.8 Effect of AM on Matrigel vessel formation counteracted by VEGFR2 inhibitor

To further elucidate the link between AM pro-angiogenic effect and VEGFR2 pathway activation, GD-HUVEC pre-treated with Ki8751 and subsequently stimulated with AM were used to perform a Matrigel tube formation assay (**Figure 30**).

GD-HUVEC showed an increasing number of nodes, junctions, segments and meshes, even if not significant, following AM treatment (**Figure 30A-D**). No differences were detected in

the mean meshes size compared to the basal condition (**Figure 30E**). Interestingly, the pre-treatment with Ki8751 promoted a reduction of the number of nodes, junctions, segments and meshes and an upregulation of the mean of meshes size, even if not significant (**Figure 30A-E**).

All these findings suggest that the AM driven pro-angiogenic role may be mediated by VEGFR2 signalling activation, as prompted by the worsening of the angiogenic parameters analysed.

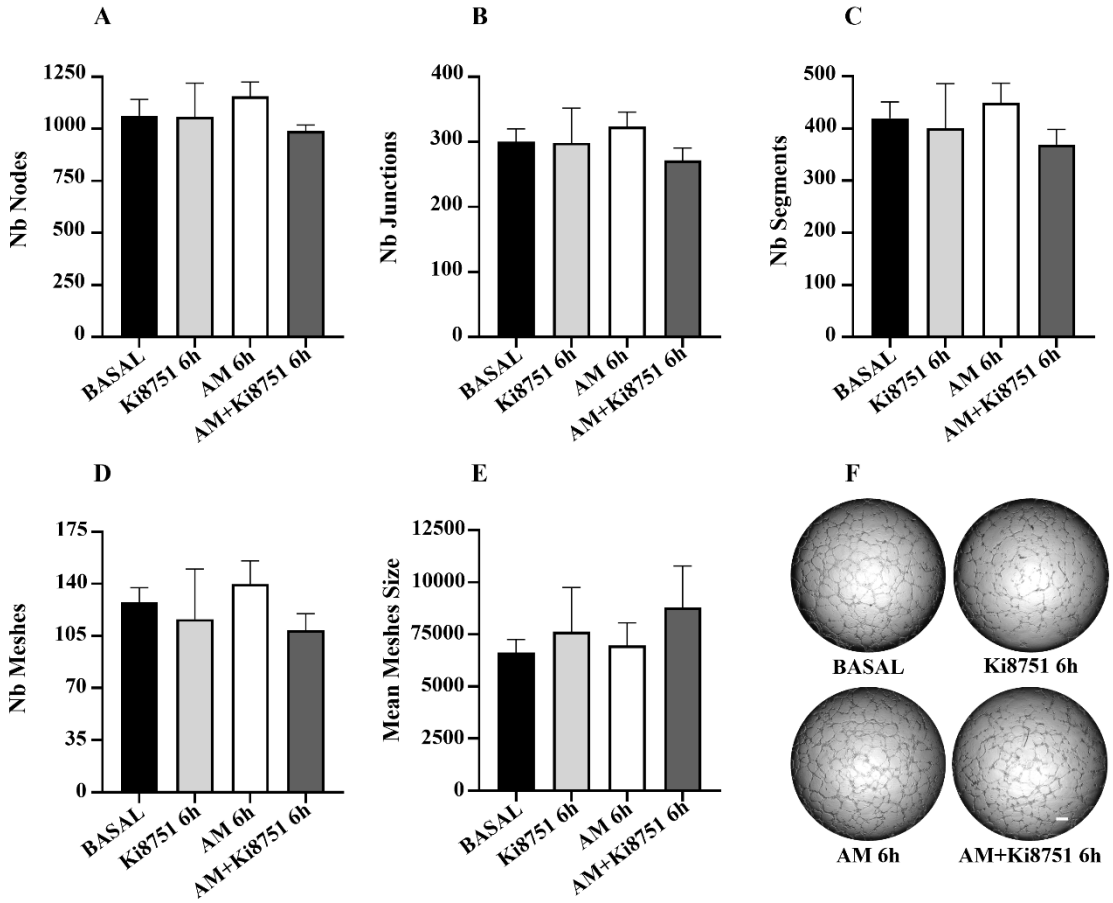


Figure 30. *GD-HUVEC show an increasing trend in number of nodes, junctions, segments and meshes following 6-hours AM treatment compared to basal condition. The pre-incubation with Ki8751 lead to a reduction of the previously mentioned parameters and to an increasing trend of the mean of meshes size.* Number of nodes (A), junctions (B), segments (C), meshes (D), mean meshes size (E) in GD-HUVEC following 6-hours AM stimulation with or without Ki8751 pre-treatment, analysed by Matrigel tube formation assay. Representative figure of all tested conditions (F). Scale bar 250µm. Data are expressed as mean ± SD ($n \geq 3$).

5.3 DISCUSSION

The present study investigated the VEGFR2/AKT/eNOS signalling pathway as one of the potential molecular mechanisms underlying the pro-angiogenic effect induced by amniotic membrane.

Chronic ulcerations in diabetic patients is a severe diabetic complication that strongly affect both patients' life quality and healthcare economics due to the absence of effective therapies (Zhang Y et al, 2020; Armstrong DG et al, 2017; Armstrong DG et al, 2023).

These ulcers are characterized by persistent inflammation and oxidative stress, reduced epithelialization, decreased proliferation and migration of fibroblasts and keratinocytes and insufficient angiogenesis (Patel S et al, 2019). For all these reasons, frequently, diabetic patients undergo to lower limb amputations (Zhang Y et al, 2020; Armstrong DG et al, 2017; Armstrong DG et al, 2023). In particular, decreased new vessel formation significantly contributes to ulcers chronicity by limiting the supply of oxygen and nutrients to the novel formed tissue (Okonkwo UA et al, 2017).

Amniotic membrane was used since the last century to treat skin burns and wounds, from different origins including diabetes related ones. It exerts many beneficial effects among which anti-inflammatory, immunomodulatory, anti-microbial, while also promoting re-epithelialization and reducing pain. These combined actions greatly support wound healing by improving both healing timing and new tissue formation (Young SM et al, 2010; Davis J, 1910; Silini AR et al, 2015; Tenenhaus M, 2017).

Although nowadays amniotic membrane-based therapies are mainly involved for compassionated studies, the molecular mechanisms behind its positive effects are not completely understood, especially regarding endothelial dysfunction and angiogenesis (Rodríguez-Valiente M et al, 2018).

We previously demonstrated, in 2022, that AM exerts both anti-inflammatory and pro-angiogenic effects on GD-HUVEC, endothelial cells obtained from the umbilical cord of gestational diabetes affected women which are epigenetically modified by *in vivo* exposure to hyperglycaemia (Pipino C et al, 2022, Di Pientrantonio N et al, 2024). These cells recapitulate the typical features of diabetic endothelium showing a pro-inflammatory and pro-oxidative phenotype and thus represent a unique *in vitro* platform to study endothelial dysfunction, angiogenesis related mechanisms and to test potential therapeutic strategies (Di Pietrantonio N et al, 2024; Di Fulvio P et al, 2014).

We previously investigated the AM role in the modulation of the inflammatory pathway mediated by the transcription factor NF-kB. Upon nuclear translocation, NF-kB activates VCAM-1 and ICAM-1 expression and their exposure to the cell membrane facilitating monocytes adhesion and thereby contributing to vascular inflammation. We demonstrated that AM treatment reduces vascular inflammation by decreasing the activation of NF-kB which in turn lowers VCAM-1 expression and exposure leading to a strong downregulation of monocytes-HUVEC interaction. In addition, AM treatment improved cell migration, promoted vessel formation on Matrigel and increased NO bioavailability thus suggesting a potential pro-angiogenic effect (Pipino C et al, 2022).

Furthermore, Noh CH et al (2023) demonstrated that the exosome rich-conditioned media obtained from human amniotic membrane derived stem cells, showing high concentrations of keratinocyte growth factor (KGF), epidermal growth factor (EGF), and VEGF, promotes new blood vessel formation in a model of rat whole-skin-excision wound (Noh CH et al, 2023).

To gain deeper insight into the molecular mechanisms underlying the AM pro-angiogenic effect, this study focused on a signalling pathway mediated by the key angiogenic receptor, VEGFR2. The modulation of VEGFa and VEGFR2 in basal conditions and following AM treatment in both GD-HUVEC and control cells was firstly analysed.

GD-HUVEC did not exhibit statistically significant differences in *VEGFa* gene expression and VEGFR2 gene and protein expression, demonstrating only a trend toward increased expression compared to control cells. However, GD-HUVEC showed a tendency toward reduced VEGFR2 activation, determined by the phosphorylation to total ratio, compared to C-HUVEC.

This observation is consistent with findings by Warren CM et al (2014) who reported that HUVEC treated for 5 days in high glucose conditions, to reproduce the diabetic environment, showed no variations in VEGFR2 total protein expression compared to cells cultivated in low glucose (Warren CM et al, 2014). In addition, also WU W et al (2016) demonstrated that HUVEC treated with high glucose showed no changes in VEGFR2 total protein levels, but they showed a reduction in VEGFR2 phosphorylation status compared to low glucose treated cells, hypothesizing a possible decrease in receptor activity due to reduced receptor availability on the cell surface (Wu W et al, 2016).

The observed trend toward reduced VEGFR2 activation in GD-HUVEC could be due to an insufficient number of receptors at the cell surface, available for ligand interaction and consequently for its phosphorylation and downstream cascade activation. This process could trigger a compensatory mechanism, leading to increased production of both VEGFa and the

receptor, explaining the trend of upregulation detected in GD-HUVEC compared to control cells, that show slightly higher levels of receptor phosphorylated to total ratio.

AM treatment promoted a non-significant upregulation of VEGFa mRNA levels and a significant increase of *VEGFR2* gene expression in both cell types, while no differences were detected for VEGFR2 total protein amount.

GD-HUVEC showed statistically significant upregulation of VEGFR2 activation following AM or VEGFa (positive control) treatment, while a non-significant trend was detected for control cells. These data suggest that AM treatment activates VEGFR2 in GD-HUVEC with a similar extend to the positive control, hypothesizing a possible activation of the downstream signalling cascade. Control cells showed not significant improvement of VEGFR2 activation probably due to the slightly higher level already in basal conditions compared to GD-HUVEC.

To further investigate the effect of AM on the VEGFR2 mediated signalling cascade, AKT activation, one of the most important mediators linked to eNOS activity and NO production, was evaluated in basal conditions and following AM or VEGFa treatment.

In particular, GD-HUVEC showed a significant reduction of AKT activation compared to control cells. In line with this, Di Pietrantonio N et al (2021) demonstrated that HUVEC treated with plasma of obese children showed reduced phosphorylated-to-total AKT ratio compared to HUVEC treated with control children plasma (Di Pietrantonio N et al, 2021). These findings are consistent with other previous studies demonstrating the compromised PI3K/AKT signalling pathway in presence of vascular insulin resistance leading to impaired eNOS activation and reduced NO bioavailability (Consoli C et al, 2008; Andreozzi F et al, 2008).

In addition, AM treatment promoted a significant enhancement of AKT activation in GD-HUVEC, while an increasing trend was observed for VEGFa incubation. On the contrary, control cells showed no changes following either AM or VEGFa treatment. Interestingly, AM or VEGFa treatment in GD-HUVEC restored AKT activation to levels comparable to control cells in basal conditions, suggesting a recovery of the signalling pathway.

AKT phosphorylation, leading to eNOS activation, is strictly linked to NO production, the key molecule involved in vascular function and in particular to vasodilatation. Indeed, bioavailable NO, promoting cGMP production, induces vasodilatation by smooth muscle cells. On the contrary, in diabetic patients who experienced strong oxidative stress, the mechanism of eNOS uncoupling determines the interaction between NO and superoxide anion resulting in peroxy-nitrite formation which, in turn, leads to nitro-tyrosine production, further contributing to diabetic nitro-oxidative stress. It was previously demonstrated by Di Fulvio P et al (2014) that GD-HUVEC showed both increased eNOS activity and NO production and enhanced

superoxide anion and nitro-tyrosine levels compared to control cells (Di Fulvio P et al, 2014). These findings highlighted the pro-oxidant phenotype of GD-HUVEC demonstrating that the excessive production of NO was involved in nitro-oxidative stress development. Moreover, Di Tomo P et al (2021) demonstrated that GD-HUVEC showed increased levels of ROS and reduced antioxidant enzymatic defence further confirming their pro-oxidative status (Di Tomo P et al, 2021).

Consistently, we further confirmed that GD-HUVEC showed increased levels of both nitro-tyrosine and superoxide anions levels compared to control cells. AM treatment significantly reduced of both nitro-tyrosine and superoxide anion levels in GD-HUVEC. Similarly, VEGFa treatment in GD-HUVEC promoted a downregulation of both oxidative markers, reaching statistical significance only for nitro-tyrosine production. No effects were detected in C-HUVEC, probably due to its low oxidative status already in basal conditions.

Of note, in our previous study, we have demonstrated that AM treatment increased cGMP levels, thus enhancing NO bioavailability, in both C- and GD-HUVEC, further confirming its role in improving nitro-oxidative stress and endothelial cell function (Pipino C et al, 2022).

These findings are in line with previous reports which show AM antioxidant effect in different contexts. In particular, human amniotic membrane stromal stem cells conditioned media increased superoxide dismutase and glutathione peroxidase levels in rats with myocardial infarction (Mokhtari B et al, 2020). Moreover, human amniotic membrane that retains viable endogenous cells protected fibroblasts from oxidant-associated damages, improved antioxidant defence and increased fibroblasts migration compared to devitalized amniotic membrane, suggesting a possible role of amniotic membrane derived stem cells as antioxidant agent (Duan-Arnold Y et al, 2015).

To further elucidate the role of VEGFR2 in AM driven antioxidant and pro-angiogenic effects, cells were pre-treated with a VEGFR2 selective inhibitor prior to AM or VEGFa incubation.

The VEGFR2 inhibitor pre-treatment significantly reduced VEGFR2 activation promoted by AM or VEGFa in GD-HUVEC, while a trend was observed in control cells. Contextually, GD-HUVEC pre-incubated with VEGFR2 inhibitor and then, treated with AM or VEGFa, showed increased trend of nitro-tyrosine levels, compared to AM or VEGFa alone. These data suggest that AM antioxidant properties partially derived from VEGFR2 activation although additional VEGFR2 independent pathways could be activated to fully explain the significant nitro-tyrosine reduction.

Moreover to further corroborate the VEGFR2 role in AM driven pro-angiogenic effect, Matrigel tube formation assay was performed in GD-HUVEC treated with AM with or without VEGFR2 inhibitor pre-incubation. GD-HUVEC showed a trend of improvements for all tested angiogenic parameters following AM treatment. Although not statistically significant, these data are consistent with the previous finding of Pipino C et al (2022) showing that GD-HUVEC treated with AM showed a better vessel formation on Matrigel promoting a more interconnected network (Pipino C et al, 2022). Interestingly, GD-HUVEC pre-treated with VEGFR2 inhibitor showed reduced number of nodes, segments, junctions and meshes and increased mean of meshes size compared to AM incubation. Although not statistically significant, these changes suggest a deterioration of the vascular network, characterized by fewer interconnection and decreased amount of meshes with bigger size.

Overall, these findings demonstrate the involvement of the VEGFR2/AKT/eNOS signalling pathway in the AM driven pro-angiogenic effect, especially focusing on its role in counteracting nitro-oxidative stress, paving the way for the identification of new therapeutic targets and further confirming the clinical importance of amniotic membrane as potential curative strategy.

Nevertheless, a key consideration of this study is the great inter-individual variability between different strains of HUVEC and between different donors of AM, as highlighted by the absence of statistical significance of some parameters that could be achieved increasing the number of biological replicates.

Although the positive results obtained using the whole amniotic membrane, the beneficial effects could be mediated by a selective or synergistic action of different components including amniotic epithelial cells, amniotic stromal cells and the matrix in which cells are embedded. For this reason, an interesting future perspective could be the investigation of the component more involved in the pro-angiogenic effect of amniotic membrane evaluating also stem cells derived conditioned media or extracellular vesicles.

6 ANGIOGENESIS: ROLE OF THE INTERACTION BETWEEN ENDOTHELIAL CELLS AND DERMAL FIBROBLASTS IN DIABETES (*AIM 3*)

Part of this project (corresponding to the results of paragraphs ranging from 6.2.6 to 6.2.11) was performed at the Laboratory for Biointerfaces, Empa, Swiss Federal Laboratories for Materials Science and Technology, St. Gallen, Switzerland, under the supervision of Dr. Markus Rottmar.

6.1 MATERIALS AND METHODS

6.1.1 HUVEC isolation and culture

Umbilical cords were obtained from randomly recruited healthy Caucasian mothers (Control, C) and women affected by Gestational Diabetes (GD) in the third trimester of pregnancy followed by 'Diabetes and Pregnancy Clinic' until delivery at the Hospital Santo Spirito of Pescara (Italy). GD women were treated with diet only and women with pre-gestational diabetes were excluded.

Women matched by age and body mass index (BMI) were divided into two groups, one normoglycemic/healthy controls (basal glycaemia < 5.1 mmol/L, oral glucose tolerance test (OGTT) 1h < 10 mmol/L and OGTT 2h < 8.5 mmol/L, n=4) and the other diagnosed with gestational diabetes (basal glycaemia ≥ 5.1 mmol/L, OGTT 1h ≥ 10 mmol/L, and OGTT 2h ≥ 8.5 mmol/L, GD, n=4) according to the criteria of the American Diabetes Association (American Diabetes Association Professional Practice Committee, 2022).

All procedures agreed with the Declaration of Helsinki principles and with the ethical standards of the Institutional Committee on Human Experimentation (*details in the paragraph 4.1.3*).

HUVEC isolation and culture protocol is detailed in the *paragraph 4.1.4*.

6.1.2 Experimental protocol

- To investigate the role of GD-HUVEC on migration and ECM remodelling by dermal fibroblasts, C- or GD-HUVEC from at least three independent donors were co-incubated with primary normal human dermal fibroblast (HDF) isolated from the dermis

of 2 independent healthy subjects' adult skin (C-12302, PromoCell) for 3 days in HUVEC culture medium using an indirect co-culture system (transwell, cat # 353180, Corning). HUVEC used for experiments were cultured between passages 3 and 5, while HDF used for experiments were cultured between passage 7 and 11. C- or GD-HUVEC were plated in the transwell while HDF were plated at bottom of the well to maintain a ratio HDF:HUVEC of 2:1.

- To investigate the role of diabetic human dermal fibroblasts (diabHDF) on vessel formation and endothelial cells migration, primary HDF isolated from the dermis of an healthy subject adult skin (C-12302, PromoCell) or primary diabHDF isolated from the dermis of type two diabetic patient adult skin (cat # HD2-6067, Cell Biologics) were co-incubated with C- or GD-HUVEC, from at least two independent donors, for 6 days in HUVEC culture medium using an indirect co-culture system (transwell, cat # 665631, Greiner Bio-One). HUVEC and diabHDF used for experiments were cultured between passages 3 and 5, while HDF used for experiments were cultured between passage 7 and 11. C- or GD-HUVEC were plated at the bottom of the well while HDF or diabHDF were plated in the transwell to maintain a ratio HDF:HUVEC of 2:1. In addition, to investigate the differences between HDF and diabHDF in basal conditions, cells were cultured 6 days in HUVEC culture medium.
  This experimental protocol and the corresponding preliminary experiments and results (related to paragraphs ranging from 6.2.6 to 6.2.11) were performed at the Laboratory for Biointerfaces, Empa, Swiss Federal Laboratories for Materials Science and Technology, St. Gallen, Switzerland, under the supervision of Dr. Markus Rottmar.

6.1.3 RNA extraction and real-time quantitative PCR

- To investigate the role of GD-HUVEC on ECM remodelling by dermal fibroblasts, the total RNA was isolated, extracted, quantified, retrotranscribed and amplified from HDF alone or co-incubated 3 days with C- or GD-HUVEC, according to the protocol detailed in the *paragraph 4.1.6.* The following TaqMan Gene Expression Assay probes for human COL1A1 (Hs00164004_m1, Thermo Fisher Scientific), FN-1

(Hs01549976_m1, Thermo Fisher Scientific) and β2M (Hs00187842_m1, Thermo Fisher Scientific) were used according to the manufacturer's instructions.

All samples were analysed in technical duplicate. The relative expression of the target genes was calculated using the $2^{-\Delta\Delta Ct}$ method (using the condition of only HDF incubated with the empty transwell as control for the normalization) using β2M as housekeeping (Applied Biosystems QuantStudio 7 Pro Real-Time PCR System, Thermo Fisher Scientific).

- To investigate the difference between HDF and diabHDF, the total RNA was isolated and extracted from HDF and diabHDF in basal conditions using the RNeasy Microkit (cat # 74004, QIAGEN) according to the manufacturer instructions. At the same time, to evaluate the effect of diabHDF on VEGFR2 gene expression by C-HUVEC, the total RNA was isolated and extracted from C-HUVEC co-incubated 6 days with diabHDF or HDF using the RNeasy Microkit (cat # 74004, QIAGEN) according to the manufacturer instructions.

  The total RNA was, then, quantified using NanodropOne (Thermo Fisher Scientific) and 120ng were retrotranscribed using iScript cDNA Synthesis Kit (cat # 1708891, BIO-RAD). The iQ SYBR Green Supermix (cat # 1708882, BIO-RAD) together with the following RT-PCR primers for human:

  - *VEGFa* (forward 5'-TCTCTACCCCAGGTCAGACG-3'; reverse 5'-AGCAATGTCCTGAAGCTCCC-3')
  - *VEGFR2* (forward 5'-GGAACCTCACTATCCGCAGAGT-3'; reverse 5'-CCAAGTTCGTCTTTTCCTGGGC-3')
  - *MCP-1* (forward 5'-CGACATCCTGGAACTGCCCTACC-3'; reverse 5'-CACTGTGCCGCTCTCGTTCAC-3')
  - *COL1* (forward 5'-CAGCCGCTTCACCTACAGC-3'; reverse 5'-TTTTGTATTCAATCACTGTCTTGCC-3')
  - *SMAD3-3* (forward 5'-GGGCTCCCTCATGTCATCTA-3'; reverse 5'-TTGAAGGCGAACTCACACAG-3')
  - *GAPDH* (forward 5'-AGTCAGCCGCATCTTCTTTT-3'; reverse 5'-CCAATACGACCAAATCCGTTG-3')

  were used according to the manufacturer's instructions.

  All samples were analysed in technical duplicate. The relative expression of the target genes was calculated using the $2^{-\Delta Ct}$ (for the comparison between HDF and diabHDF)

and the $2^{-\Delta\Delta Ct}$ method (for the comparison between the two co-incubation conditions using the condition of only C-HUVEC co-incubated with the empty transwell as control for the normalization) using GAPDH as housekeeping (CFX96™ Real-Time System C1000 Touch™ Thermal Cycler, BIO-RAD).

6.1.4 Flow cytometry analysis

The flow cytometry analysis protocol is detailed in the *paragraph 4.1.8*.

HDF were co-incubated 3 days with C- or GD-HUVEC to evaluate ECM remodelling and cell migration markers. Briefly, HDF were fixed, permeabilized (according to the protocol detailed in the *paragraph 4.1.8*) and incubated with primary antibodies: anti-Smad2/3 (cat #5678S, Cell Signaling, 1:100), anti-phospho-Smad2 (S465/467)/Smad3 (S423/425) (cat #8828S, Cell Signaling, 1:50), anti-p44/42MAPK (ERK1/2) (cat #9102S, Cell Singaling, 1:50), anti-phospho-p42/44MAPK T202/Y204 (cat #9101S, Cell Signaling Technology, 1:100), anti-Collagen1 (ab34710, Abcam, 1:100), anti-MMP2 (ab92536, Abcam, 1:100), anti-TIMP2 (NBP2-53347, NOVUS, 1:100), anti-FAK (A32309, Antibodies.com, 1:100), anti-YAP (A32371, Antibodies.com, 1:50), anti-phospho YAP S127 (cat # 13008S, Cell Signaling, 1:200), anti-TAZ (cat # 71192S, Cell Singaling, 1:50), anti-phospho TAZ S89 (WWTR1-S89, cat # SAB5701813, Merck, 1:500) for 30 minutes at 4°C. A subsequent incubation with Alexa Fluor 488-conjugated secondary antibody (cat #A-11034, Thermo Fisher Scientific, 1:100 and cat #A11001 Life Technologies, 1:100) was performed for 30 minutes at 4°C.

All results are expressed as the Mean Fluorescence Intensity (M.F.I.) Ratio, calculated by dividing the M.F.I. of positive events by the M.F.I. of negative events (M.F.I. of the secondary antibody), normalized as FOLD vs HDF (HDF co-incubated with the empty transwell).

6.1.5 Immunofluorescence analysis

The immunofluorescence analysis protocol is detailed in the *paragraph 4.1.7*.

HDF, alone or co-incubated 3 days with C- or GD-HUVEC, (for Collagen1 staining) as well as C-HUVEC, co-incubated 6 days with HDF or diabHDF, (for VEGFR2 staining) were fixed with 4% paraformaldehyde for 20 minutes at room temperature. Paraformaldehyde was then removed, and cells were washed with PBS for 5 minutes twice and permeabilized with 0.1% Triton X-100 (SigmaAldrich, Germany) in PBS for 10 minutes. Cells were blocked with 1%

bovine serum (cat # A4503, Sigma-Aldrich, Germany) or 3% BSA in PBS for 1-hour at room temperature. Subsequently, cells were incubated 1-hour with primary antibody anti-Collagen1 (ab34710, Abcam, 1:100) or anti-VEGFR2 (ab237634, Abcam, 1:100). After washing with PBS, cells were incubated with Cy3-conjugated secondary antibody (cat #A-10520, Thermo Fisher Scientific, 1:300) or Alexa488-conjugated secondary antibody (A11008, Invitrogen, 1:200) and with Phalloidin (AlexaFluor633 Phalloidin, A22284, Invitrogen, 1:200) at room temperature for 1-hour.

Nuclei were stained with DAPI mounting medium (4′6′-diamidino-2-phenylindole; Thermo Fisher Scientific, Karlsruhe, Germany). Finally, cells were washed with PBS and mounted with Fluorescence Mounting Medium (cat # S3023, Agilent Dako, USA).

For the acquisition of the immunofluorescence signals, slides were observed under a confocal microscope (Zeiss LSM-800 and Zeiss LSM-780; Carl Zeiss Meditec AG, Oberkochen, Germany). All results are expressed as FOLD vs HDF (for Collagen1 staining) or FOLD vs C-HUVEC (for VEGFR2 staining).

6.1.6 Zymography

To investigate the role of GD-HUVEC on MMP activity by dermal fibroblasts, HDF were co-incubated 3 days with C- or GD-HUVEC, then were washed to remove FBS residues and incubated, without the transwell, for 24-hours with only DMEM. Then, the conditioned media was collected, centrifuged and stored at -80°C until further use. The day of the experiment, conditioned media was thawed on ice, diluted 1:1 in sample buffer and incubated 1-hour at 37°C. In the meantime, a 0.75mm polyacrylamide gel containing 2.5mg/mL of gelatine was prepared. Samples were run into the gel and then the gel was incubated 1-hour with a solution containing 2% Triton-X 100 and subsequently, incubated overnight with a reaction solution, to allow gelatine enzymatic digestion, at 37°C. At the end of the incubation time, the gel was stained with a standard Coomassie blue staining. The gel was scanned and analysed using ImageJ to evaluate the density of the bands. All results are expressed as FOLD vs HDF.

6.1.7 Wound healing scratch assay

To investigate the role of GD-HUVEC on migration by dermal fibroblasts, HDF co-incubated for 3 days with C- or GD-HUVEC were used to perform a wound healing scratch assay. At the

same time, to investigate the role of diabHDF on HUVEC migration, C-HUVEC co-incubated 6 days with HDF or diabHDF were used to perform wound healing scratch assay.

For both experimental plans, following the co-incubation time, the wound was performed by scratching a line across the bottom of the well on a confluent cell's monolayer using a sterile p-200 pipette tip. The cells were rinsed gently with warm DMEM and then cultivated in the medium with 1% FBS, re-positioning each transwell in the corresponding well. Pictures were obtained using an inverted microscope (PAULA, Leica Microsystem and Primovert, Zeiss). To quantify migration, the empty area, obtained by the scratch, was quantified using ImageJ software. For each timepoint, the area of the same gap was measured again. The difference between the initial and final areas was calculated as percentage (%).

6.1.8 Presto Blue assay

To investigate the differences regarding metabolic activity between HDF and diabHDF in basal conditions, the PrestoBlue assay (PrestoBlue Cell Viability Reagent, A13262, Invitrogen) was carried out according to the manufacturer' instruction.

Briefly, HDF and diabHDF were seeded in 96-well plates at a density of 2560 cells/well in HUVEC medium. After 6 days in culture, cells were washed with warm PBS and incubated for 1.5-hours at 37°C with PrestoBlue working solution, previously diluted 1:10 in cell culture media according to manufacturer's instructions. Thereafter, the mixture was pipetted up and down to mix reduced and oxidized PrestoBlue solution. Finally, the fluorescence of each sample was recorded at excitation wavelength of 547nm and at emission wavelength of 582nm using the Mithras plate reader (Mithras^2 LB 943 Multimode Reader). Data were normalized with the fluorescent value of the cell culture media diluted with the PrestoBlue working solution.

6.1.9 PicoGreen assay

To investigate the differences in the double-strand DNA amount, as indirect measurement of amount of viable cells present in the well, between HDF and diabHDF in basal conditions, the PicoGreen assay (Quant-IT^{TM} PicoGreen^{TM} dsDNAassay kit, P7589, Invitrogen) was carried out according to the manufacturer's instructions.

Briefly, HDF and diabHDF were seeded in 96-well plates at a density of 2560 cells/well in HUVEC medium. After 6 days in culture, cells were washed with warm PBS and incubated for

5 minutes on a shaker at room temperature with 200µl of lysing solution. Samples were frozen at -20°C and then thawed. Samples and standards, appropriately prepared to obtain an appropriate standard curve, were pipetted into a black bottom 96-well plate and incubated 2 minutes with PicoGreen solution appropriately diluted. Finally, the fluorescence of each sample and standard was recorded at excitation wavelength of 485nm and at emission wavelength of 528nm using the Mithras plate reader (Mithras^2 LB 943 Multimode Reader).

6.1.10 Matrigel tube formation assay

To investigate the role of diabHDF on vessel formation, C- and GD-HUVEC were co-incubated with HDF or diabHDF for 6 days, then HUVEC were detached and plated 1.0×10^4 cells/well in the growth factor–reduced basement membrane matrix gel (Matrigel, cat # 356230, Corning) coated µ-Plate angiogenesis 96-well ibiTreat (part of the cat # 89646, ibidi) using 10% FBS HUVEC culture medium. 6-hours later representative photographs were acquired using optical microscope (Primovert, Zeiss). Images were processed using ImageJ software (Angiogenesis analyser tool) to analyse angiogenic parameters (i.e., number of segments, meshes, and master junctions) in all the tested conditions. All results are expressed as FOLD vs C-HUVEC or FOLD vs GD-HUVEC.

6.1.11 Statistical analysis

All experimental data are expressed as mean ± Standard Deviation (SD). Each experiment, regarding the role of GD-HUVEC on ECM remodelling and migration by dermal fibroblasts, was conducted in technical triplicates using at least 3 independent donors of C- and GD-HUVEC and 2 independent donors of HDF. Each experiment, regarding the role of diabHDF on endothelial cells migration and vessel formation as well as the comparison between HDF and diabHDF, were conducted at least in technical duplicates using at least 2 independent donors of C- and GD-HUVEC, one donor of HDF and one donor of diabHDF. The normal distribution of quantitative data was assessed by the Shapiro–Wilk test. T-test or Mann-Whitney test, according to data normal distribution, were used to compare two data sets. One sample Wilcoxon signed-rank test were used to compare the median of the experimental group *"HDF co-incubated with C-HUVEC"* to the baseline value of 1 corresponding to the experimental

group "*HDF*". Probability values were calculated considering 95% compatibility interval. All analyses were performed with GraphPad Prism (version 9, GraphPad Software).

6.2 RESULTS

6.2.1 Effect of GD-HUVEC on ECM production by dermal fibroblasts

To investigate the role of GD-HUVEC, which retain epigenetic modifications following *in vivo* exposure to hyperglycaemia and therefore, show a pro-inflammatory and pro-oxidative phenotype typical of the diabetic endothelium, on ECM production by dermal fibroblasts, the expression of FN1 and COL1A1 was assessed in HDF co-incubated with C- or GD-HUVEC (**Figure 31)**.

HDF, co-incubated with GD-HUVEC, showed a decreasing trend of *FN1* mRNA levels and a significant reduction of *COL1A1* gene expression compared to HDF co-incubated with C-HUVEC (**Figure 31A,B).** Contextually, HDF co-incubated with GD-HUVEC exhibited a significant downregulation of COL1A1 intracellular production, revealed by flow cytometry analysis, and a trend of downregulation of total COL1A1 amount, revealed by immunofluorescence images quantification (**Figure 31C-E**). These findings suggest a potential role of soluble factors secreted by GD-HUVEC in negatively modulating COL1A1 gene and protein expression.

Of note, consistently with the literature, HDF co-incubated with control endothelial cells showed an increased COL1A1 production, both intracellular and total amount, as demonstrated by **Figure 34A-C**, highlighting an ECM production upregulation in this experimental condition compared to HDF alone.

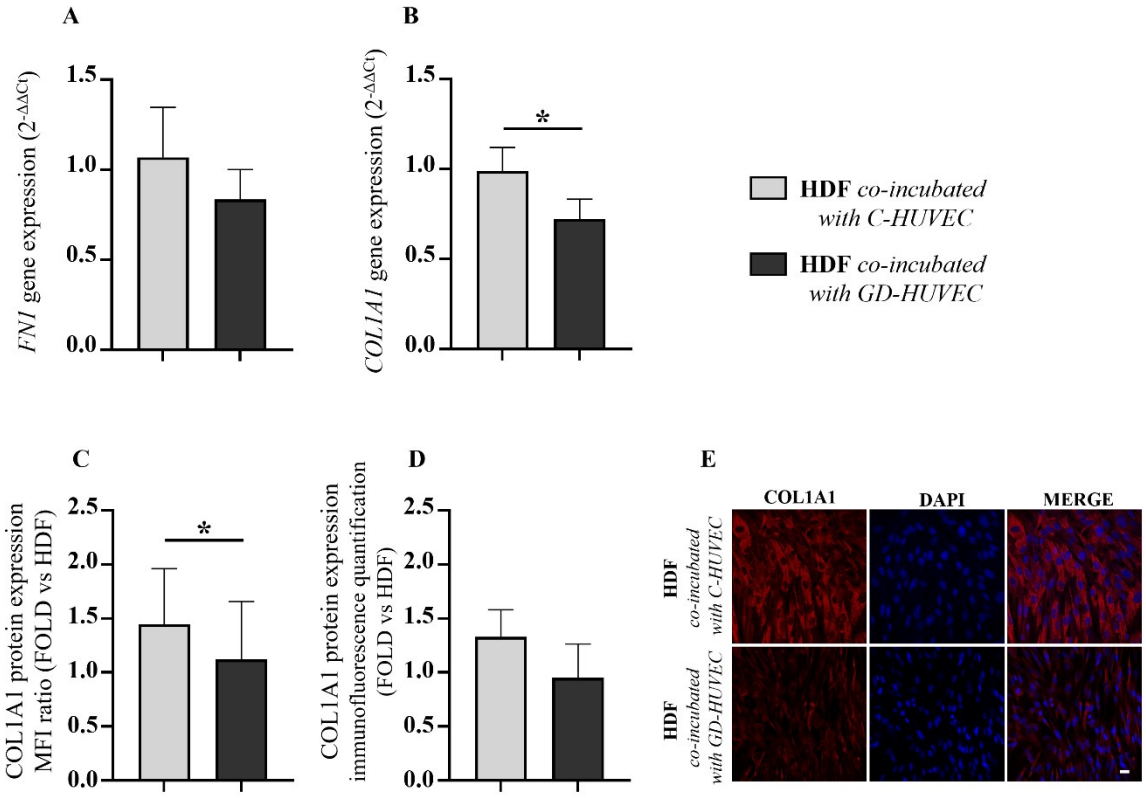


Figure 31. *HDF co-incubated with GD-HUVEC showed decreased FN1 mRNA levels and COL1A1 gene and protein expression compared to HDF co-incubated with C-HUVEC.* Relative mRNA expression of *FN1* (A) and *COL1A1* (B), intracellular (C) and total (D) protein expression of COL1A1 of HDF co-incubated 3 days with C- or GD-HUVEC analysed by RT-PCR, flow cytometry and immunofluorescence, respectively. Immunofluorescence representative images (E). Scale bar 20µm. RT-PCR data are expressed as mean ($2^{-\Delta\Delta Ct}$) ± SD, flow cytometry and immunofluorescence data are expressed as mean (FOLD vs HDF) ± SD (HUVEC n ≥ 3; HDF n=2). Asterisks point out statistically significant differences between the selected conditions (*p<0.05).

6.2.2 Effect of GD-HUVEC on Smad2-3 and MAPK activation by dermal fibroblasts

To deeply study the potential mechanisms affected by the presence of GD-HUVEC resulting in reduced COL1A1 production, the activation, revealed by the phosphorylated to total ratio, of Smad2-3 (TGF-β dependent pathway) and MAPK (one of the TGF-β independent pathways) was evaluated in HDF co-incubated with C- or GD-HUVEC (**Figure 32**).

HDF co-incubated with GD-HUVEC showed a trend of reduction of Smad2-3 activation and a significant downregulation of MAPK activation, compared to HDF co-incubated with C-HUVEC (**Figure 32A,B**).

Overall, these results indicate that GD-HUVEC could regulate ECM production, in particular COL1, by modulating mainly TGF-β independent pathways such as MAPK activation.

Of note, HDF co-incubated with C-HUVEC showed increased activation of both factors but mainly MAPK, compared to HDF alone (**Figure 34D,E**), further confirming the role of HUVEC in ECM production management.

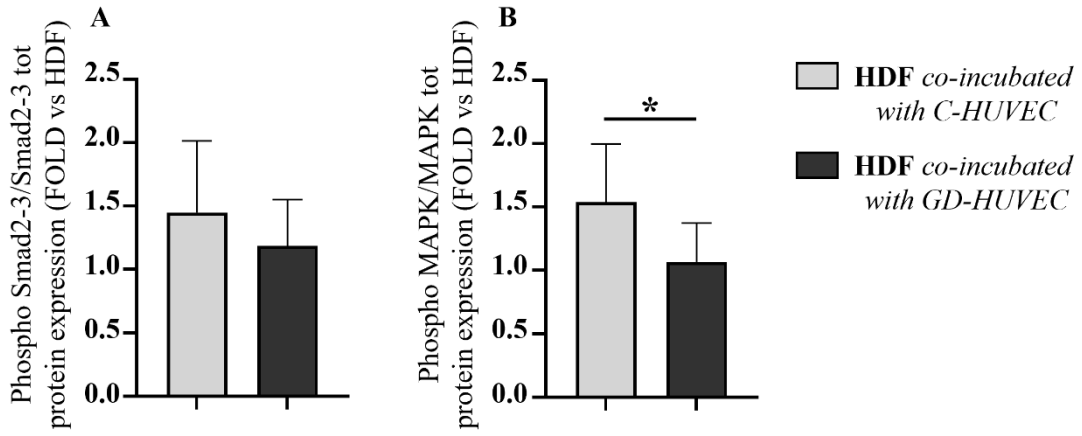


Figure 32. *HDF co-incubated with GD-HUVEC showed reduced activation of Smad2-3 and MAPK compared to HDF co-incubated with C-HUVEC.* Smad2(S465/467)-Smad3(S423/425) phosphorylated to total ratio (A) and MAPK (T202/Y204) phosphorylated to total ratio (B) in HDF co-incubated 3 days with C- or GD-HUVEC, analysed by flow cytometry. Data are expressed as mean (FOLD vs HDF) ± SD (HUVEC n ≥ 3; HDF n=2). Asterisks point out statistically significant differences between the selected conditions (*p<0.05).

6.2.3 Effect of GD-HUVEC on ECM degradation by dermal fibroblasts

To further elucidate the role of GD-HUVEC on ECM remodelling by dermal fibroblasts, ECM degradation by the synergistic action of MMP and TIMP was evaluated in HDF co-incubated with C- or GD-HUVEC (**Figure 33**).

Firstly, HDF co-incubated with GD-HUVEC showed significant upregulation of MMP2 production and significant downregulation of TIMP2 expression (**Figure 33A,B**).

Contextually, MMP2 activity was studied by zymography analysis. In particular, HDF co-incubated with GD-HUVEC exhibited a higher MMP activity, even if not significant, compared to HDF co-incubated with control cells (**Figure 33C**).

These findings highlight the potential ability of GD-HUVEC secreted factors to move the ECM remodelling balance toward an increased ECM degradation, characterized by the upregulation of MMP activity, and a reduced ECM production, as revealed by decreased COL1A1 expression.

Of note, HDF co-incubated with C-HUVEC showed increased MMP2 and TIMP2 production compared to HDF alone (**Figure 34F,G**). This data results in no differences in MMP activity of HDF co-incubated with C-HUVEC compared to HDF alone, highlighting a maintenance of ECM remodelling equilibrium (**Figure 34H**).

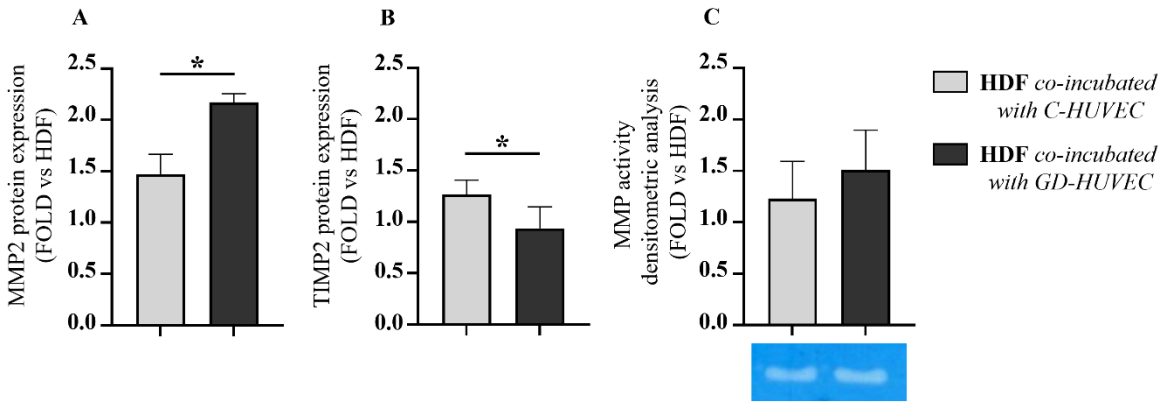


Figure 33. *HDF co-incubated with GD-HUVEC showed increased MMP2 levels and activity as well as decreased TIMP2 protein expression compared to HDF co-incubated with C-HUVEC*. MMP2 (A) and TIMP2 (B) protein expression and MMP2 activity (C) in HDF co-incubated 3 days with C- or GD-HUVEC analysed by flow cytometry and zymography, respectively. Data are expressed as mean (FOLD vs HDF) ± SD (HUVEC n ≥ 3; HDF n=2). Asterisks point out statistically significant differences between the selected conditions (*p<0.05).

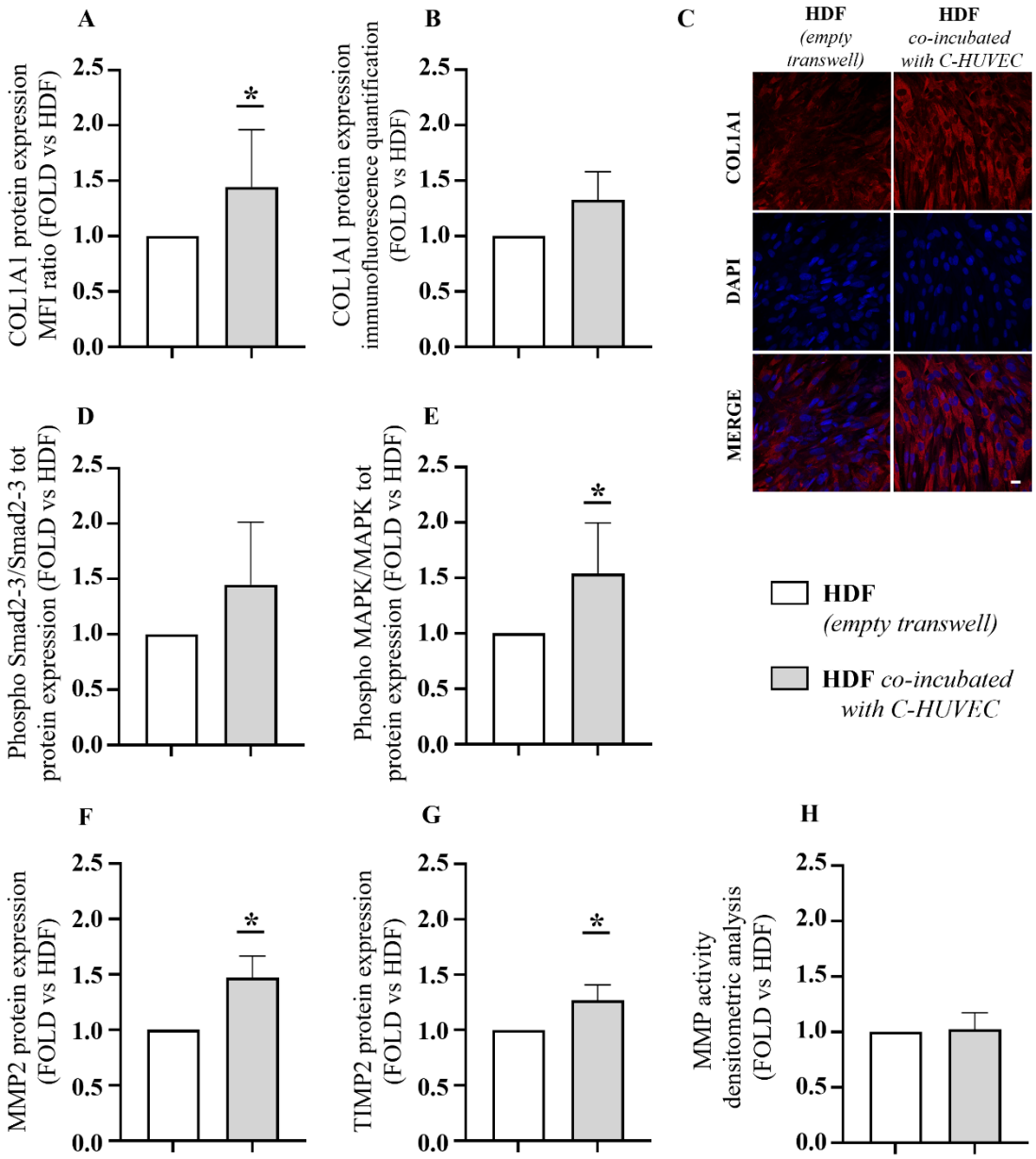


Figure 34. *HDF co-incubated with C-HUVEC showed an ECM remodelling balance moved toward an increased ECM production, revealed by increased COL1A expression, and an unaltered ECM degradation, revealed by increased levels of both MMP2 and TIMP2 and no changes in MMP activity.* COL1A1 (A), MMP2 (F) and TIMP2 (G) protein expression as well as Smad2-3 (D) and MAPK (E) activation, in HDF alone or co-incubated with C-HUVEC, analysed by flow cytometry. COL1A1 total amount quantification (B) and representative images (C), in HDF alone or co-incubated with C-HUVEC, analysed by immunofluorescence. Scale bar 20µm. MMP activity (H), in HDF alone or co-incubated with C-HUVEC, analysed by zymography. Data are expressed as mean (FOLD vs HDF) ± SD (HUVEC n ≥ 3; HDF n=2). Asterisks point out statistically significant differences between the selected condition and the hypothetical value of 1 set up as baseline for the "HDF" experimental condition (*p<0.05).

6.2.4 Effect of GD-HUVEC on migration by dermal fibroblasts

To investigate the role of GD-HUVEC on dermal fibroblasts migration, wound healing scratch assay has been performed on HDF co-incubated with C- or GD-HUVEC, monitoring cells at different timepoints (**Figure 35**).

HDF co-incubated with GD-HUVEC showed reduced cell migration ability, especially at timepoints ranging from 18 to 42 hours after the scratch, compared to HDF co-incubated with C-HUVEC (**Figure 35B,C**). Particularly, HDF co-incubated with GD-HUVEC exhibited significant reduction in cell migration capacity at 24h following scratch compared to HDF co-incubated with endothelial control cells (**Figure 35A**).

These findings suggest that GD-HUVEC could negatively impact HDF migration.

Interestingly, HDF co-incubated with C-HUVEC showed an increased migration ability compared to HDF alone, although this difference did not reach significant significance (**Figure 37B,C**).

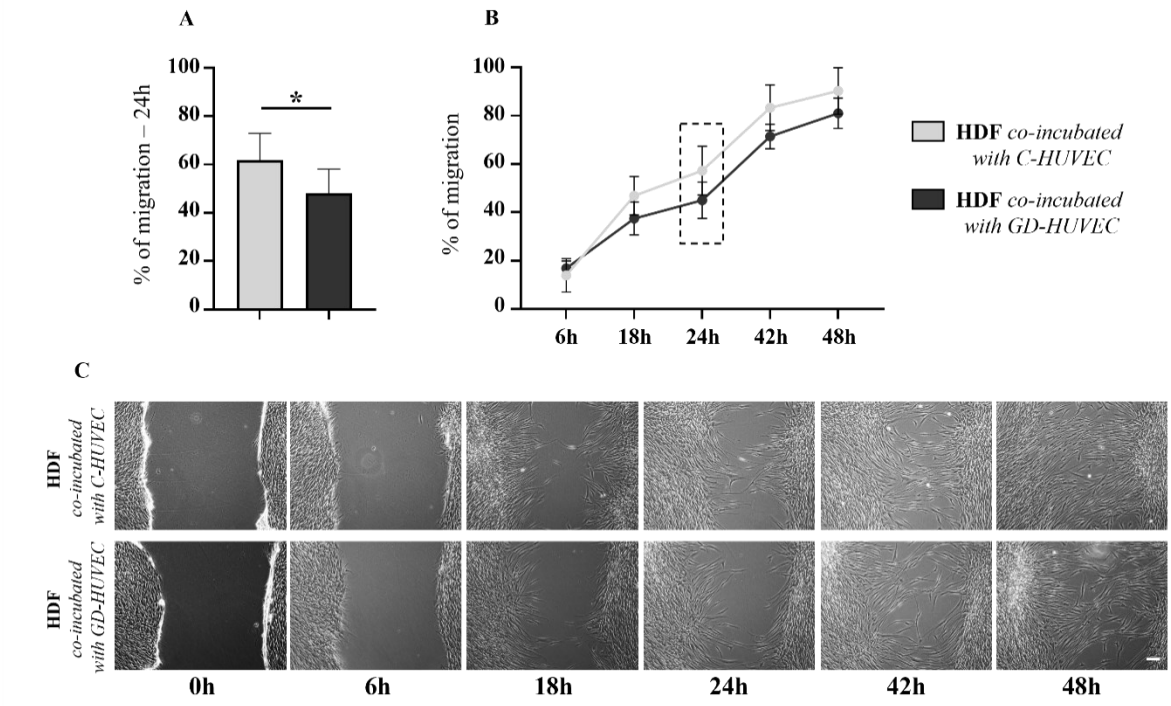


Figure 35. *HDF co-incubation with GD-HUVEC showed reduced migration ability compared to HDF co-incubated with C-HUVEC.* Percentage (%) of migration at different timepoints (A,B) in HDF co-incubated 3 days with C- or GD-HUVEC analysed by wound healing scratch assay. Data are expressed as mean (% of migration) ± SD (HUVEC n ≥ 3; HDF n=2). Representative figures of all timepoints analysed (C). Scale bar 100µm. Asterisks point out statistically significant differences between the selected conditions (*p<0.05).

6.2.5 Effect of GD-HUVEC on Hippo pathway and FAK expression by dermal fibroblasts

To deeply investigate the role of GD-HUVEC on dermal fibroblast migration, the Hippo pathway, characterized by the phosphorylation of TAZ and YAP, and the expression of FAK, the main mechanisms involved in HDF migration, were studied on HDF co-incubated with C- or GD-HUVEC (**Figure 36**).

When the Hippo pathway gets activated, YAP and TAZ are phosphorylated and, in turn, degraded abolishing their nuclear translocation. Thus, the transcriptional activation of migration related genes is suppressed. On the contrary, when the Hippo pathway is deactivated, YAP and TAZ phosphorylation do not occur, thus, they translocate into the nucleus triggering the transcription of migration related genes. ECM could deactivate Hippo pathway promoting fibroblasts migration. Moreover, FAK expression connected to focal adhesion remodelling is another important pathway involved in HDF migration.

HDF co-incubated with GD-HUVEC showed significant upregulation of the phosphorylated to total ratio of both TAZ and YAP compared to HDF co-incubated with C-HUVEC (**Figure 36 A,B**). Moreover, HDF co-incubated with GD-HUVEC exhibited significant downregulation of FAK expression compared to HDF co-incubated with endothelial control cells (**Figure 36C**).

These finding suggest that GD-HUVEC released factors could activate the Hippo pathway promoting TAZ and YAP phosphorylation blocking the expression of genes that promote fibroblasts migration. At the same time, GD-HUVEC could also downregulate FAK expression decreasing focal adhesion remodelling and thus, reducing cell migration. Of note, HDF co-incubated with C-HUVEC showed increased FAK expression compared to HDF alone (**Figure 37A**), while no differences were detected for TAZ and YAP phosphorylated to total ratio (data not shown). This data, together with the increase of migration ability following C-HUVEC co-incubation, suggest that endothelial control cells could release factors that promote HDF migration mainly modulating focal adhesion remodelling.

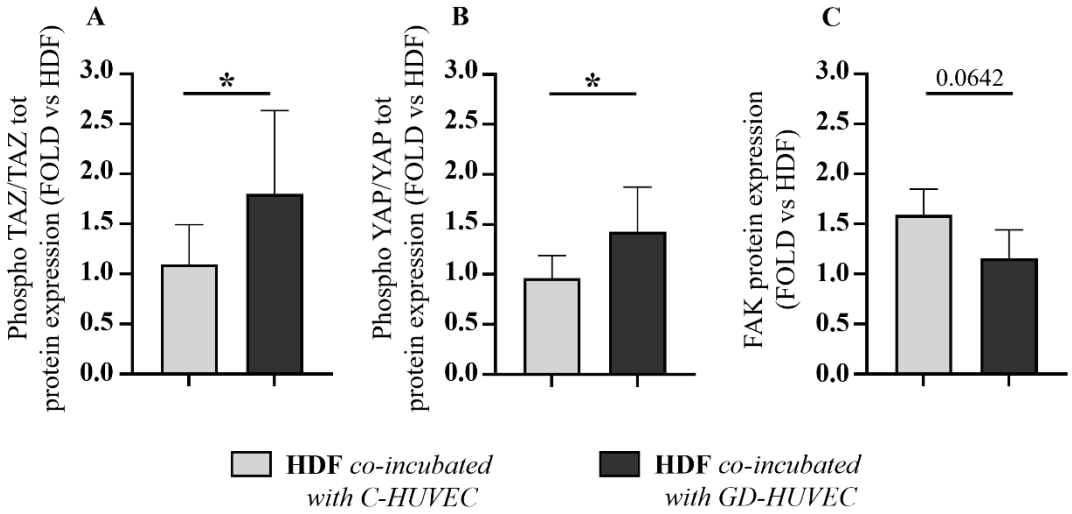


Figure 36. *HDF co-incubated with GD-HUVEC showed increased TAZ and YAP phosphorylated to total ratio and reduced FAK protein expression compared to HDF co-incubated with C-HUVEC.* TAZ phosphorylated (S89) to total ratio (A), YAP phosphorylated (S127) to total ratio (B) and FAK protein expression (C) in HDF co-incubated 3 days with C- or GD-HUVEC, analysed by flow cytometry. Data are expressed as mean (FOLD vs HDF) ± SD (HUVEC n ≥ 3; HDF n=2). Asterisks point out statistically significant differences between the selected conditions (*p<0.05).

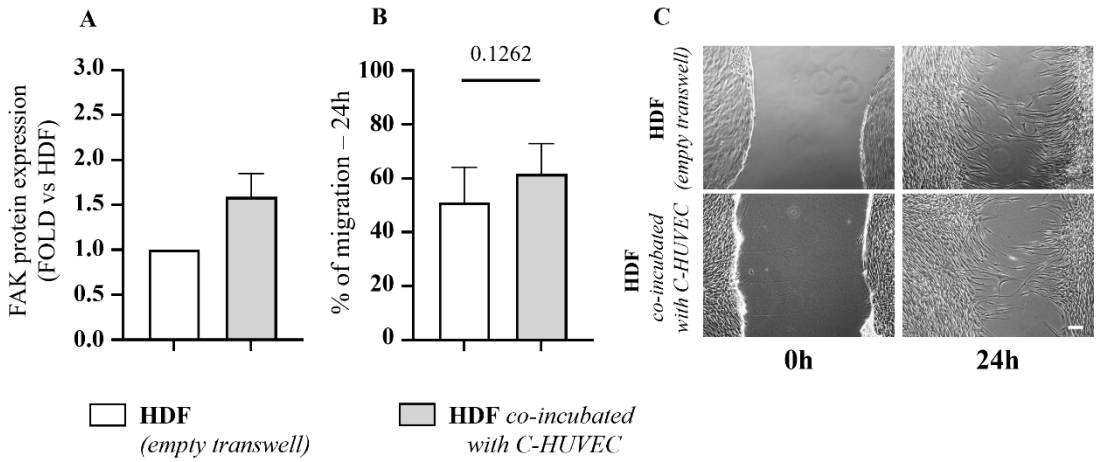


Figure 37. *HDF co-incubated with C-HUVEC showed increased FAK expression and migration ability compared to HDF alone.* FAK protein expression (A) and percentage (%) of migration (B) in HDF alone or co-incubated with C-HUVEC, analysed by flow cytometry and wound healing scratch assay, respectively. Representative figures of all timepoints analysed (C). Scale bar 100µm. Data are expressed as mean (FOLD vs HDF) ± SD, for FAK protein expression, and as mean (as % of migration) ± SD, for wound healing scratch assay, (HUVEC

n ≥ 3; HDF n=2). Asterisks point out statistically significant differences between the selected condition and the hypothetical value of 1 set up as baseline for the "HDF" experimental condition (*p<0.05).

6.2.6 Differences between HDF and diabHDF on metabolic activity and dsDNA amount

Before investigating the role of diabHDF on endothelial cell migration and vessel formation, the differences on metabolic activity and double strand DNA (dsDNA) amount between HDF and diabHDF in basal conditions were investigated (**Figure 38**).

HDF showed an increased amount of dsDNA and an enhancement of metabolic activity, even if not significant, compared to diabHDF in basal conditions (**Figure 38A,B**).

These preliminary data suggest that diabHDF may exhibit a lower proliferation rate, as indirectly indicated by the lower dsDNA levels and metabolic activity, compared to HDF.

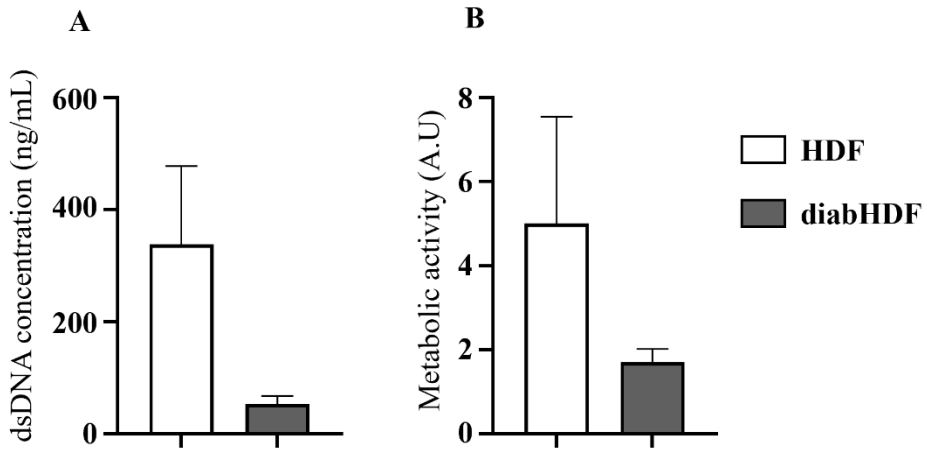


Figure 38. *HDF showed increased dsDNA amount and metabolic activity compared to diabHDF.* dsDNA concentration (ng/mL) (A) and metabolic activity (B) of HDF and diabHDF in basal conditions, analysed by PicoGreen and PrestoBlue assays, respectively. Data are expressed as mean ± SD (HDF n=1; diabHDF n=1).

6.2.7 Differences between HDF and diabHDF on *COL1*, *SMAD3-3*, *MCP-1* and *VEGFa* gene expression

To further investigate the differences between HDF and diabHDF in basal conditions, *COL1, SMAD3-,3 MCP-1* and *VEGFa* gene expression were evaluated (**Figure 39**).

HDF exhibited decreased *COL1* mRNA levels, even if not significant, compared to diabHDF (**Figure 39A**), while no differences were detected for *SMAD3-3* mRNA levels (**Figure 39B**). Moreover, HDF showed an increasing trend of *MCP-1* and *VEGFa* gene expression compared to diabHDF (**Figure 39C,D**).

These preliminary findings suggest that diabHDF showing reduced *COL1* mRNA levels, without a significant alteration of *SMAD3-3* expression, exhibit the same molecular features, regarding ECM production, of HDF co-incubated with GD-HUVEC. In addition, the elevated *MCP-1* expression suggest a potential pro-inflammatory phenotype of diabHDF compared to HDF. The increasing trend of *VEGFa* gene expression in diabHDF is consistent with the *VEGFa* mRNA levels upregulated in GD-HUVEC compared to C-HUVEC.

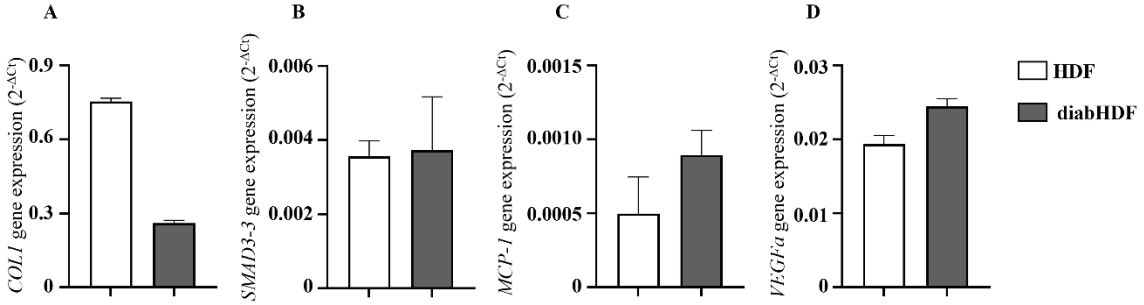


Figure 39. *diabHDF showed reduced COL1 mRNA levels, increased MCP-1 and VEGFa gene expression, while no differences were detected for SMAD3-3 mRNA expression.* Relative mRNA expression of *COL1* (A), *SMAD3-3* (B), *MCP-1* (C) and *VEGFa* (D) of HDF or diabHDF in basal conditions, analysed by RT-PCR. Data are expressed as mean ($2^{-\Delta Ct}$) ± SD (HDF n=1; diabHDF n=1).

6.2.8 Effect of diabHDF on migration by C-HUVEC

To investigate the effect of diabHDF on endothelial cell migration, wound healing scratch assay was performed on C-HUVEC co-incubated with HDF or diabHDF (**Figure 40**).

C-HUVEC co-incubated with diabHDF showed a reduced migration ability compared to those co-incubated with HDF, although the difference was not statistically significant (**Figure 40A,B**).

No differences were detected between C-HUVEC alone or co-incubated with HDF (data not shown).

These preliminary results suggest a potential involvement of diabHDF secreted factors in reducing endothelial cells migration abilities.

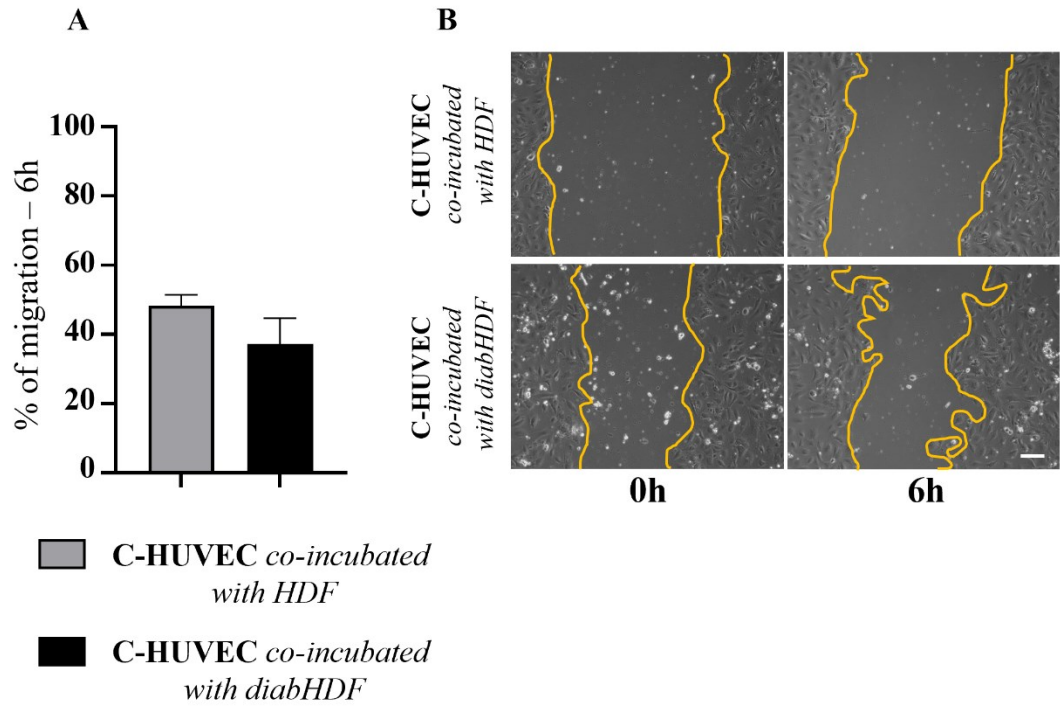


Figure 40. *C-HUVEC co-incubated with diabHDF showed reduced cell migration ability compared to C-HUVEC co-incubated with HDF.* Percentage (%) of migration at 6-hours following scratch in C-HUVEC co-incubated 6 days with HDF or diabHDF analysed by wound healing scratch assay. Data are expressed as mean (as % of migration) ± SD (HUVEC n=2; HDF n=1; diabHDF n=1). Representative figures of all timepoints analysed (B). Scale bar 100µm.

6.2.9 Effect of diabHDF on Matrigel vessel formation by C-HUVEC

To deeply investigate the potential role of diabHDF on vessel formation by endothelial cells, Matrigel tube formation assay was performed on C-HUVEC co-incubated with HDF or diabHDF (**Figure 41**).

C-HUVEC co-incubated with diabHDF showed reduced number of all analysed parameters including the number of extremities, nodes, junctions, master junctions, pieces, segments and branches (**Figure 41A-G**) compared to C-HUVEC co-incubated with HDF.

Moreover, C-HUVEC co-incubated with diabHDF exhibited decreased branches length and total network length compared to C-HUVEC co-incubated with HDF (**Figure 41H,I**).

No differences were detected between C-HUVEC alone or co-incubated with HDF (data not shown).

These preliminary data suggest a possible role of diabHDF in negatively modulating the angiogenesis process worsening all the tested angiogenic parameters and thus, resulting in a less interconnected network compared to the effect promoted by HDF.

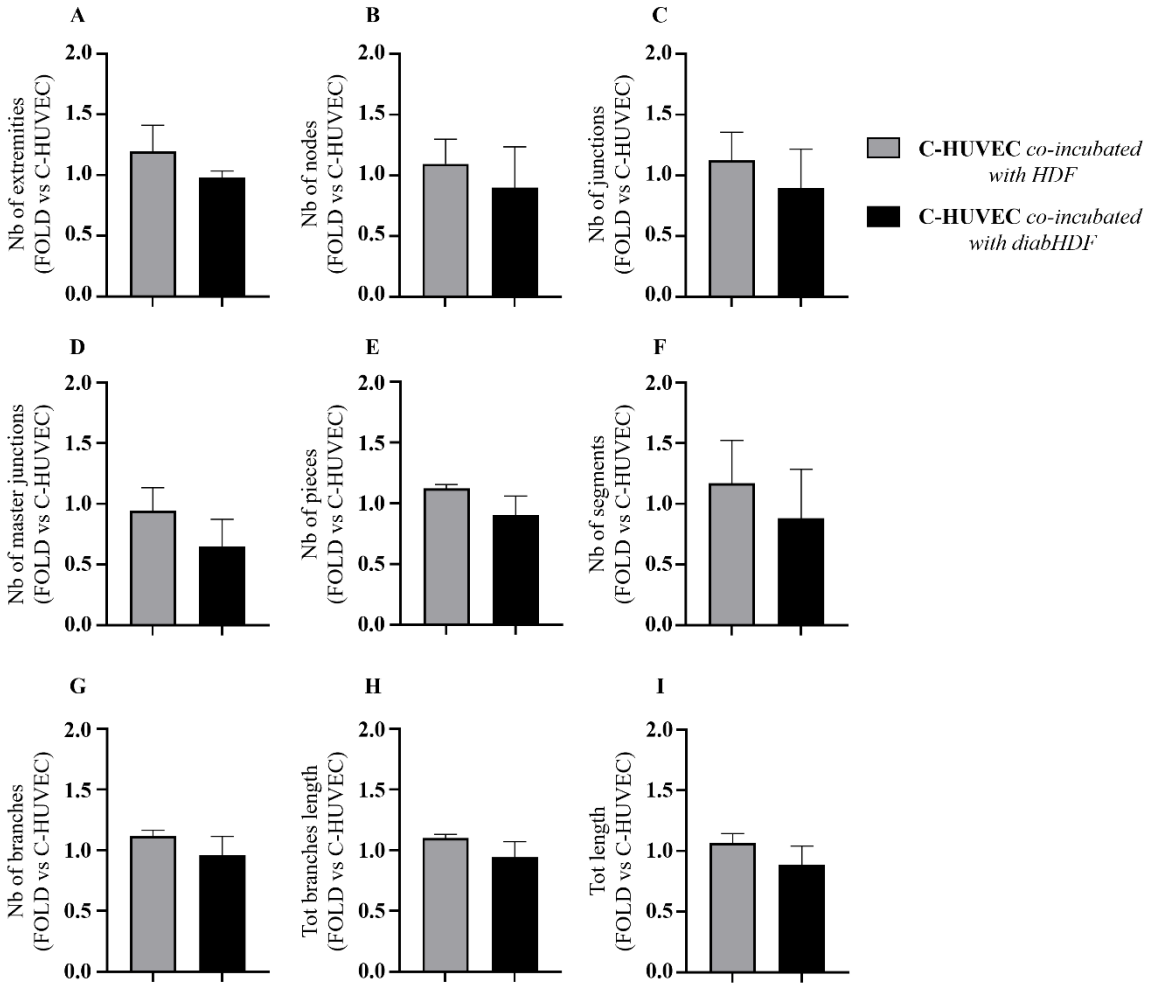


Figure 41. *C-HUVEC co-incubated with diabHDF showed reduced levels of all tested angiogenic parameters compared to C-HUVEC co-incubated with HDF.* Number of extremities (A), nodes (B), junctions (C), master junctions (D), pieces (E), segments (F), branches (G), total branches length (H) and total length (I) in C-HUVEC co-incubated 6 days with HDF or diabHDF, analysed by Matrigel tube formation assay. Data are expressed as mean (FOLD vs C-HUVEC) ± SD (C-HUVEC n=2; HDF n=1; diabHDF n=1).

6.2.10 Effect of diabHDF on VEGFR2 gene and protein expression by C-HUVEC

To investigate the potential mechanism promoted by diabHDF at the base of the reduction in cell migration and vessel formation by C-HUVEC, VEGFR2 gene and protein expression were evaluated in C-HUVEC co-incubated with HDF or diabHDF (**Figure 42**).

C-HUVEC co-incubated with diabHDF showed increased trend of VEGFR2 gene expression compared to C-HUVEC co-incubated with HDF (**Figure 42A**). In contrast, immunofluorescence quantification revealed that C-HUVEC co-incubated with diabHDF exhibited reduced VEGFR2 total protein expression compared to those co-incubated with HDF, although this difference did not reach statistical significance (**Figure 42B**).

A trend toward increased VEGFR2 protein expression was observed in C-HUVEC co-incubated with HDF compared to C-HUVEC cultured alone, while no differences were detected in VEGFR2 mRNA levels (data not shown).

These preliminary findings suggest a potential involvement of VEGFR2 pathway in the negative modulation of both endothelial cells' migration and vessel formation.

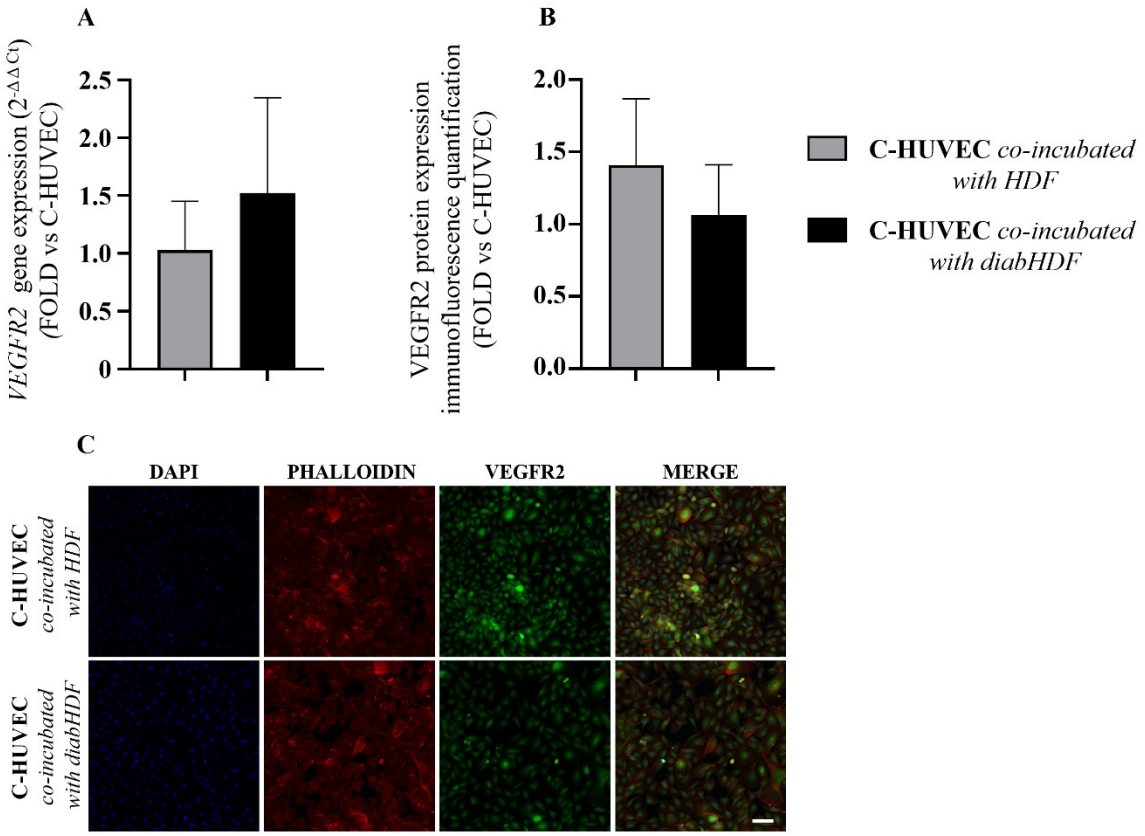


Figure 42. *C-HUVEC co-incubated with diabHDF showed increased VEGR2 mRNA levels and reduced VEGFR2 protein expression compared to C-HUVEC co-incubated with HDF.* VEGFR2 gene (A) and protein (B) expression in C-HUVEC co-incubated 6 days with HDF or diabHDF, analysed by RT-PCR and immunofluorescence, respectively. RT-PCR data are expressed as mean ($2^{-\Delta\Delta Ct}$) ± SD, immunofluorescence data are expressed as mean (FOLD vs C-HUVEC) ± SD (HUVEC n ≥ 3; HDF n=2). Representative figures of immunofluorescence analysis (C). Scale bar 100µm.

6.2.11 Effect of diabHDF on Matrigel vessel formation by GD-HUVEC

To further investigate the role of diabHDF on vessel formation under diabetic condition, Matrigel tube formation assay was performed using GD-HUVEC, endothelial cells epigenetically modified by *in vivo* chronic exposure to hyperglycaemia which reproduce the typical features of diabetic endothelium. Indeed, we have previously demonstrated that GD-HUVEC showed impaired vessel formation on Matrigel compared to C-HUVEC. Thus, Matrigel tube formation assay was conducted on GD-HUVEC co-incubated with HDF or diabHDF (**Figure 43**).

GD-HUVEC co-incubated with diabHDF showed reduced levels of most analysed parameters including the number of nodes, junctions, master junctions, pieces, segments, branches, total branches length and total length (**Figure 43B-I**) compared to GD-HUVEC co-incubated with HDF. No differences were detected for the number of extremities between the two tested conditions (**Figure 43A**).

Moreover, no differences were detected for all tested parameters between GD-HUVEC alone and GD-HUVEC co-incubated with HDF (data not shown).

These preliminary data suggest that factors secreted by diabHDF may promote the formation of a less interconnected vascular network even in GD-HUVEC, which reproduce the typical inflammatory, oxidative and angiogenic phenotype of the diabetic endothelium, thereby contributing to the insufficient angiogenesis underlying diabetic foot ulcer healing.

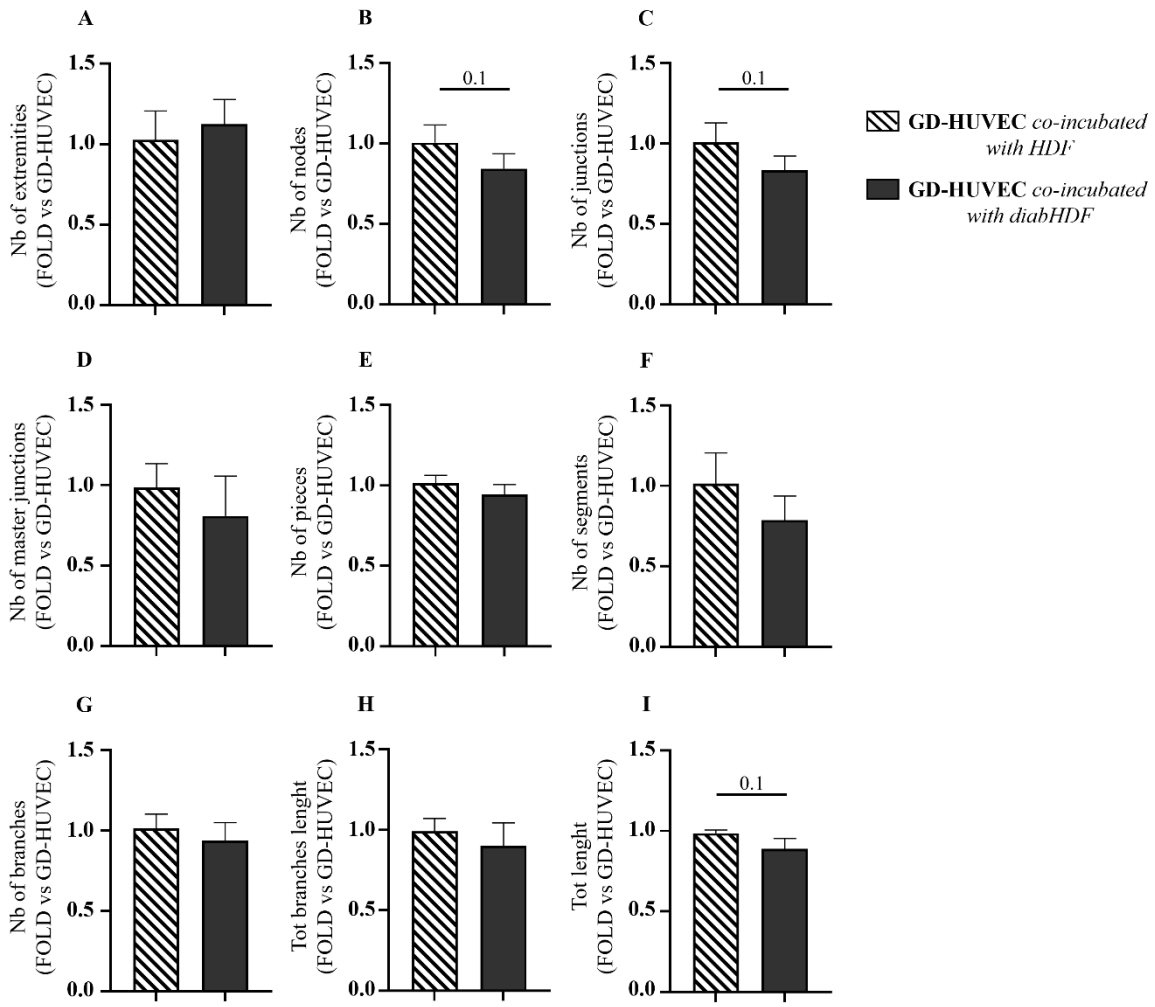


Figure 43. *GD-HUVEC co-incubated with diabHDF showed a reduced trend of the vast majority of analysed angiogenic parameters compared to GD-HUVEC co-incubated with HDF.* Number of extremities (A), nodes (B), junctions (C), master junctions (D), pieces (E), segments (F), branches (G), total branches length (H) and total length (I) in GD-HUVEC co-incubated 6 days with HDF or diabHDF, analysed by Matrigel tube formation assay. Data are expressed as mean (FOLD vs GD-HUVEC) ± SD (GD-HUVEC n=3; HDF n=1; diabHDF n=1).

6.3 DISCUSSION

The present study investigated the interaction between endothelial cells and dermal fibroblasts in the context of diabetes. Specifically, this project aimed to elucidate the role of GD-HUVEC in regulating dermal fibroblast migration and ECM remodelling, as well as the impact of diabetic fibroblasts on endothelial cell migration and vessel formation.

Wound healing is an extremely complex process composed of four different phases. The third step, also called proliferative phase, exhibited a great action of both dermal fibroblasts, involved in replacing the temporary ECM to new granulation tissue, and endothelial cells, strongly involved in the angiogenesis process (Wilkinson HN et al, 2020).

Thus, during the proliferation phase of the finely tuned process of wound healing, endothelial cells and dermal fibroblasts show an intense crosstalk in physiological conditions (Okonkwo UA et al, 2017). Indeed, endothelial cells, interacting with integrins of the ECM and responding to different growth factors and cytokines secreted by fibroblasts, enhance new blood vessel formation and cells' migration ability. On the other side, also fibroblasts positively respond to endothelial cells' secreted factors enhancing ECM production and cell migration, indirectly contributing to the angiogenesis process (Stunova A et al, 2018; Berthod F et al, 2006).

Although their crosstalk is well-established in physiological conditions, in pathological contexts, such as diabetes, the endothelial cell-dermal fibroblast interaction is not completely understood. Therefore, the deeply investigation of the interplay between endothelial cells and dermal fibroblasts in diabetes could help to elucidate the mechanisms behind the impaired healing process and in particular behind the insufficient angiogenesis, laying the foundation for new therapeutic targets discovery.

Firstly, we confirmed that HDF co-incubated with control endothelial cells, compared to HDF alone, showed an unbalanced ECM remodelling toward a greater ECM production, characterized by increased COL1A1 expression due to an increased MAPK activation, and an unaltered ECM degradation, marked by enhanced MMP2 and TIMP2 expression thus resulting in no differences in MMP activity. These findings are consistent with Yuan H et al (2025) who reported that extracellular vesicles obtained from endothelial cells promoted ECM deposition and fibroblasts infiltration in the wound bed of mice (Yuan H et al, 2025).

To investigate the role of GD-HUVEC, which reproduce the typical features of diabetic endothelium, on ECM remodelling by dermal fibroblasts, ECM production was investigated in HDF co-incubated with C- or GD-HUVEC. In particular, we mainly focused on COL1A1 modulation, which accounts more than 70% of ECM composition.

Particularly, HDF co-incubated with GD-HUVEC showed a reduced trend of *FN1* mRNA levels and total COL1A1 production, and a significant downregulation of COL1A1 gene and intracellular protein expression compared to HDF co-incubated with C-HUVEC.

Several studies, consistent with our findings, demonstrated the reduced collagen and ECM production in the skin of diabetic mice compared to control animals (Bowersox JC, 1986; Huang Y et al, 2020).

The collagen synthesis is mediated mainly by two different pathways triggered by TGFβ: the canonical pathway, mediated by Smad proteins activation, and the non-canonical pathways, which involved several mediators including MAPK (ERK1/2) (Shi X et al, 2020).

To gain deeper into the potential mechanism resulting in lower collagen production induced by GD-HUVEC, Smad2-3 as well as MAPK (ERK1/2) phosphorylated to total ratio were investigated. Notably, HDF co-incubated with GD-HUVEC showed a reducing trend of Smad2-3 phosphorylation and a significant reduction of MAPK activation, compared to HDF co-incubated with endothelial control cells, suggesting an involvement of both signalling pathways but more significantly of the MAPK mediated non-canonical mechanism.

To further study the ECM remodelling by HDF promoted by GD-HUVEC, ECM degradation was elucidated. In particular, these cells showed increased MMP2 production and decreased TIMP2 expression resulting in an increasing trend of MMP activity compared to HDF co-incubated with C-HUVEC.

These results are in line with previous findings showing elevated amount of MMP in the wound area of diabetic patients and, especially, in diabetic foot ulcers leading to excessive ECM degradation and impaired healing (Fu K et al, 2022; Izzo V et al, 2014).

These findings suggest that GD-HUVEC secreted factors promoted an unbalanced ECM remodelling by HDF, resulting in decreased ECM production and enhanced ECM degradation, reproducing the condition of diabetic wounds, further contributing to reduced angiogenesis. Indeed, chronic diabetic wounds, characterized by elevated MMP activity which strongly degrade ECM, result in a disorganized matrix micro-structure with low mechanical properties that not correctly support pro-angiogenic mediators signalling and endothelial cells migration and sprouting (Libby JR et al, 2024).

Additionally, fibroblasts migration is an important feature contributing to wound healing. For this reason, we confirmed that HDF co-incubated with control endothelial cells showed increased migration characterized by upregulated FAK expression, thus resulting in a better focal adhesion remodelling, compared to HDF alone. Many studies, concordant with our

findings, demonstrated that endothelial cells promote fibroblasts migration in physiological conditions (Hou T et al, 2022; Yuan H et al, 2025).

Diabetic wounds are characterized by decreased fibroblasts proliferation and migration, thus, the potential role of GD-HUVEC in modulating HDF migration was investigated.

HFD co-incubated with GD-HUVEC showed decreased migration compared to fibroblasts co-incubated with control endothelial cells. To deeply study the mechanisms underlying this effect, the Hippo pathway as well as FAK expression were explored. In particular, HDF co-incubated with GD-HUVEC exhibited a significant upregulation of both YAP and TAZ phosphorylated-to-total ratio determining the activation of the Hippo pathway and a consequent downregulation of migratory related downstream genes, compared to HDF co-incubated with C-HUVEC. Moreover, GD-HUVEC co-incubation induced a significant downregulation of FAK protein expression by HDF, promoting a reduction of focal adhesion remodelling, further contributing to decreased HDF migration.

Several studies, consistent with our findings, reported that YAP and TAZ nuclear translocation is fundamental to achieve wound healing in physiological conditions and that the deletion of both mediators severely impaired the healing process (Schmidt A et al, 2025; Dey A et al, 2020). Notably, some studies reported that YAP and TAZ also regulate TGFβ-activated SMAD transcription factors. Indeed, YAP and TAZ degradation, in turn, block TGF-β mediated myofibroblasts differentiation targeting Smad mediated signalling pathway (Dey A et al, 2020; Hiemer SE et al, 2014). Moreover, Liu W et al (2017) reported results, in line with our findings, showing that fibroblasts under high glucose conditions or from diabetic mice exhibited reduced FAK expression due to an increased activity of Calpain 1, an enzyme involved in FAK degradation (Liu W et al, 2017).

Overall, these results suggest a key role of secreted factors by GD-HUVEC in modulating ECM remodelling toward an increased ECM degradation by dermal fibroblasts and in reducing HDF migration, paving the way for a deeper comprehension of the endothelial cell-dermal fibroblast interaction and in turn, of the insufficient angiogenesis which occur during the impaired healing process of diabetic chronic wounds.

Nevertheless, these results need to be confirmed at longer co-incubation timepoints to further substantiate the role of GD-HUVEC in the regulation of ECM remodelling.

Before investigating the impact of diabHDF on endothelial cell migration and vessel formation, the differences between diabHDF and HDF were studied. In particular, diabHDF showed reduced metabolic activity and dsDNA content compared to HDF suggesting, indirectly, a potential reduction in their proliferation rate. These results are in line with the

findings of Loots MA et al (1999) that reported lower proliferation capacity as well as abnormal morphology of fibroblasts isolated from diabetic ulcers compared to healthy controls (Loots MA et al, 1999).

Additionally, diabHDF showed reduced COL1 gene expression, while no differences were detected for SMAD3-3 mRNA levels. The reduction in COL1 gene expression is consistent with the downregulation obtained in HDF following GD-HUVEC co-incubation and with the previously mentioned findings from the literature (Bowersox JC, 1986; Huang Y et al, 2020).

Moreover, diabHDF exhibited increased *MCP-1* and *VEGFa* gene expression compared to HDF. The enhanced expression of MCP-1 is consistent with Kasiewicz LN et al (2016) results which reported that TNFα produced by macrophages induces MCP-1 production by dermal fibroblasts which, in turn, recruits more macrophages boosting the chronic inflammation typical of diabetic foot ulcers (Kasiewicz LN et al, 2016).

Overall, diabHDF exhibited important differences compared to healthy fibroblasts in terms of both proliferation and gene expression profile. However, these preliminary results require further validation using more biological replicates to reach statistical significance.

Lastly, diabHDF were co-incubated with C-HUVEC to further elucidate the potential role of these cells on endothelial cell migration and vessel formation.

Particularly, C-HUVEC co-incubated with diabHDF showed reduced cell migration and decreased all the tested angiogenic parameters resulting in a structurally less interconnected network characterized by reduced total and branches length, compared to control endothelial cells incubated with HDF.

These preliminary findings are consistent with the results reported by Gao R et al (2023) who showed that dermal fibroblasts, treated with IL7 (which is increased in high glucose condition), impair endothelial cell proliferation, migration and angiogenesis, by secreting angiopoietin-like-4 (ANGPTL4) (Gao R et al, 2023).

To gain insight into the potential mechanism behind the reduction in endothelial cell migration and vessel formation induced by diabHDF co-incubation, VEGFR2 gene and protein expression was evaluated. In particular, C-HUVEC showed increased receptor mRNA levels, but reduced VEGFR2 protein expression compared to endothelial cells co-incubated with HDF.

These preliminary findings suggest a potential involvement of the VEGFR2 mediated pathway as possible mechanism underling the diabHDF mediated reduction in C-HUVEC migration and angiogenesis.

To further investigate the effects of diabHDF in reducing vessel formation in diabetic context, diabHDF were co-incubated with GD-HUVEC, which, as demonstrated by Pipino C et al

(2022), show increased number of isolated elements and reduced amount of interconnections, resulting in a worsening of the developed network, compared to C-HUVEC. Notably, diabHDF co-incubation induced an impairment in the vast majority of the analysed parameters in GD-HUVEC, additionally corroborating its potential effects in negatively modulating the angiogenesis process.

These results, even if preliminary, pave the way for a better comprehension of the impact of dermal fibroblasts secreted factors on angiogenesis. Nevertheless, these findings need to be confirmed on more biological replicates to validate our hypothesis.

Additionally, a future perspective could be to investigate the potential mediators secreted by dermal fibroblasts and endothelial cells which are the key drivers of their interaction to explore new potential therapeutic targets.

7 CONCLUSIONS

This thesis aims to gain insight into the mechanisms underlying the endothelial dysfunction in diabetes with a specific emphasis on the reduced angiogenesis-associated molecular pathways, typical of chronic diabetic wounds, and on innovative therapeutic strategies.

To this end, the unique *in vitro* model of GD-HUVEC has been employed. Owing to stable epigenetic modifications acquired following *in vivo* exposure to hyperglycaemia during pregnancy, this model faithfully reproduces the typical features of diabetic endothelial dysfunction including the pro-inflammatory and pro-oxidative phenotype and the reduced angiogenesis.

Firstly, the findings showed in this thesis demonstrate the role of Picual and Changlot Real olive leaf phenolic extracts in counteracting vascular inflammation by modulating NF-kB activation and thus, reducing the expression and membrane exposure of vascular adhesion molecules resulting in reduced monocytes adhesion.

Additionally, the results previously displayed assess the pro-angiogenic role of amniotic membrane via VEGFR2/AKT/eNOS signalling pathway. Particularly, amniotic membrane, promoting the activation of VEGFR2 and AKT, leads to nitro-oxidative stress reduction and, consequently, to structurally more interconnected vessel formation.

To further investigate the molecular mechanisms that regulate reduced angiogenesis in chronic diabetic wounds, the interaction between endothelial cells and dermal fibroblasts was studied. Specifically, the findings showed in the thesis demonstrate that GD-HUVEC compromise ECM remodelling by HDF toward a greater matrix degradation and a lower matrix production, mainly regulated by MAPK-associated TGF-β non-canonical pathway, indirectly affecting angiogenesis. Additionally, the preliminary results showed in the thesis suggest that diabHDF negatively modulate endothelial cell migration and vessel formation.

Overall, these findings lay the foundation for a better understanding of different molecular pathways associated to endothelial dysfunction and reduced angiogenesis, which are characteristic of diabetic chronic wounds, thereby facilitating the identification of new therapeutic targets. Furthermore, by highlighting the anti-inflammatory and pro-angiogenic effects of phenolic extracts and amniotic membrane, respectively, these results strongly support their potential future application in clinical practice. Ultimately, this work not only advances our mechanistic understanding of diabetic endothelial dysfunction but also paves the way for innovative therapies that could transform the management of chronic diabetic wounds.

8 REFERENCES

Abbott CA, Malik RA, van Ross ER, Kulkarni J, Boulton AJ. Prevalence and characteristics of painful diabetic neuropathy in a large community-based diabetic population in the U.K. Diabetes Care. 2011 Oct;34(10):2220-4. doi: 10.2337/dc11-1108.

Ahmad S, Hewett PW, Wang P, Al-Ani B, Cudmore M, Fujisawa T, Haigh JJ, le Noble F, Wang L, Mukhopadhyay D, Ahmed A. Direct evidence for endothelial vascular endothelial growth factor receptor-1 function in nitric oxide-mediated angiogenesis. Circ Res. 2006 Sep 29;99(7):715-22. doi: 10.1161/01.RES.0000243989.46006.b9.

Akil AA, Yassin E, Al-Maraghi A, Aliyev E, Al-Malki K, Fakhro KA. Diagnosis and treatment of type 1 diabetes at the dawn of the personalized medicine era. J Transl Med. 2021 Apr 1;19(1):137. doi: 10.1186/s12967-021-02778-6.

Albers JW, Pop-Busui R. Diabetic neuropathy: mechanisms, emerging treatments, and subtypes. Curr Neurol Neurosci Rep. 2014 Aug;14(8):473. doi: 10.1007/s11910-014-0473-5.

Alicic RZ, Rooney MT, Tuttle KR. Diabetic Kidney Disease: Challenges, Progress, and Possibilities. Clin J Am Soc Nephrol. 2017 Dec 7;12(12):2032-2045. doi: 10.2215/CJN.11491116.

American Diabetes Association Professional Practice Committee. 2. Diagnosis and Classification of Diabetes: Standards of Care in Diabetes-2024. Diabetes Care. 2024 Jan 1;47(Suppl 1):S20-S42. doi: 10.2337/dc24-S002.

American Diabetes Association Professional Practice Committee. 2. Classification and Diagnosis of Diabetes: Standards of Medical Care in Diabetes-2022. Diabetes Care. 2022 Jan 1;45(Suppl 1):S17-S38. doi: 10.2337/dc22-S002.

American Diabetes Association. 2. Classification and Diagnosis of Diabetes: *Standards of Medical Care in Diabetes-2018*. Diabetes Care. 2018 Jan;41(Suppl 1):S13-S27. doi: 10.2337/dc18-S002.

American Diabetes Association. Diagnosis and classification of diabetes mellitus. Diabetes Care 2014;37(Suppl. 1):S81–S90

American Diabetes Association. Diagnosis and classification of diabetes mellitus. Diabetes Care. 2011 Jan;34 Suppl 1(Suppl 1):S62-9. doi: 10.2337/dc11-S062.

American Diabetes Association. Economic Costs of Diabetes in the U.S. in 2017. Diabetes Care. 2018 May;41(5):917-928. doi: 10.2337/dci18-0007.

Andreadou I, Sigala F, Iliodromitis EK, Papaefthimiou M, Sigalas C, Aligiannis N, Savvari P, Gorgoulis V, Papalabros E, Kremastinos DT. Acute doxorubicin cardiotoxicity is successfully treated with the phytochemical oleuropein through suppression of oxidative and nitrosative stress. J Mol Cell Cardiol. 2007 Mar;42(3):549-58. doi: 10.1016/j.yjmcc.2006.11.016.

Andreozzi F, Formoso G, Prudente S, Hribal ML, Pandolfi A, Bellacchio E, Di Silvestre S, Trischitta V, Consoli A, Sesti G. TRIB3 R84 variant is associated with impaired insulin-

mediated nitric oxide production in human endothelial cells. Arterioscler Thromb Vasc Biol. 2008 Jul;28(7):1355-60. doi: 10.1161/ATVBAHA.108.162883.

Armstrong DG, Boulton AJM, Bus SA. Diabetic Foot Ulcers and Their Recurrence. N Engl J Med. 2017 Jun 15;376(24):2367-2375. doi: 10.1056/NEJMra1615439.

Armstrong DG, Tan TW, Boulton AJM, Bus SA. Diabetic Foot Ulcers: A Review. JAMA. 2023 Jul 3;330(1):62-75. doi: 10.1001/jama.2023.10578.

Atkinson MA, Eisenbarth GS, Michels AW. Type 1 diabetes. Lancet. 2014 Jan 4;383(9911):69-82. doi: 10.1016/S0140-6736(13)60591-7.

Aubry EM, Raio L, Oelhafen S. Effect of the IADPSG screening strategy for gestational diabetes on perinatal outcomes in Switzerland. Diabetes Res Clin Pract. 2021 May;175:108830. doi: 10.1016/j.diabres.2021.108830.

Bernabé-García Á, Liarte S, Moraleda JM, Castellanos G, Nicolás FJ. Amniotic membrane promotes focal adhesion remodeling to stimulate cell migration. Sci Rep. 2017 Nov 10;7(1):15262. doi: 10.1038/s41598-017-15509-z.

Berthod F, Germain L, Tremblay N, Auger FA. Extracellular matrix deposition by fibroblasts is necessary to promote capillary-like tube formation in vitro. J Cell Physiol. 2006 May;207(2):491-8. doi: 10.1002/jcp.20584.

Bo S, Signorile A, Menato G, Gambino R, Bardelli C, Gallo ML, Cassader M, Massobrio M, Pagano GF. C-reactive protein and tumor necrosis factor-alpha in gestational hyperglycemia. J Endocrinol Invest. 2005 Oct;28(9):779-86. doi: 10.1007/BF03347566.

Bongarzone S, Savickas V, Luzi F, Gee AD. Targeting the Receptor for Advanced Glycation Endproducts (RAGE): A Medicinal Chemistry Perspective. J Med Chem. 2017 Sep 14;60(17):7213-7232. doi: 10.1021/acs.jmedchem.7b00058.

Bowersox JC. In vivo collagen metabolism in spontaneously diabetic (db/db) mice. Exp Mol Pathol. 1986 Oct;45(2):221-6. doi: 10.1016/0014-4800(86)90061-4.

Brindeau A. Creation d'un vagin artificiel A l'aide des membranes ovulaires d'un oeuf A terme. J. Gynecol. Obstet. Biol. Reprod (Paris) 1934; 13, 821–824.

Burger K. Weitere erfahrungen iiber die kunstliche scheidenbildung mit eihauten. Zentralbl. Gynäkol. 1937; 69, 1153–1154.

Burgess JL, Wyant WA, Abdo Abujamra B, Kirsner RS, Jozic I. Diabetic Wound-Healing Science. Medicina (Kaunas). 2021 Oct 8;57(10):1072. doi: 10.3390/medicina57101072.

Campbell BCV, De Silva DA, Macleod MR, Coutts SB, Schwamm LH, Davis SM, Donnan GA. Ischaemic stroke. Nat Rev Dis Primers. 2019 Oct 10;5(1):70. doi: 10.1038/s41572-019-0118-8.

Cappellacci I, Di Pietrantonio N, Viola D, Formoso G, Zujko ME, Martín-García B, Gomez-Caravaca AM, Verardo V, Pandolfi A, Pipino C. Unveiling the anti-inflammatory potential of olive leaf phenolic extracts in diabetes-related endothelial dysfunction. Front Endocrinol (Lausanne). 2025 Oct 14;16:1671932. doi: 10.3389/fendo.2025.1671932.

Carmeliet P. Angiogenesis in life, disease and medicine. Nature. 2005 Dec 15;438(7070):932-6. doi: 10.1038/nature04478.

Castellano JM, Ramos-Romero S, Perona JS. Oleanolic Acid: Extraction, Characterization and Biological Activity. Nutrients. 2022 Jan 31;14(3):623. doi: 10.3390/nu14030623.

Catalano PM, Tyzbir ED, Roman NM, Amini SB, Sims EA. Longitudinal changes in insulin release and insulin resistance in nonobese pregnant women. Am J Obstet Gynecol. 1991 Dec;165(6 Pt 1):1667-72. doi: 10.1016/0002-9378(91)90012-g.

Chandrasekaran P, Weiskirchen R. The Role of Obesity in Type 2 Diabetes Mellitus-An Overview. Int J Mol Sci. 2024 Feb 4;25(3):1882. doi: 10.3390/ijms25031882.

Chellan G, Shivaprakash S, Karimassery Ramaiyar S, Varma AK, Varma N, Thekkeparambil Sukumaran M, Rohinivilasam Vasukutty J, Bal A, Kumar H. Spectrum and prevalence of fungi infecting deep tissues of lower-limb wounds in patients with type 2 diabetes. J Clin Microbiol. 2010 Jun;48(6):2097-102. doi: 10.1128/JCM.02035-09.

Chen K, Tang L, Wang X, Li Y, Zhang X, Cui S, Chen W, Jin Z, Zhu D. Prevalence and risk factors for type 2 diabetes mellitus in women with gestational diabetes mellitus: a systematic review and meta-analysis. Front Endocrinol (Lausanne). 2024 Dec 23;15:1486861. doi: 10.3389/fendo.2024.1486861.

Chen P, Piaggi P, Traurig M, Bogardus C, Knowler WC, Baier LJ, Hanson RL. Differential methylation of genes in individuals exposed to maternal diabetes in utero. Diabetologia. 2017 Apr;60(4):645-655. doi: 10.1007/s00125-016-4203-1.

Chen RR, Silva EA, Yuen WW, Mooney DJ. Spatio-temporal VEGF and PDGF delivery patterns blood vessel formation and maturation. Pharm Res. 2007 Feb;24(2):258-64. doi: 10.1007/s11095-006-9173-4.

Chen S, Zeng L, Hu Z. Progressing haemorrhagic stroke: categories, causes, mechanisms and managements. J Neurol. 2014 Nov;261(11):2061-78. doi: 10.1007/s00415-014-7291-1. Epub 2014 Mar 5. PMID: 24595959; PMCID: PMC4221651.

Chen X, Li H, Wang Z, Zhou Q, Chen S, Yang B, Yin D, He H, He M. Quercetin protects the vascular endothelium against iron overload damages via ROS/ADMA/DDAHII/eNOS/NO pathway. Eur J Pharmacol. 2020 Feb 5;868:172885. doi: 10.1016/j.ejphar.2019.172885.

Chistiakov DA, Melnichenko AA, Grechko AV, Myasoedova VA, Orekhov AN. Potential of anti-inflammatory agents for treatment of atherosclerosis. Exp Mol Pathol. 2018 Apr;104(2):114-124. doi: 10.1016/j.yexmp.2018.01.008.

Christensen AA, Gannon M. The Beta Cell in Type 2 Diabetes. Curr Diab Rep. 2019 Aug 9;19(9):81. doi: 10.1007/s11892-019-1196-4.

Ciumărnean L, Milaciu MV, Runcan O, Vesa ȘC, Răchișan AL, Negrean V, Perné MG, Donca VI, Alexescu TG, Para I, Dogaru G. The Effects of Flavonoids in Cardiovascular Diseases. Molecules. 2020 Sep 21;25(18):4320. doi: 10.3390/molecules25184320.

Claesson-Welsh L, Welsh M. VEGFA and tumour angiogenesis. J Intern Med. 2013 Feb;273(2):114-27. doi: 10.1111/joim.12019.

Clegg LW, Mac Gabhann F. Site-Specific Phosphorylation of VEGFR2 Is Mediated by Receptor Trafficking: Insights from a Computational Model. PLoS Comput Biol. 2015 Jun 12;11(6):e1004158. doi: 10.1371/journal.pcbi.1004158.

Clewell AE, Béres E, Vértesi A, Glávits R, Hirka G, Endres JR, Murbach TS, Szakonyiné IP. A Comprehensive Toxicological Safety Assessment of an Extract of Olea Europaea L. Leaves (Bonolive™). Int J Toxicol. 2016 Mar-Apr;35(2):208-21. doi: 10.1177/1091581815619764.

Consoli C, Martelli E, D'Adamo M, Menghini R, Arcelli D, Porzio O, Pandolfi A, Pistolese GR, Consoli A, Lauro R, Ippoliti A, Federici M. Insulin resistance affects gene expression in endothelium. Arterioscler Thromb Vasc Biol. 2008 Feb;28(2):e7-9. doi: 10.1161/ATVBAHA.107.152264.

Czech MP. Mechanisms of insulin resistance related to white, beige, and brown adipocytes. Mol Metab. 2020 Apr;34:27-42. doi: 10.1016/j.molmet.2019.12.014.

Daiber A, Chlopicki S. Revisiting pharmacology of oxidative stress and endothelial dysfunction in cardiovascular disease: Evidence for redox-based therapies. Free Radic Biol Med. 2020 Sep;157:15-37. doi: 10.1016/j.freeradbiomed.2020.02.026.

Dali-Youcef N, Mecili M, Ricci R, Andrès E. Metabolic inflammation: connecting obesity and insulin resistance. Ann Med. 2013 May;45(3):242-53. doi: 10.3109/07853890.2012.705015.

Davis J. Skin transplantation with a review of 550 cases at the Johns Hopkins hospital. Johns Hopkins Med. J. 1910; 15, 15.

de Alencar Silva A, Pereira-de-Morais L, Rodrigues da Silva RE, de Menezes Dantas D, Brito Milfont CG, Gomes MF, Araújo IM, Kerntopf MR, Alencar de Menezes IR, Barbosa R. Pharmacological screening of the phenolic compound caffeic acid using rat aorta, uterus and ileum smooth muscle. Chem Biol Interact. 2020 Dec 1;332:109269. doi: 10.1016/j.cbi.2020.109269.

de Bock M, Derraik JG, Brennan CM, Biggs JB, Morgan PE, Hodgkinson SC, Hofman PL, Cutfield WS. Olive (Olea europaea L.) leaf polyphenols improve insulin sensitivity in middle-aged overweight men: a randomized, placebo-controlled, crossover trial. PLoS One. 2013;8(3):e57622. doi: 10.1371/journal.pone.0057622.

De Meyts P. The Insulin Receptor and Its Signal Transduction Network. 2016 Apr 27. In: Feingold KR, Ahmed SF, Anawalt B, Blackman MR, Boyce A, Chrousos G, Corpas E, de Herder WW, Dhatariya K, Dungan K, Hofland J, Kalra S, Kaltsas G, Kapoor N, Koch C, Kopp P, Korbonits M, Kovacs CS, Kuohung W, Laferrère B, Levy M, McGee EA, McLachlan R, Muzumdar R, Purnell J, Rey R, Sahay R, Shah AS, Singer F, Sperling MA, Stratakis CA, Trence DL, Wilson DP, editors. *Endotext [Internet]. South Dartmouth (MA): MDText.com, Inc.; 2000–*. PMID: 27512793.

De Rotth A. Plastic repair of conjunctival defects with fetal membranes. Arch. Ophthalmol. 1940; 23, 522. doi:10.1097/ICO.0b013e318156cb08

Del Chierico F, Rapini N, Deodati A, Matteoli MC, Cianfarani S, Putignani L. Pathophysiology of Type 1 Diabetes and Gut Microbiota Role. Int J Mol Sci. 2022 Nov 24;23(23):14650. doi: 10.3390/ijms232314650.

Demidova-Rice TN, Durham JT, Herman IM. Wound Healing Angiogenesis: Innovations and Challenges in Acute and Chronic Wound Healing. Adv Wound Care (New Rochelle). 2012 Feb;1(1):17-22. doi: 10.1089/wound.2011.0308.

Dendup T, Feng X, Clingan S, Astell-Burt T. Environmental Risk Factors for Developing Type 2 Diabetes Mellitus: A Systematic Review. Int J Environ Res Public Health. 2018 Jan 5;15(1):78. doi: 10.3390/ijerph15010078.

Deng H, Li B, Shen Q, Zhang C, Kuang L, Chen R, Wang S, Ma Z, Li G. Mechanisms of diabetic foot ulceration: A review. J Diabetes. 2023 Apr;15(4):299-312. doi: 10.1111/1753-0407.13372.

Deus IA, Mano JF, Custódio CA. Perinatal tissues and cells in tissue engineering and regenerative medicine. Acta Biomater. 2020 Jul 1;110:1-14. doi: 10.1016/j.actbio.2020.04.035.

Dey A, Varelas X, Guan KL. Targeting the Hippo pathway in cancer, fibrosis, wound healing and regenerative medicine. Nat Rev Drug Discov. 2020 Jul;19(7):480-494. doi: 10.1038/s41573-020-0070-z.

Di Cianni G, Miccoli R, Volpe L, Lencioni C, Del Prato S. Intermediate metabolism in normal pregnancy and in gestational diabetes. Diabetes Metab Res Rev. 2003 Jul-Aug;19(4):259-70. doi: 10.1002/dmrr.390.

Di Fulvio P, Pandolfi A, Formoso G, Di Silvestre S, Di Tomo P, Giardinelli A, De Marco A, Di Pietro N, Taraborrelli M, Sancilio S, Di Pietro R, Piantelli M, Consoli A. Features of endothelial dysfunction in umbilical cord vessels of women with gestational diabetes. Nutr Metab Cardiovasc Dis. 2014 Dec;24(12):1337-45. doi: 10.1016/j.numecd.2014.06.005.

Di Pietrantonio N, Palmerini C, Pipino C, Baldassarre MPA, Bologna G, Mohn A, Giannini C, Lanuti P, Chiarelli F, Pandolfi A, Di Pietro N. Plasma from obese children increases monocyte-endothelial adhesion and affects intracellular insulin signaling in cultured endothelial cells: Potential role of mTORC1-S6K1. Biochim Biophys Acta Mol Basis Dis. 2021 Apr 1;1867(4):166076. doi: 10.1016/j.bbadis.2021.166076.

Di Pietrantonio N, Sánchez-Ceinos J, Shumliakivska M, Rakow A, Mandatori D, Di Tomo P, Formoso G, Bonfini T, Baldassarre MPA, Sennström M, Almahmeed W, Pandolfi A, Cosentino F. The inflammatory and oxidative phenotype of gestational diabetes is epigenetically transmitted to the offspring: role of methyltransferase MLL1-induced H3K4me3. Eur Heart J. 2024 Dec 23;45(48):5171-5185. doi: 10.1093/eurheartj/ehae688.

Di Tomo P, Alessio N, Falone S, Pietrangelo L, Lanuti P, Cordone V, Santini SJ, Di Pietrantonio N, Marchisio M, Protasi F, Di Pietro N, Formoso G, Amicarelli F, Galderisi U, Pandolfi A. Endothelial cells from umbilical cord of women affected by gestational diabetes: A suitable in vitro model to study mechanisms of early vascular senescence in diabetes. FASEB J. 2021 Jun;35(6):e21662. doi: 10.1096/fj.202002072RR.

Di Tomo P, Canali R, Ciavardelli D, Di Silvestre S, De Marco A, Giardinelli A, Pipino C, Di Pietro N, Virgili F, Pandolfi A. β-Carotene and lycopene affect endothelial response to TNF-α

reducing nitro-oxidative stress and interaction with monocytes. Mol Nutr Food Res. 2012 Feb;56(2):217-27. doi: 10.1002/mnfr.201100500.

DiMeglio LA, Evans-Molina C, Oram RA. Type 1 diabetes. Lancet. 2018 Jun 16;391(10138):2449-2462. doi: 10.1016/S0140-6736(18)31320-5.

Dimmeler S, Zeiher AM. Endothelial cell apoptosis in angiogenesis and vessel regression. Circ Res. 2000 Sep 15;87(6):434-9. doi: 10.1161/01.res.87.6.434.

Dong H, Sun Y, Nie L, Cui A, Zhao P, Leung WK, Wang Q. Metabolic memory: mechanisms and diseases. Signal Transduct Target Ther. 2024 Feb 28;9(1):38. doi: 10.1038/s41392-024-01755-x.

Drela E, Stankowska K, Kulwas A, Rość D. Endothelial progenitor cells in diabetic foot syndrome. Adv Clin Exp Med. 2012 Mar-Apr;21(2):249-54.

Du Cheyne C, Tay H, De Spiegelaere W. The complex TIE between macrophages and angiogenesis. Anat Histol Embryol. 2020 Sep;49(5):585-596. doi: 10.1111/ahe.12518.

Duan-Arnold Y, Gyurdieva A, Johnson A, Jacobstein DA, Danilkovitch A. Soluble Factors Released by Endogenous Viable Cells Enhance the Antioxidant and Chemoattractive Activities of Cryopreserved Amniotic Membrane. Adv Wound Care (New Rochelle). 2015 Jun 1;4(6):329-338. doi: 10.1089/wound.2015.0637.

Elliott A, Walters RK, Pirinen M, Kurki M, Junna N, Goldstein JI, Reeve MP, Siirtola H, Lemmelä SM, Turley P, Lahtela E, Mehtonen J, Reis K, Elnahas AG, Reigo A, Palta P, Esko T, Mägi R; Estonian Biobank Research Team; FinnGen; Palotie A, Daly MJ, Widén E. Distinct and shared genetic architectures of gestational diabetes mellitus and type 2 diabetes. *Nat Genet*. 2024 Mar;56(3):377-382. doi: 10.1038/s41588-023-01607-4.

Farhadihosseinabadi B, Farahani M, Tayebi T, Jafari A, Biniazan F, Modaresifar K, Moravvej H, Bahrami S, Redl H, Tayebi L, Niknejad H. Amniotic membrane and its epithelial and mesenchymal stem cells as an appropriate source for skin tissue engineering and regenerative medicine. Artif Cells Nanomed Biotechnol. 2018;46(sup2):431-440. doi: 10.1080/21691401.2018.1458730.

Favaron PO, Carvalho RC, Borghesi J, Anunciação AR, Miglino MA. The Amniotic Membrane: Development and Potential Applications - A Review. Reprod Domest Anim. 2015 Dec;50(6):881-92. doi: 10.1111/rda.12633.

Fedele F, Mancone M, Chilian WM, Severino P, Canali E, Logan S, De Marchis ML, Volterrani M, Palmirotta R, Guadagni F. Role of genetic polymorphisms of ion channels in the pathophysiology of coronary microvascular dysfunction and ischemic heart disease. Basic Res Cardiol. 2013 Nov;108(6):387. doi: 10.1007/s00395-013-0387-4.

Feldman EL, Nave KA, Jensen TS, Bennett DLH. New Horizons in Diabetic Neuropathy: Mechanisms, Bioenergetics, and Pain. Neuron. 2017 Mar 22;93(6):1296-1313. doi: 10.1016/j.neuron.2017.02.005.

Fonseca VA. Defining and characterizing the progression of type 2 diabetes. Diabetes Care. 2009 Nov;32 Suppl 2(Suppl 2):S151-6. doi: 10.2337/dc09-S301.

Forbes JM, Cooper ME. Mechanisms of diabetic complications. Physiol Rev. 2013 Jan;93(1):137-88. doi: 10.1152/physrev.00045.2011.

Förstermann U, Münzel T. Endothelial nitric oxide synthase in vascular disease: from marvel to menace. Circulation. 2006 Apr 4;113(13):1708-14. doi: 10.1161/CIRCULATIONAHA.105.602532.

Frank RN. Diabetic retinopathy. N Engl J Med. 2004 Jan 1;350(1):48-58. doi: 10.1056/NEJMra021678.

Fu K, Zheng X, Chen Y, Wu L, Yang Z, Chen X, Song W. Role of matrix metalloproteinases in diabetic foot ulcers: Potential therapeutic targets. Front Pharmacol. 2022 Oct 20;13:1050630. doi: 10.3389/fphar.2022.1050630.

Fu Z, Gilbert ER, Liu D. Regulation of insulin synthesis and secretion and pancreatic Beta-cell dysfunction in diabetes. Curr Diabetes Rev. 2013 Jan 1;9(1):25-53.

Fuchsberger C, Flannick J, Teslovich TM et al. The genetic architecture of type 2 diabetes. Nature. 2016 Aug 4;536(7614):41-47. doi: 10.1038/nature18642..

Fugmann M, Breier M, Rottenkolber M, Banning F, Ferrari U, Sacco V, Grallert H, Parhofer KG, Seissler J, Clavel T, Lechner A. The stool microbiota of insulin resistant women with recent gestational diabetes, a high risk group for type 2 diabetes. Sci Rep. 2015 Aug 17;5:13212. doi: 10.1038/srep13212.

Fukumura D, Jain RK. Imaging angiogenesis and the microenvironment. APMIS. 2008 Jul-Aug;116(7-8):695-715. doi: 10.1111/j.1600-0463.2008.01148.x.

Galicia-Garcia U, Benito-Vicente A, Jebari S, Larrea-Sebal A, Siddiqi H, Uribe KB, Ostolaza H, Martín C. Pathophysiology of Type 2 Diabetes Mellitus. Int J Mol Sci. 2020 Aug 30;21(17):6275. doi: 10.3390/ijms21176275.

Galiero R, Caturano A, Vetrano E, Beccia D, Brin C, Alfano M, Di Salvo J, Epifani R, Piacevole A, Tagliaferri G, Rocco M, Iadicicco I, Docimo G, Rinaldi L, Sardu C, Salvatore T, Marfella R, Sasso FC. Peripheral Neuropathy in Diabetes Mellitus: Pathogenetic Mechanisms and Diagnostic Options. Int J Mol Sci. 2023 Feb 10;24(4):3554. doi: 10.3390/ijms24043554.

Gao L, Mann GE. Vascular NAD(P)H oxidase activation in diabetes: a double-edged sword in redox signalling. Cardiovasc Res. 2009 Apr 1;82(1):9-20. doi: 10.1093/cvr/cvp031.

Gao R, Zhou P, Li Y, Li Q. High glucose-induced IL-7/IL-7R upregulation of dermal fibroblasts inhibits angiogenesis in a paracrine way in delayed diabetic wound healing. J Cell Commun Signal. 2023 Sep;17(3):1023-1038. doi: 10.1007/s12079-023-00754-x.

Gargano JW, Wehner S, Reeves MJ. Presenting symptoms and onset-to-arrival time in patients with acute stroke and transient ischemic attack. J Stroke Cerebrovasc Dis. 2011 Nov;20(6):494-502. doi: 10.1016/j.jstrokecerebrovasdis.2010.02.022.

Gazzini S, Cerullo R, Soloperto D. VEGF as a Key Actor in Recurrent Respiratory Papillomatosis: A Narrative Review. Curr Issues Mol Biol. 2024 Jul 1;46(7):6757-6768. doi: 10.3390/cimb46070403.

Godos J, Marventano S, Mistretta A, Galvano F, Grosso G. Dietary sources of polyphenols in the Mediterranean healthy Eating, Aging and Lifestyle (MEAL) study cohort. Int J Food Sci Nutr. 2017 Sep;68(6):750-756. doi: 10.1080/09637486.2017.1285870.

Golebiewska EM, Poole AW. Platelet secretion: From haemostasis to wound healing and beyond. Blood Rev. 2015 May;29(3):153-62. doi: 10.1016/j.blre.2014.10.003.

González-Hedström D, García-Villalón ÁL, Amor S, de la Fuente-Fernández M, Almodóvar P, Prodanov M, Priego T, Martín AI, Inarejos-García AM, Granado M. Olive leaf extract supplementation improves the vascular and metabolic alterations associated with aging in Wistar rats. Sci Rep. 2021 Apr 14;11(1):8188. doi: 10.1038/s41598-021-87628-7.

Goyal R, Singhal M, Jialal I. Type 2 Diabetes. [Updated 2023 Jun 23]. In: StatPearls [Internet]. Treasure Island (FL): StatPearls Publishing; 2025 Jan-. Available from: https://www.ncbi.nlm.nih.gov/books/NBK513253/.

Grosso G, Godos J, Currenti W, Micek A, Falzone L, Libra M, Giampieri F, Forbes-Hernández TY, Quiles JL, Battino M, La Vignera S, Galvano F. The Effect of Dietary Polyphenols on Vascular Health and Hypertension: Current Evidence and Mechanisms of Action. Nutrients. 2022 Jan 27;14(3):545. doi: 10.3390/nu14030545.

Gurtner GC, Werner S, Barrandon Y, Longaker MT. Wound repair and regeneration. Nature. 2008 May 15;453(7193):314-21. doi: 10.1038/nature07039.

Gurung M, Li Z, You H, Rodrigues R, Jump DB, Morgun A, Shulzhenko N. Role of gut microbiota in type 2 diabetes pathophysiology. EBioMedicine. 2020 Jan;51:102590. doi: 10.1016/j.ebiom.2019.11.051.

Hiemer SE, Szymaniak AD, Varelas X. The transcriptional regulators TAZ and YAP direct transforming growth factor β-induced tumorigenic phenotypes in breast cancer cells. J Biol Chem. 2014 May 9;289(19):13461-74. doi: 10.1074/jbc.M113.529115.

Hou T, Du M, Gao X, An M. Human Vascular Endothelial Cells Promote the Secretion of Vascularization Factors and Migration of Human Skin Fibroblasts under Co-Culture and Its Preliminary Application. Int J Mol Sci. 2022 Nov 13;23(22):13995. doi: 10.3390/ijms232213995.

Huang Y, Kyriakides TR. The role of extracellular matrix in the pathophysiology of diabetic wounds. Matrix Biol Plus. 2020 Apr 22;6-7:100037. doi: 10.1016/j.mbplus.2020.100037.

Hyppönen E, Läärä E, Reunanen A, Järvelin MR, Virtanen SM. Intake of vitamin D and risk of type 1 diabetes: a birth-cohort study. Lancet. 2001 Nov 3;358(9292):1500-3. doi: 10.1016/S0140-6736(01)06580-1.

Insausti CL, Blanquer M, García-Hernández AM, Castellanos G, Moraleda JM. Amniotic membrane-derived stem cells: immunomodulatory properties and potential clinical application. Stem Cells Cloning. 2014 Mar 24;7:53-63. doi: 10.2147/SCCAA.S58696.

International Diabetes Federation. IDF Diabetes Atlas. 11th ed. 2025. Available from: https://diabetesatlas.org/resources/idf-diabetes-atlas-2025/

Iqbal I, Wilairatana P, Saqib F, Nasir B, Wahid M, Latif MF, Iqbal A, Naz R, Mubarak MS. Plant Polyphenols and Their Potential Benefits on Cardiovascular Health: A Review. Molecules. 2023 Sep 1;28(17):6403. doi: 10.3390/molecules28176403.

Izzo V, Meloni M, Vainieri E, Giurato L, Ruotolo V, Uccioli L. High matrix metalloproteinase levels are associated with dermal graft failure in diabetic foot ulcers. Int J Low Extrem Wounds. 2014 Sep;13(3):191-6. doi: 10.1177/1534734614544959.

Janus A, Szahidewicz-Krupska E, Mazur G, Doroszko A. Insulin Resistance and Endothelial Dysfunction Constitute a Common Therapeutic Target in Cardiometabolic Disorders. Mediators Inflamm. 2016;2016:3634948. doi: 10.1155/2016/3634948.

Jemai H, El Feki A, Sayadi S. Antidiabetic and antioxidant effects of hydroxytyrosol and oleuropein from olive leaves in alloxan-diabetic rats. J Agric Food Chem. 2009 Oct 14;57(19):8798-804. doi: 10.1021/jf901280r.

Jemai H, Fki I, Bouaziz M, Bouallagui Z, El Feki A, Isoda H, Sayadi S. Lipid-lowering and antioxidant effects of hydroxytyrosol and its triacetylated derivative recovered from olive tree leaves in cholesterol-fed rats. J Agric Food Chem. 2008 Apr 23;56(8):2630-6. doi: 10.1021/jf072589s.

Jeun R. Immunotherapies for prevention and treatment of type 1 diabetes. Immunotherapy. 2025 Feb;17(3):201-210. doi: 10.1080/1750743X.2025.2473311.

Jian K, Yang C, Li T, Wu X, Shen J, Wei J, Yang Z, Yuan D, Zhao M, Shi J. PDGF-BB-derived supramolecular hydrogel for promoting skin wound healing. J Nanobiotechnology. 2022 Apr 26;20(1):201. doi: 10.1186/s12951-022-01390-0.

Josefson JL, Catalano PM, Lowe WL, Scholtens DM, Kuang A, Dyer AR, Lowe LP, Metzger BE. The Joint Associations of Maternal BMI and Glycemia with Childhood Adiposity. J Clin Endocrinol Metab. 2020 Jul 1;105(7):2177–88. doi: 10.1210/clinem/dgaa180.

Kahn SE, Cooper ME, Del Prato S. Pathophysiology and treatment of type 2 diabetes: perspectives on the past, present, and future. Lancet. 2014 Mar 22;383(9922):1068-83. doi: 10.1016/S0140-6736(13)62154-6.

Kämpfer H, Pfeilschifter J, Frank S. Expressional regulation of angiopoietin-1 and -2 and the tie-1 and -2 receptor tyrosine kinases during cutaneous wound healing: a comparative study of normal and impaired repair. Lab Invest. 2001 Mar;81(3):361-73. doi: 10.1038/labinvest.3780244.

Karbach S, Wenzel P, Waisman A, Munzel T, Daiber A. eNOS uncoupling in cardiovascular diseases--the role of oxidative stress and inflammation. Curr Pharm Des. 2014;20(22):3579-94. doi: 10.2174/13816128113196660748.

Karjalainen J, Martin JM, Knip M, Ilonen J, Robinson BH, Savilahti E, Akerblom HK, Dosch HM. A bovine albumin peptide as a possible trigger of insulin-dependent diabetes mellitus. N Engl J Med. 1992 Jul 30;327(5):302-7. doi: 10.1056/NEJM199207303270502. Erratum in: N Engl J Med 1992 Oct 22;327(17):1252.

Kasiewicz LN, Whitehead KA. Silencing TNFα with lipidoid nanoparticles downregulates both TNFα and MCP-1 in an in vitro co-culture model of diabetic foot ulcers. Acta Biomater. 2016 Mar 1;32:120-128. doi: 10.1016/j.actbio.2015.12.023.

Khosla K, Heimberger S, Nieman KM, Tung A, Shahul S, Staff AC, Rana S. Long-Term Cardiovascular Disease Risk in Women After Hypertensive Disorders of Pregnancy: Recent Advances in Hypertension. Hypertension. 2021 Sep;78(4):927-935. doi: 10.1161/HYPERTENSIONAHA.121.16506.

Kim JH, Kim S, Piao S, Kim M, Kim DW, Jeon BH, Oh SH, Kim CS. Non-Thermal Plasma Attenuates TNF-α-Induced Endothelial Inflammation via ROS Modulation and NF-κB Inhibition. Int J Mol Sci. 2025 May 7;26(9):4449. doi: 10.3390/ijms26094449.

Kim SY, England L, Wilson HG, Bish C, Satten GA, Dietz P. Percentage of gestational diabetes mellitus attributable to overweight and obesity. Am J Public Health. 2010 Jun;100(6):1047-52. doi: 10.2105/AJPH.2009.172890.

Kivimäki M, Bartolomucci A, Kawachi I. The multiple roles of life stress in metabolic disorders. Nat Rev Endocrinol. 2023 Jan;19(1):10-27. doi: 10.1038/s41574-022-00746-8.

Kleinberger JW, Pollin TI. Personalized medicine in diabetes mellitus: current opportunities and future prospects. Ann N Y Acad Sci. 2015 Jun;1346(1):45-56. doi: 10.1111/nyas.12757.

Knapp P, Dunn-Roberts A, Sahib N, Cook L, Astin F, Kontou E, Thomas SA. Frequency of anxiety after stroke: An updated systematic review and meta-analysis of observational studies. Int J Stroke. 2020 Apr;15(3):244-255. doi: 10.1177/1747493019896958. Epub 2020 Jan 24. Erratum in: Int J Stroke. 2021 Dec;16(9):NP2. doi: 10.1177/17474930211037143.

Knip M, Åkerblom HK, Becker D, Dosch HM, Dupre J, Fraser W, Howard N, Ilonen J, Krischer JP, Kordonouri O, Lawson ML, Palmer JP, Savilahti E, Vaarala O, Virtanen SM; TRIGR Study Group. Hydrolyzed infant formula and early β-cell autoimmunity: a randomized clinical trial. JAMA. 2014 Jun 11;311(22):2279-87. doi: 10.1001/jama.2014.5610.

Koh TJ, DiPietro LA. Inflammation and wound healing: the role of the macrophage. Expert Rev Mol Med. 2011 Jul 11;13:e23. doi: 10.1017/S1462399411001943.

Kondrashova A, Hyöty H. Role of viruses and other microbes in the pathogenesis of type 1 diabetes. Int Rev Immunol. 2014 Jul-Aug;33(4):284-95. doi: 10.3109/08830185.2014.889130.

Kramer CK, Campbell S, Retnakaran R. Gestational diabetes and the risk of cardiovascular disease in women: a systematic review and meta-analysis. Diabetologia. 2019 Jun;62(6):905-914. doi: 10.1007/s00125-019-4840-2.

Kussmann M, Abe Cunha DH, Berciano S. Bioactive compounds for human and planetary health. Front Nutr. 2023 Jul 17;10:1193848. doi: 10.3389/fnut.2023.1193848.

LaPierre MP, Stoffel M. MicroRNAs as stress regulators in pancreatic beta cells and diabetes. Mol Metab. 2017 Jul 18;6(9):1010-1023. doi: 10.1016/j.molmet.2017.06.020.

Leclercq IA, Da Silva Morais A, Schroyen B, Van Hul N, Geerts A. Insulin resistance in hepatocytes and sinusoidal liver cells: mechanisms and consequences. J Hepatol. 2007 Jul;47(1):142-56. doi: 10.1016/j.jhep.2007.04.002.

Lee J, Lee NK, Moon JH. Gestational Diabetes Mellitus: Mechanisms Underlying Maternal and Fetal Complications. Endocrinol Metab (Seoul). 2025 Feb;40(1):10-25. doi: 10.3803/EnM.2024.2264.

Li H, Fu X, Zhang L, Huang Q, Wu Z, Sun T. Research of PDGF-BB gel on the wound healing of diabetic rats and its pharmacodynamics. J Surg Res. 2008 Mar;145(1):41-8. doi: 10.1016/j.jss.2007.02.044.

Li J, Chen J, Kirsner R. Pathophysiology of acute wound healing. Clin Dermatol. 2007 Jan-Feb;25(1):9-18. doi: 10.1016/j.clindermatol.2006.09.007.

Li J, Zhong Z, Yuan J, Chen X, Huang Z, Wu Z. Resveratrol improves endothelial dysfunction and attenuates atherogenesis in apolipoprotein E-deficient mice. J Nutr Biochem. 2019 May;67:63-71. doi: 10.1016/j.jnutbio.2019.01.022.

Li M, Hinkle SN, Grantz KL, Kim S, Grewal J, Grobman WA, Skupski DW, Newman RB, Chien EK, Sciscione A, Zork N, Wing DA, Nageotte M, Tekola-Ayele F, Louis GMB, Albert PS, Zhang C. Glycaemic status during pregnancy and longitudinal measures of fetal growth in a multi-racial US population: a prospective cohort study. *Lancet Diabetes Endocrinol*. 2020 Apr;8(4):292-300. doi: 10.1016/S2213-8587(20)30024-3.

Li W, Dong M, Guo P, Liu Y, Jing Y, Chen R, Zhang M. Luteolin-induced coronary arterial relaxation involves activation of the myocyte voltage-gated K^+ channels and inward rectifier K^+ channels. Life Sci. 2019 Mar 15;221:233-240. doi: 10.1016/j.lfs.2019.02.028.

Li Y, Ren X, He L, Li J, Zhang S, Chen W. Maternal age and the risk of gestational diabetes mellitus: A systematic review and meta-analysis of over 120 million participants. Diabetes Res Clin Pract. 2020 Apr;162:108044. doi: 10.1016/j.diabres.2020.108044.

Liarte S, Bernabé-García Á, Rodríguez-Valiente M, Moraleda JM, Castellanos G, Nicolás FJ. Amniotic Membrane Restores Chronic Wound Features to Normal in a Keratinocyte TGF-β-Chronified Cell Model. Int J Mol Sci. 2023 Mar 25;24(7):6210. doi: 10.3390/ijms24076210.

Libby JR, Royce H, Walker SR, Li L. The role of extracellular matrix in angiogenesis: Beyond adhesion and structure. Biomater Biosyst. 2024 Jul 8;15:100097. doi: 10.1016/j.bbiosy.2024.100097.

Lin X, Li H. Obesity: Epidemiology, Pathophysiology, and Therapeutics. Front Endocrinol (Lausanne). 2021 Sep 6;12:706978. doi: 10.3389/fendo.2021.706978.

Lins PG, Marina Piccoli Pugine S, Scatolini AM, de Melo MP. *In vitro* antioxidant activity of olive leaf extract (*Olea europaea* L.) and its protective effect on oxidative damage in human erythrocytes. Heliyon. 2018 Sep 20;4(9):e00805. doi: 10.1016/j.heliyon.2018.e00805.

Liu W, Ma K, Kwon SH, Garg R, Patta YR, Fujiwara T, Gurtner GC. The Abnormal Architecture of Healed Diabetic Ulcers Is the Result of FAK Degradation by Calpain 1. J Invest Dermatol. 2017 May;137(5):1155-1165. doi: 10.1016/j.jid.2016.11.039.

Long Y, Li D, Yu S, Zhang YL, Liu SY, Wan JY, Shi A, Deng J, Wen J, Li XQ, Ma Y, Li N, Yang M. Natural essential oils: A promising strategy for treating cardio-cerebrovascular diseases. J Ethnopharmacol. 2022 Oct 28;297:115421. doi: 10.1016/j.jep.2022.115421.

Loots MA, Lamme EN, Mekkes JR, Bos JD, Middelkoop E. Cultured fibroblasts from chronic diabetic wounds on the lower extremity (non-insulin-dependent diabetes mellitus) show disturbed proliferation. Arch Dermatol Res. 1999 Feb-Mar;291(2-3):93-9. doi: 10.1007/s004030050389.

Lowe WL Jr, Scholtens DM, Kuang A, Linder B, Lawrence JM, Lebenthal Y, McCance D, Hamilton J, Nodzenski M, Talbot O, Brickman WJ, Clayton P, Ma RC, Tam WH, Dyer AR, Catalano PM, Lowe LP, Metzger BE; HAPO Follow-up Study Cooperative Research Group. Hyperglycemia and Adverse Pregnancy Outcome Follow-up Study (HAPO FUS): Maternal Gestational Diabetes Mellitus and Childhood Glucose Metabolism. Diabetes Care. 2019 Mar;42(3):372-380. doi: 10.2337/dc18-1646.

Maahs DM, West NA, Lawrence JM, Mayer-Davis EJ. Epidemiology of type 1 diabetes. Endocrinol Metab Clin North Am. 2010 Sep;39(3):481-97. doi: 10.1016/j.ecl.2010.05.011.

Magenta A, Greco S, Capogrossi MC, Gaetano C, Martelli F. Nitric oxide, oxidative stress, and p66Shc interplay in diabetic endothelial dysfunction. Biomed Res Int. 2014;2014:193095. doi: 10.1155/2014/193095.

Mahdavian Delavary B, van der Veer WM, van Egmond M, Niessen FB, Beelen RH. Macrophages in skin injury and repair. Immunobiology. 2011 Jul;216(7):753-62. doi: 10.1016/j.imbio.2011.01.001.

Mamede AC, Carvalho MJ, Abrantes AM, Laranjo M, Maia CJ, Botelho MF. Amniotic membrane: from structure and functions to clinical applications. Cell Tissue Res. 2012 Aug;349(2):447-58. doi: 10.1007/s00441-012-1424-6.

Manna C, Migliardi V, Golino P, Scognamiglio A, Galletti P, Chiariello M, Zappia V. Oleuropein prevents oxidative myocardial injury induced by ischemia and reperfusion. J Nutr Biochem. 2004 Aug;15(8):461-6. doi: 10.1016/j.jnutbio.2003.12.010.

Marso SP, Hiatt WR. Peripheral arterial disease in patients with diabetes. J Am Coll Cardiol. 2006 Mar 7;47(5):921-9. doi: 10.1016/j.jacc.2005.09.065.

Martin JM, Trink B, Daneman D, Dosch HM, Robinson B. Milk proteins in the etiology of insulin-dependent diabetes mellitus (IDDM). Ann Med. 1991 Oct;23(4):447-52. doi: 10.3109/07853899109148088.

Martin P, Leibovich SJ. Inflammatory cells during wound repair: the good, the bad and the ugly. Trends Cell Biol. 2005 Nov;15(11):599-607. doi: 10.1016/j.tcb.2005.09.002.

McDermott MM, Ferrucci L, Liu K, Guralnik JM, Tian L, Liao Y, Criqui MH. Leg symptom categories and rates of mobility decline in peripheral arterial disease. J Am Geriatr Soc. 2010 Jul;58(7):1256-62. doi: 10.1111/j.1532-5415.2010.02941.x.

McIntyre HD, Chang AM, Callaway LK, Cowley DM, Dyer AR, Radaelli T, Farrell KA, Huston-Presley L, Amini SB, Kirwan JP, Catalano PM; Hyperglycemia and Adverse Pregnancy Outcome (HAPO) Study Cooperative Research Group. Hormonal and metabolic factors associated with variations in insulin sensitivity in human pregnancy. Diabetes Care. 2010 Feb;33(2):356-60. doi: 10.2337/dc09-1196.

Metzger BE, Persson B, Lowe LP, Dyer AR, Cruickshank JK, Deerochanawong C, Halliday HL, Hennis AJ, Liley H, Ng PC, Coustan DR, Hadden DR, Hod M, Oats JJ, Trimble ER; HAPO Study Cooperative Research Group. Hyperglycemia and adverse pregnancy outcome study: neonatal glycemia. Pediatrics. 2010 Dec;126(6):e1545-52. doi: 10.1542/peds.2009-2257.

Mirza R, Koh TJ. Dysregulation of monocyte/macrophage phenotype in wounds of diabetic mice. Cytokine. 2011 Nov;56(2):256-64. doi: 10.1016/j.cyto.2011.06.016.

Mittal R, Prasad K, Lemos JRN, Arevalo G, Hirani K. Unveiling Gestational Diabetes: An Overview of Pathophysiology and Management. Int J Mol Sci. 2025 Mar 5;26(5):2320. doi: 10.3390/ijms26052320.

Mizukami H, Kudoh K. Diversity of pathophysiology in type 2 diabetes shown by islet pathology. J Diabetes Investig. 2022 Jan;13(1):6-13. doi: 10.1111/jdi.13679.

Młynarska E, Czarnik W, Dzieża N, Jędraszak W, Majchrowicz G, Prusinowski F, Stabrawa M, Rysz J, Franczyk B. Type 2 Diabetes Mellitus: New Pathogenetic Mechanisms, Treatment and the Most Important Complications. Int J Mol Sci. 2025 Jan 27;26(3):1094. doi: 10.3390/ijms26031094.

Mokhtari B, Azizi Y, Rostami Abookheili A, Aboutaleb N, Nazarinia D, Naderi N. Human amniotic membrane mesenchymal stem cells-conditioned medium attenuates myocardial ischemia-reperfusion injury in rats by targeting oxidative stress. Iran J Basic Med Sci. 2020 Nov;23(11):1453-1461. doi: 10.22038/ijbms.2020.47572.10952.

Morley RL, Sharma A, Horsch AD, Hinchliffe RJ. Peripheral artery disease. BMJ. 2018 Feb 1;360:j5842. doi: 10.1136/bmj.j5842.

Moyce BL, Dolinsky VW. Maternal β-Cell Adaptations in Pregnancy and Placental Signalling: Implications for Gestational Diabetes. Int J Mol Sci. 2018 Nov 5;19(11):3467. doi: 10.3390/ijms19113467.

Neyrinck AM, Catry E, Taminiau B, Cani PD, Bindels LB, Daube G, Dessy C, Delzenne NM. Chitin-glucan and pomegranate polyphenols improve endothelial dysfunction. Sci Rep. 2019 Oct 2;9(1):14150. doi: 10.1038/s41598-019-50700-4.

Noh CH, Park S, Seong HR, Lee AY, Tsolmon KE, Geum D, Hong SC, Kim TM, Choi EK, Kim YB. An Exosome-Rich Conditioned Medium from Human Amniotic Membrane Stem Cells Facilitates Wound Healing via Increased Reepithelization, Collagen Synthesis, and Angiogenesis. Cells. 2023 Nov 24;12(23):2698. doi: 10.3390/cells12232698.

Okonkwo UA, DiPietro LA. Diabetes and Wound Angiogenesis. Int J Mol Sci. 2017 Jul 3;18(7):1419. doi: 10.3390/ijms18071419.

Padhi S, Nayak AK, Behera A. Type II diabetes mellitus: a review on recent drug based therapeutics. Biomed Pharmacother. 2020 Nov;131:110708. doi: 10.1016/j.biopha.2020.110708.

Pandur E, Micalizzi G, Mondello L, Horváth A, Sipos K, Horváth G. Antioxidant and Anti-Inflammatory Effects of Thyme (*Thymus vulgaris* L.) Essential Oils Prepared at Different Plant Phenophases on *Pseudomonas aeruginosa* LPS-Activated THP-1 Macrophages. Antioxidants (Basel). 2022 Jul 6;11(7):1330. doi: 10.3390/antiox11071330.

Patel S, Srivastava S, Singh MR, Singh D. Mechanistic insight into diabetic wounds: Pathogenesis, molecular targets and treatment strategies to pace wound healing. Biomed Pharmacother. 2019 Apr;112:108615. doi: 10.1016/j.biopha.2019.108615.

Pérez-Pérez A, Maymó JL, Gambino YP, Guadix P, Dueñas JL, Varone CL, Sánchez-Margalet V. Activated translation signaling in placenta from pregnant women with gestational diabetes mellitus: possible role of leptin. Horm Metab Res. 2013 Jun;45(6):436-42. doi: 10.1055/s-0032-1333276.

Petersen KF, Shulman GI. Cellular mechanism of insulin resistance in skeletal muscle. J R Soc Med. 2002;95 Suppl 42(Suppl 42):8-13.

Pickup JC. Insulin-pump therapy for type 1 diabetes mellitus. N Engl J Med. 2012 Apr 26;366(17):1616-24. doi: 10.1056/NEJMct1113948.

Pipino C, Bernabé-García Á, Cappellacci I, Stelling-Férez J, Di Tomo P, Santalucia M, Navalón C, Pandolfi A, Nicolás FJ. Effect of the Human Amniotic Membrane on the Umbilical Vein Endothelial Cells of Gestational Diabetic Mothers: New Insight on Inflammation and Angiogenesis. Front Bioeng Biotechnol. 2022 Jul 5;10:854845. doi: 10.3389/fbioe.2022.854845.

Pipino C, Bernabé-García Á, Cappellacci I, Stelling-Férez J, Di Tomo P, Santalucia M, Navalón C, Pandolfi A, Nicolás FJ. Effect of the Human Amniotic Membrane on the Umbilical Vein Endothelial Cells of Gestational Diabetic Mothers: New Insight on Inflammation and Angiogenesis. Front Bioeng Biotechnol. 2022 Jul 5;10:854845. doi: 10.3389/fbioe.2022.854845.

Pipino C, Shangaris P, Resca E, Zia S, Deprest J, Sebire NJ, David AL, Guillot PV, De Coppi P. Placenta as a reservoir of stem cells: an underutilized resource? Br Med Bull. 2013;105:43-68. doi: 10.1093/bmb/lds033.

Plows JF, Stanley JL, Baker PN, Reynolds CM, Vickers MH. The Pathophysiology of Gestational Diabetes Mellitus. Int J Mol Sci. 2018 Oct 26;19(11):3342. doi: 10.3390/ijms19113342.

Prasad RB, Kristensen K, Katsarou A, Shaat N. Association of single nucleotide polymorphisms with insulin secretion, insulin sensitivity, and diabetes in women with a history of gestational diabetes mellitus. *BMC Med Genomics*. 2021 Nov 20;14(1):274. doi: 10.1186/s12920-021-01123-6.

Primavera M, Giannini C, Chiarelli F. Prediction and Prevention of Type 1 Diabetes. Front Endocrinol (Lausanne). 2020 Jun 2;11:248. doi: 10.3389/fendo.2020.00248.

Qi W, Yang C, Dai Z, Che D, Feng J, Mao Y, Cheng R, Wang Z, He X, Zhou T, Gu X, Yan L, Yang X, Ma JX, Gao G. High levels of pigment epithelium-derived factor in diabetes impair wound healing through suppression of Wnt signaling. Diabetes. 2015 Apr;64(4):1407-19. doi: 10.2337/db14-1111.

Quillen DM, Samraj G, Kuritzky L. Improving management of type 2 diabetes mellitus: 2. Biguanides. Hosp Pract (1995). 1999 Oct 15;34(11):41-4. doi: 10.1080/21548331.1999.11443925.

Reddy MA, Zhang E, Natarajan R. Epigenetic mechanisms in diabetic complications and metabolic memory. Diabetologia. 2015 Mar;58(3):443-55. doi: 10.1007/s00125-014-3462-y.

Reidy K, Kang HM, Hostetter T, Susztak K. Molecular mechanisms of diabetic kidney disease. J Clin Invest. 2014 Jun;124(6):2333-40. doi: 10.1172/JCI72271.

Retnakaran R, Ye C, Hanley AJ, Connelly PW, Sermer M, Zinman B. Treatment of Gestational Diabetes Mellitus and Maternal Risk of Diabetes After Pregnancy. Diabetes Care. 2023 Mar 1;46(3):587-592. doi: 10.2337/dc22-1786.

Rice JB, Desai U, Cummings AK, Birnbaum HG, Skornicki M, Parsons NB. Burden of diabetic foot ulcers for medicare and private insurers. Diabetes Care. 2014;37(3):651-8. doi: 10.2337/dc13-2176.

Rodrigo-Carbó C, Madinaveitia-Nisarre L, Pérez-Calahorra S, Gracia-Rubio I, Cebollada A, Galindo-Lalana C, Mateo-Gallego R, Lamiquiz-Moneo I. Low-calorie, high-protein diets, regardless of protein source, improve glucose metabolism and cardiometabolic profiles in subjects with prediabetes or type 2 diabetes and overweight or obesity. Diabetes Obes Metab. 2025 Jan;27(1):268-279. doi: 10.1111/dom.16013.

Rodrigues M, Kosaric N, Bonham CA, Gurtner GC. Wound Healing: A Cellular Perspective. Physiol Rev. 2019 Jan 1;99(1):665-706. doi: 10.1152/physrev.00067.2017.

Rodríguez-Valiente M, García-Hernández AM, Fuente-Mora C, Sánchez-Gálvez J, García-Vizcaino EM, Tristante Barrenechea E, Castellanos Escrig G, Liarte Lastra SD, Nicolás FJ. Management of Foot Ulcers and Chronic Wounds with Amniotic Membrane in Comorbid Patients: A Successful Experience. Biomedicines. 2024 Oct 18;12(10):2380. doi: 10.3390/biomedicines12102380.

Rodríguez-Valiente M, Nicolás FJ, García-Hernández AM, Fuente Mora C, Blanquer M, Alcaraz PJ, Almansa S, Merino GR, Lucas MDL, Algueró MC, Insausti CL, Piñero A, Moraleda JM, Castellanos G. Cryopreserved amniotic membrane in the treatment of diabetic foot ulcers: a case series. J Wound Care. 2018 Dec 2;27(12):806-815. doi: 10.12968/jowc.2018.27.12.806.

Romani A, Ieri F, Urciuoli S, Noce A, Marrone G, Nediani C, Bernini R. Health Effects of Phenolic Compounds Found in Extra-Virgin Olive Oil, By-Products, and Leaf of *Olea europaea* L. Nutrients. 2019 Aug 1;11(8):1776. doi: 10.3390/nu11081776.

Rossboth S, Lechleitner M, Oberaigner W. Risk factors for diabetic foot complications in type 2 diabetes-A systematic review. Endocrinol Diabetes Metab. 2020 Aug 17;4(1):e00175. doi: 10.1002/edm2.175.

Rousselle P, Braye F, Dayan G. Re-epithelialization of adult skin wounds: Cellular mechanisms and therapeutic strategies. Adv Drug Deliv Rev. 2019 Jun;146:344-365. doi: 10.1016/j.addr.2018.06.019.

Ruan GX, Kazlauskas A. Axl is essential for VEGF-A-dependent activation of PI3K/Akt. EMBO J. 2012 Apr 4;31(7):1692-703. doi: 10.1038/emboj.2012.21.

Ruchat SM, Houde AA, Voisin G, St-Pierre J, Perron P, Baillargeon JP, Gaudet D, Hivert MF, Brisson D, Bouchard L. Gestational diabetes mellitus epigenetically affects genes predominantly involved in metabolic diseases. Epigenetics. 2013 Sep;8(9):935-43. doi: 10.4161/epi.25578.

Ruiz-Cañada C, Bernabé-García Á, Liarte S, Insausti CL, Angosto D, Moraleda JM, Castellanos G, Nicolás FJ. Amniotic membrane stimulates cell migration by modulating transforming growth factor-β signalling. J Tissue Eng Regen Med. 2018 Mar;12(3):808-820. doi: 10.1002/term.2501.

Sabella N. Use of fetal membranes in skin grafting. Med. Rec. 1913; 83, 478–480

Sacks DB, Arnold M, Bakris GL, Bruns DE, Horvath AR, Lernmark Å, Metzger BE, Nathan DM, Kirkman MS. Guidelines and Recommendations for Laboratory Analysis in the Diagnosis and Management of Diabetes Mellitus. Diabetes Care. 2023 Oct 1;46(10):e151-e199. doi: 10.2337/dci23-0036.

Saely CH, Rein P, Vonbank A, Huber K, Drexel H. Type 2 diabetes and the progression of visualized atherosclerosis to clinical cardiovascular events. Int J Cardiol. 2013 Aug 10;167(3):776-80. doi: 10.1016/j.ijcard.2012.03.042.

Samsudeen H, De Varaj SP, Kandasamy K. Unraveling the Therapeutic Potential of Muscle Strengthening Exercises for Reversing Diabetes Mellitus. Curr Diabetes Rev. 2025;21(3):7-12. doi: 10.2174/0115733998275876240125064716.

Satoh T. Molecular mechanisms for the regulation of insulin-stimulated glucose uptake by small guanosine triphosphatases in skeletal muscle and adipocytes. Int J Mol Sci. 2014 Oct 16;15(10):18677-92. doi: 10.3390/ijms151018677.

Schiavone V, Romasco T, Di Pietrantonio N, Garzoli S, Palmerini C, Di Tomo P, Pipino C, Mandatori D, Fioravanti R, Butturini E, Sabatino M, Baldassarre MPA, Ragno R, Pandolfi A, Di Pietro N. Essential Oils from Mediterranean Plants Inhibit In Vitro Monocyte Adhesion to Endothelial Cells from Umbilical Cords of Females with Gestational Diabetes Mellitus. Int J Mol Sci. 2023 Apr 13;24(8):7225. doi: 10.3390/ijms24087225.

Schmidt A, von Woedtke T, Weltmann KD, Bekeschus S. YAP/TAZ, beta-catenin, and TGFb pathway activation in medical plasma-induced wound healing in diabetic mice. J Adv Res. 2025 Jun;72:387-400. doi: 10.1016/j.jare.2024.07.004.

Schulz E, Wenzel P, Münzel T, Daiber A. Mitochondrial redox signaling: Interaction of mitochondrial reactive oxygen species with other sources of oxidative stress. Antioxid Redox Signal. 2014 Jan 10;20(2):308-24. doi: 10.1089/ars.2012.4609.

Seino S, Sugawara K, Yokoi N, Takahashi H. β-Cell signalling and insulin secretagogues: A path for improved diabetes therapy. Diabetes Obes Metab. 2017 Sep;19 Suppl 1:22-29. doi: 10.1111/dom.12995.

Sha W, Liu M, Sun D, Qiu J, Xu B, Chen L, Shen T, Chen C, Wang H, Zhang C, Lei T. Resveratrol ameliorated endothelial injury of thoracic aorta in diabetic mice and Gly-LDL-induced HUVECs through inhibiting TLR4/HIF-1α. J Cell Mol Med. 2021 Jun 10;25(13):6258–70. doi: 10.1111/jcmm.16584.

Shah FH, Nam YS, Bang JY, Hwang IS, Kim DH, Ki M, Lee HW. Targeting vascular endothelial growth receptor-2 (VEGFR-2): structural biology, functional insights, and therapeutic resistance. Arch Pharm Res. 2025 May;48(5):404-425. doi: 10.1007/s12272-025-01545-1.

Shepherd PR, Kahn BB. Glucose transporters and insulin action--implications for insulin resistance and diabetes mellitus. N Engl J Med. 1999 Jul 22;341(4):248-57. doi: 10.1056/NEJM199907223410406.

Shi X, Young CD, Zhou H, Wang X. Transforming Growth Factor-β Signaling in Fibrotic Diseases and Cancer-Associated Fibroblasts. Biomolecules. 2020 Dec 12;10(12):1666. doi: 10.3390/biom10121666.

Silini AR, Cargnoni A, Magatti M, Pianta S, Parolini O. The Long Path of Human Placenta, and Its Derivatives, in Regenerative Medicine. Front Bioeng Biotechnol. 2015 Oct 19;3:162. doi: 10.3389/fbioe.2015.00162.

Somova LI, Shode FO, Ramnanan P, Nadar A. Antihypertensive, antiatherosclerotic and antioxidant activity of triterpenoids isolated from Olea europaea, subspecies africana leaves. J Ethnopharmacol. 2003 Feb;84(2-3):299-305. doi: 10.1016/s0378-8741(02)00332-x.

Soni MG, Burdock GA, Christian MS, Bitler CM, Crea R. Safety assessment of aqueous olive pulp extract as an antioxidant or antimicrobial agent in foods. Food Chem Toxicol. 2006 Jul;44(7):903-15. doi: 10.1016/j.fct.2006.01.008.

Sorsby A, Symons HM. AMNIOTIC MEMBRANE GRAFTS IN CAUSTIC BURNS OF THE EYE: (Burns of the second degree). Br J Ophthalmol. 1946 Jun;30(6):337-45. doi:10.1136/bjo.30.1.64

Staton CA, Valluru M, Hoh L, Reed MW, Brown NJ. Angiopoietin-1, angiopoietin-2 and Tie-2 receptor expression in human dermal wound repair and scarring. Br J Dermatol. 2010 Nov;163(5):920-7. doi: 10.1111/j.1365-2133.2010.09940.x.

Steffes MW, Sibley S, Jackson M, Thomas W. Beta-cell function and the development of diabetes-related complications in the diabetes control and complications trial. Diabetes Care. 2003 Mar;26(3):832-6. doi: 10.2337/diacare.26.3.832.

Stelling-Férez J, Cappellacci I, Pandolfi A, Gabaldón JA, Pipino C, Nicolás FJ. Oleanolic acid rescues critical features of umbilical vein endothelial cells permanently affected by hyperglycemia. Front Endocrinol (Lausanne). 2023 Dec 13;14:1308606. doi: 10.3389/fendo.2023.1308606.

Stern M. The grafting of preserved amniotic membranes to burned and ulcerated surfaces, substituting skin grafts. JAMA 1913; 60, 973. doi:10.1001/ jama.1913.04340130021008.

Stumvoll M, Goldstein BJ, van Haeften TW. Type 2 diabetes: principles of pathogenesis and therapy. Lancet. 2005 Apr 9-15;365(9467):1333-46. doi: 10.1016/S0140-6736(05)61032-X.

Stunova A, Vistejnova L. Dermal fibroblasts-A heterogeneous population with regulatory function in wound healing. Cytokine Growth Factor Rev. 2018 Feb;39:137-150. doi: 10.1016/j.cytogfr.2018.01.003.

Sweeting A, Wong J, Murphy HR, Ross GP. A Clinical Update on Gestational Diabetes Mellitus. Endocr Rev. 2022 Sep 26;43(5):763-793. doi: 10.1210/endrev/bnac003.

Talhaoui N, Gómez-Caravaca AM, Roldán C, León L, De la Rosa R, Fernández-Gutiérrez A, Segura-Carretero A. Chemometric analysis for the evaluation of phenolic patterns in olive leaves from six cultivars at different growth stages. J Agric Food Chem. 2015 Feb 18;63(6):1722-9. doi: 10.1021/jf5058205.

Tandara AA, Mustoe TA. Oxygen in wound healing--more than a nutrient. World J Surg. 2004 Mar;28(3):294-300. doi: 10.1007/s00268-003-7400-2.

Tenenhaus M. The Use of Dehydrated Human Amnion/Chorion Membranes in the Treatment of Burns and Complex Wounds: Current and Future Applications. Ann Plast Surg. 2017 Feb;78(2 Suppl 1):S11-S13. doi: 10.1097/SAP.0000000000000983.

The Expert Committee on the Diagnosis and Classification of Diabetes Mellitus. Report of the Expert Committee on the Diagnosis and Classification of Diabetes Mellitus. Diabetes Care. 1997 Jul;20(7):1183-97. doi: 10.2337/diacare.20.7.1183.

Tonnesen MG, Feng X, Clark RA. Angiogenesis in wound healing. J Investig Dermatol Symp Proc. 2000 Dec;5(1):40-6. doi: 10.1046/j.1087-0024.2000.00014.x.

Tyagi S, Gupta P, Saini AS, Kaushal C, Sharma S. The peroxisome proliferator-activated receptor: A family of nuclear receptors role in various diseases. J Adv Pharm Technol Res. 2011 Oct;2(4):236-40. doi: 10.4103/2231-4040.90879.

Ucci M, Di Tomo P, Tritschler F, Cordone VGP, Lanuti P, Bologna G, Di Silvestre S, Di Pietro N, Pipino C, Mandatori D, Formoso G, Pandolfi A. Anti-inflammatory Role of Carotenoids in Endothelial Cells Derived from Umbilical Cord of Women Affected by Gestational Diabetes Mellitus. Oxid Med Cell Longev. 2019 Jan 30;2019:8184656. doi: 10.1155/2019/8184656.

Vaarala O, Atkinson MA, Neu J. The "perfect storm" for type 1 diabetes: the complex interplay between intestinal microbiota, gut permeability, and mucosal immunity. Diabetes. 2008 Oct;57(10):2555-62. doi: 10.2337/db08-0331.

Vestweber D. How leukocytes cross the vascular endothelium. Nat Rev Immunol. 2015 Nov;15(11):692-704. doi: 10.1038/nri3908.

Villaschi S, Nicosia RF. Paracrine interactions between fibroblasts and endothelial cells in a serum-free coculture model. Modulation of angiogenesis and collagen gel contraction. Lab Invest. 1994 Aug;71(2):291-9.

Vinik AI, Maser RE, Mitchell BD, Freeman R. Diabetic autonomic neuropathy. Diabetes Care. 2003 May;26(5):1553-79. doi: 10.2337/diacare.26.5.1553.

Vounzoulaki E, Khunti K, Abner SC, Tan BK, Davies MJ, Gillies CL. Progression to type 2 diabetes in women with a known history of gestational diabetes: systematic review and meta-analysis. BMJ. 2020 May 13;369:m1361. doi: 10.1136/bmj.m1361.

Vounzoulaki E, Khunti K, Abner SC, Tan BK, Davies MJ, Gillies CL. Progression to type 2 diabetes in women with a known history of gestational diabetes: systematic review and meta-analysis. BMJ. 2020 May 13;369:m1361. doi: 10.1136/bmj.m1361.

Wang N, Yang BH, Wang G, Gao Y, Cao X, Zhang XF, Yan CC, Lian XT, Liu BH, Ju S. A meta-analysis of the relationship between foot local characteristics and major lower extremity amputation in diabetic foot patients. J Cell Biochem. 2019 Jun;120(6):9091-9096. doi: 10.1002/jcb.28183.

Wang X, Bove AM, Simone G, Ma B. Molecular Bases of VEGFR-2-Mediated Physiological Function and Pathological Role. Front Cell Dev Biol. 2020 Nov 16;8:599281. doi: 10.3389/fcell.2020.599281.

Warren CM, Ziyad S, Briot A, Der A, Iruela-Arispe ML. A ligand-independent VEGFR2 signaling pathway limits angiogenic responses in diabetes. Sci Signal. 2014 Jan 7;7(307):ra1. doi: 10.1126/scisignal.2004235.

Weyer C, Bogardus C, Mott DM, Pratley RE. The natural history of insulin secretory dysfunction and insulin resistance in the pathogenesis of type 2 diabetes mellitus. J Clin Invest. 1999 Sep;104(6):787-94. doi: 10.1172/JCI7231.

Wicklow B, Retnakaran R. Gestational Diabetes Mellitus and Its Implications across the Life Span. Diabetes Metab J. 2023 May;47(3):333-344. doi: 10.4093/dmj.2022.0348.

Wilkinson HN, Hardman MJ. Wound healing: cellular mechanisms and pathological outcomes. Open Biol. 2020 Sep;10(9):200223. doi: 10.1098/rsob.200223.

Williams MA, Qiu C, Muy-Rivera M, Vadachkoria S, Song T, Luthy DA. Plasma adiponectin concentrations in early pregnancy and subsequent risk of gestational diabetes mellitus. J Clin Endocrinol Metab. 2004 May;89(5):2306-11. doi: 10.1210/jc.2003-031201.

Writing Group for the TRIGR Study Group; Knip M, Åkerblom HK, Al Taji E, Becker D, Bruining J, Castano L, Danne T, de Beaufort C, Dosch HM, Dupre J, Fraser WD, Howard N, Ilonen J, Konrad D, Kordonouri O, Krischer JP, Lawson ML, Ludvigsson J, Madacsy L, Mahon JL, Ormisson A, Palmer JP, Pozzilli P, Savilahti E, Serrano-Rios M, Songini M, Taback S, Vaarala O, White NH, Virtanen SM, Wasikowa R. Effect of Hydrolyzed Infant Formula vs Conventional Formula on Risk of Type 1 Diabetes: The TRIGR Randomized Clinical Trial. JAMA. 2018 Jan 2;319(1):38-48. doi: 10.1001/jama.2017.19826.

Wu W, Zhang D, Pan D, Zuo G, Ren X, Chen S. Downregulation of vascular endothelial growth factor receptor-2 under oxidative stress conditions is mediated by β-transduction repeat-containing protein via glycogen synthase kinase-3β signaling. Int J Mol Med. 2016 Apr;37(4):911-20. doi: 10.3892/ijmm.2016.2493.

Xu J, Zgheib C, Hu J, Wu W, Zhang L, Liechty KW. The role of microRNA-15b in the impaired angiogenesis in diabetic wounds. Wound Repair Regen. 2014 Sep-Oct;22(5):671-7. doi: 10.1111/wrr.12217.

Xu S, Ilyas I, Little PJ, Li H, Kamato D, Zheng X, Luo S, Li Z, Liu P, Han J, Harding IC, Ebong EE, Cameron SJ, Stewart AG, Weng J. Endothelial Dysfunction in Atherosclerotic Cardiovascular Diseases and Beyond: From Mechanism to Pharmacotherapies. Pharmacol Rev. 2021 Jul;73(3):924-967. doi: 10.1124/pharmrev.120.000096.

Xue M, Jackson CJ. Extracellular Matrix Reorganization During Wound Healing and Its Impact on Abnormal Scarring. Adv Wound Care (New Rochelle). 2015 Mar 1;4(3):119-136. doi: 10.1089/wound.2013.0485.

Yang DR, Wang MY, Zhang CL, Wang Y. Endothelial dysfunction in vascular complications of diabetes: a comprehensive review of mechanisms and implications. Front Endocrinol (Lausanne). 2024 Apr 5;15:1359255. doi: 10.3389/fendo.2024.1359255.

Yates C, May K, Hale T, Allard B, Rowlings N, Freeman A, Harrison J, McCann J, Wraight P. Wound chronicity, inpatient care, and chronic kidney disease predispose to MRSA infection in diabetic foot ulcers. Diabetes Care. 2009 Oct;32(10):1907-9. doi: 10.2337/dc09-0295.

Young SM, Benyshek DC. In search of human placentophagy: a cross-cultural survey of human placenta consumption, disposal practices, and cultural beliefs. Ecol Food Nutr. 2010 Nov-Dec;49(6):467-84. doi: 10.1080/03670244.2010.524106.

Yuan H, Salapatas AM, Leonardo TR, Han C, Vegesna B, Debnath K, Chen L, Ravindran S, DiPietro LA. The Role of Endothelial Cell-Derived Extracellular Vesicles in Modulating Fibroblast Function in Skin Wound Healing. J Invest Dermatol. 2025 Oct 27:S0022-202X(25)03499-2. doi: 10.1016/j.jid.2025.10.584.

Zaccardi F, Webb DR, Yates T, Davies MJ. Pathophysiology of type 1 and type 2 diabetes mellitus: a 90-year perspective. Postgrad Med J. 2016 Feb;92(1084):63-9. doi: 10.1136/postgradmedj-2015-133281.

Zhang Y, Lazzarini PA, McPhail SM, van Netten JJ, Armstrong DG, Pacella RE. Global disability burdens of diabetes-related lower-extremity complications in 1990 and 2016. Diabetes Care. 2020;43(5):964–974. doi:10.2337/dc19-1614

Zhang YE. Non-Smad Signaling Pathways of the TGF-β Family. Cold Spring Harb Perspect Biol. 2017 Feb 1;9(2):a022129. doi: 10.1101/cshperspect.a022129.

Zheng L, Li M, Li H. High Glucose Promotes and Aggravates the Senescence and Dysfunction of Vascular Endothelial Cells in Women with Hyperglycemia in Pregnancy. Biomolecules. 2024 Mar 10;14(3):329. doi: 10.3390/biom14030329.

Zhou K, Ma Y, Brogan MS. Chronic and non-healing wounds: The story of vascular endothelial growth factor. Med Hypotheses. 2015 Oct;85(4):399-404. doi: 10.1016/j.mehy.2015.06.017.